

UNIVERSITY OF RIJEKA
FACULTY OF MEDICINE

Lara Valenčić Seršić

CHARACTERISATION OF microRNA IN CEREBROSPINAL
FLUID-DERIVED EXTRACELLULAR VESICLES AFTER
SEVERE TRAUMATIC BRAIN INJURY

Doctoral thesis

Rijeka, 2025

UNIVERSITY OF RIJEKA
FACULTY OF MEDICINE

Lara Valenčić Seršić

CHARACTERISATION OF microRNA IN CEREBROSPINAL
FLUID-DERIVED EXTRACELLULAR VESICLES AFTER
SEVERE TRAUMATIC BRAIN INJURY

Doctoral thesis

Mentor: Assoc. Prof. Kristina Grabušić

Rijeka, 2025

SVEUČILIŠTE U RIJECI
MEDICINSKI FAKULTET

Lara Valenčić Seršić

KARAKTERIZACIJA mikroRNA U IZVANSTANIČNIM
VEZIKULAMA CEREBROSPINALNE TEKUĆINE NAKON
TEŠKE TRAUMATSKE OZLJEDE MOZGA

Doktorski rad

Rijeka, 2025

Mentor rada: izv. prof. dr. sc. Kristina Grabušić, dipl. ing. biol.

Doktorska disertacija obranjena je dana _____ u/na
_____, pred povjerenstvom u sastavu:

1. _____(titula, ime i prezime)
2. _____(titula, ime i prezime)
3. _____(titula, ime i prezime)
4. _____(titula, ime i prezime)
5. _____(titula, ime i prezime)

Rad ima ____listova.

UDK: _____(UDK broj dodjeljuje knjižnica Medicinskog fakulteta u Rijeci)

PREDGOVOR

Doktorska disertacija izrađena je na Katedri za anesteziologiju, reanimatologiju, hitnu i intenzivnu medicinu te Zavodu za fiziologiju, imunologiju i patofiziologiju Medicinskog fakulteta Sveučilišta u Rijeci. Klinički dio doktorske disertacije izrađen je na Klinici za anesteziologiju, intenzivnu medicinu i liječenje boli Kliničkog bolničkog centra Rijeka te na Odjelu za anesteziju, reanimatologiju, intenzivnu medicinu i liječenje boli Opće bolnice Pula.

Istraživanje je provedeno u sklopu projekta Hrvatske zaklade za znanost pod naslovom "Identifikacija cirkulirajućih biomarkera neurološkog oporavka u bolesnika s ozljedom mozga" (IP-2019-04-1511) te projekta s potporom Sveučilišta u Rijeci, naslova "Izvanstanične vezikule kao klinički marker neuroregeneracije nakon teške ozljede mozga (uniri-biomed-18- 5). Voditeljica oba projekta je mentorica, izv. prof. dr. sc. Kristina Grabušić, dipl. ing. biol.

ZAHVALE

Zahvaljujem se svojoj mentorici, prof. dr. sc. Kristini Grabušić, dipl. ing. biol., što me vodila kroz proces stvaranja ovog doktorskog rada i što je uvijek bila dostupna za korisnu informaciju, potporu i riječ utjehe.

Zahvaljujem se kolegama s Klinike za anesteziologiju, intenzivnu medicinu i liječenje boli što su imali dovoljno strpljenja te želje i volje za prilagodbom u danima kad mi je to bilo potrebno kako bih savladala još jedan korak k završetku ovog rada.

Najveće hvala ide mojoj boljoj polovici na nesebičnoj podršci i ljubavi, kao i mojoj obitelji zbog usađivanja upornosti i konstantne želje za učenjem što me dovelo do trenutne životne pozicije.

Posebno mjesto s posebnim **hvala** pripada mom sinu Oliveru koji je od dana rođenja majčino nepresušno vrelo snage i motivacije.

SUMMARY

Objectives: Severe traumatic brain injury (sTBI) refers to a life-threatening acquired alteration of brain function caused by an external mechanical force. The silent epidemic of today remains one of the leading causes of mortality and morbidity with long-term implications for survivors. After the initial injury, a broad pathophysiological spectrum of events develops in the background of sTBI and triggers further brain damage. A prerequisite to treating or mitigating post-sTBI damage is the timely recognition of harmful brain processes. A potential source of valuable information about ongoing brain events is the intracranial cerebrospinal fluid (CSF) drained as part of sTBI management. Here, we focus on CSF-derived microRNAs (miRNAs), small molecules that affect numerous cellular processes by impacting gene expression. The research goal was to characterize types and dynamics of CSF-miRNAs after sTBI and determine if miRNAs are present in CSF in free form or as a cargo of extracellular vesicles (EVs), nanoparticles included in cell-to-cell communication.

Subjects and Methods: A total of 35 intracranial CSF samples were collected from 5 sTBI patients through 12 days following the injury. Samples were combined into the day (d) d1–2, d3–4, d5–6, and d7–12 CSF pools and separated by size exclusion chromatography (SEC) into SEC fractions followed by immunoblot and tunable resistive pulse sensing (TRPS) analyses of SEC-fractions. MiRNA was isolated from SEC fractions enriched for CD81-positive EVs or albumin as well as from unseparated CSF pools. After cDNA synthesis with added quantification spike-ins, samples were analyzed by a commercial PCR array with primers to detect 87 targeted miRNAs.

Results: The 87 targeted miRNAs differed up to a million-fold across CSF pools, with the highest levels found at d1–2, followed by a decreasing trend in subsequent pools. Ten most abundant miRNAs across the CSF pools were miR-451a, miR-16-5p, miR-144-3p, miR-20a-5p, let-7b-5p, miR-15a-5p, miR-21-5p, miR-223-3p, miR-106a-5p, and miR-15b-5p. Detected miRNAs had a high abundance in pools burdened with elevated haemolysis levels. Most detected miRNAs were mainly associated with free proteins, while small portions were identified as cargo of CD81-positive EVs, including miR-142-3p, miR-204-5p, and miR-223-3p.

Conclusion: Findings of the performed study of human intracranial CSF indicate that sTBI generates dynamic alterations in extracellular miRNAs, which may serve as carriers of critical informations regarding processes occurring in the early phase of brain injury and potentially initial steps towards neurorecovery. Future research should focus on both free and EV-associated miRNAs to further elucidate the role of miRNAs in pathogenesis and healing after sTBI.

Key words: Brain Injuries, Traumatic; Cerebrospinal Fluid; Extracellular Vesicles; MicroRNAs.

PROŠIRENI SAŽETAK

Cilj istraživanja: Teška traumatska ozljeda mozga (tTOM) predstavlja životno ugrožavajuće stanje koje dovodi do oštećenja strukture i funkcije mozga. Nastaje uslijed djelovanja vanjske sile uz posljedični poremećaj stanja svijesti i mogući razvoj kome. Jedan je od vodećih uzroka smrtnosti uz dugoročne neurološke posljedice za preživjele. Primarna ozljeda moždanog tkiva nastaje u trenutku zadobivanja traume i pokreće niz patofizioloških mehanizama s posljedičnom sekundarnom ozljedom mozga. U odnosu na primarnu ozljedu mozga koja je ireverzibilna, pravovremeno prepoznata i prevenirana, sekundarna ozljeda može biti izlječena. Vrijedne biološke informacije o podležućim moždanim zbivanjima prisutne su u cerebrospinalnoj tekućini (CSF), koja postaje dostupna putem vanjskog drenažnog sustava u sklopu liječenja. U ovom istraživanju fokus je bio na mikroRNA (miRNA) molekulama koje djeluju na gensku ekspresiju zbog čega se razmatraju kao potencijalni biomarkeri zbijanja tijekom tTOM-a. Naime, miRNA može biti otpuštena u CSF s mjesta ozljede mozga kao posljedica oštećenja tkiva, no isto tako može biti produkt sekrecije različitih stanica. U biološkim tekućinama miRNA cirkulira u slobodnom obliku ili vezana uz izvanstanične vezikule (IV), nanočestice koje posreduju međustaničnu komunikaciju. Cilj istraživanja je bio istražiti vrste miRNA molekula i njihovu dinamiku u CSF-u nakon tTOM-a i utvrditi jesu li miRNA u CSF-u prisutne u slobodnom obliku ili kao dio IV-a.

Ispitanici i metode: Studija je provedena na ukupno 35 uzoraka CSF-a uzorkovanih jedanput dnevno kroz 12 dana u 5 pacijenata koji su doživjeli tTOM. Uzorci su bili združeni u skupne CSF uzorke prema sljedećim danima (d) prikupljanja: d1–2, d3–4, d5–6 i d7–12. Na združenim CSF uzorcima provedena je western blot analiza markera za IV-e te markera prisutnosti krvi, uključujući albumin, hemoglobin i apolipoproteine. Iz združenih CSF uzoraka izolirana je miRNA, koja je poslužila za sintezu komplementarne DNA (engl., *complementary DNA*, cDNA). Sinteza cDNA provedena je uz dodavanje sintetskih miRNA poznatih količina (engl., *spike-in*) u svrhu omogućavanja apsolutne kvantifikacije ciljnih miRNA molekula. Uzorci cDNA analizirani su potom pomoću lančane reakcije u stvarnom vremenu (engl., *real-time polymerase chain reaction*, RT-PCR) na komercijalno dostupnoj ploči s početnicama za detekciju 87 miRNA. Radi analize IV-a, združeni CSF uzorci su razdvojeni u frakcije korištenjem kromatografije isključenjem po veličini (engl., *size-exclusion chromatography*, SEC) na koloni napunjenoj sefarozum CL-6B. Dobivene frakcije analizirane su imunoblotom radi detekcije markera IV-a i krvnih komponenata te metodom opažanja podesivog otpornog pulsa (engl., *tunable resistive pulse sensing*, TRPS) radi određivanja veličine i koncentracije nanočestica. Frakcije pozitivne na CD81 marker karakterističan za IV-e te frakcije pozitivne na

albumin, korištene su za izolaciju miRNA uz naknadni postupak sinteze cDNA i detekciju 87 ciljnih miRNA na komercijalnoj RT-PCR ploči kao što je prethodno opisano.

Rezultati: Svih 87 ciljnih miRNA detektirano je u združenim CST uzorcima no s rasponom koncentracija od nekoliko nanograma do manje od femtograma pri čemu su vrijednosti opadale s napredovanjem dana od nastanka ozljede. U ranim danima nakon ozljede zabilježena je visoka razina hemolize, osobito u uzorku d1–2, a sljedećih 10 miRNA bile su najzastupljenije: miR-451a, miR-16-5p, miR-144-3p, miR-20a-5p, let-7b-5p, miR-15a-5p, miR-21-5p, miR-223-3p, miR-106a-5p i miR-15b-5p. Nakon što je na združenim CST uzorcima provedena kromatografska separacija IV-a i slobodnih proteina, većina ciljnih miRNA detektirana je u frakciji slobodnih proteina, a svega nekoliko sljedećih ciljnih miRNA je bilo detektirano u frakcijama s CD81 pozitivnim IV-ama: miR-142-3p, miR-204-5p i miR-223-3p. Zanimljivo je da su te miRNA bile detektirane u združenim uzorcima d5–6 i d7–12 koji su pokazali najmanji stupanj hemolize.

Zaključak: Rezultati istraživanja intrakranijalne CST upućuju na to da tTOM uzrokuje dinamične promjene u izvanstaničnim miRNA molekulama koje predstavljaju potencijalne nositelje vrijednih informacija o zbivanjima povezanim s oštećenjem mozga i ranim procesima neurološkog oporavka. Buduća bi se istraživanja trebala usmjeriti na analizu slobodnih miRNA kao i onih povezanih s IV-ama, kako bi se razjasnila njihova uloga u patofiziološkim mehanizmima nakon tTOM-a u cilju prevencije nastanka sekundarne ozljede mozga.

Ključne riječi: cerebrospinalna tekućina; izvanstanične vezikule; mikroRNA; ozljeda mozga, traumatska.

TABLE OF CONTENTS

PREDGOVOR	4
ZAHVALE	5
SUMMARY	6
PROŠIRENI SAŽETAK	7
1. INTRODUCTION AND LITERATURE REVIEW	5
1.1. Traumatic brain injury	5
1.1.1. Classification of brain injury severity	5
1.1.2. Epidemiology and demographics	7
1.1.3. Biophysical aspects	8
1.1.4. Pathoanatomical changes	9
1.1.5. Current strategies and challenges in acute treatment	11
1.2. Molecular mechanisms of acute intracranial pathophysiology	13
1.2.1. Excitotoxicity and calcium disbalance	14
1.2.2. Mitochondrial dysfunction and oxidative stress	14
1.2.3. Neuroinflammation	16
1.2.4. Apoptosis	16
1.2.5. The brain-blood barrier dysfunction	17
1.3. MicroRNA	18
1.3.1. Biogenesis of miRNA	18
1.3.2. Mode of action of miRNAs	20
1.3.3. The role of microRNAs in brain function	21
1.3.4. Biomarker potential of microRNAs in traumatic brain injury	23
1.4. Extracellular vesicles	24
1.4.1. Overview of extracellular vesicle biogenesis	24
1.4.2. Isolation, characterisation and quantification of extracellular vesicles (EVs) – what do the guidelines say?	27
1.4.3. Extracellular vesicles and severe traumatic brain injury	28
1.4.4. MicroRNA as cargo of extracellular vesicles after severe traumatic brain injury	29

2. RESEARCH OBJECTIVES	30
3. SUBJECTS AND METHODS	31
3.1. Subjects	31
3.2. Materials	32
3.2.1. Chemicals, cell culture and molecular biology reagents and materials.....	32
3.2.2. Solutions	33
3.2.3. miRNA isolation and quantification kits and reagents	34
3.2.4. Antibodies.....	36
3.3. Methods	37
3.3.1. CSF collection and pooling	37
3.3.2. Cell culture.....	37
3.3.3. Western blot	37
3.3.4. Size-exclusion chromatography	38
3.3.5. Slot blot.....	39
3.3.6. Tunable resistive pulse sensing (TRPS).....	39
3.3.7. RNA isolation and quantification	39
3.3.8. Synthesis of complementary DNA (cDNA)	40
3.3.9. Real-time polymerase chain reaction (RT-PCR).....	40
3.3.10. Statistical analysis	40
3.3.11. Figures and tables.....	40
4. RESULTS.....	41
4.1. Clinical characteristics of severe traumatic brain injury patients.....	41
4.2. Dynamics of intracranial CSF molecular content in acute phase of sTBI patient recovery 42	
4.2.1. CSF biobank is created from samples collected during 12 days after the injury	42
4.2.2. Plasma and cell protein levels in CSF are increased in the first 4 days after the injury	43
4.2.3. miR451 quantification shows varying levels of haemolysis in post-TBI CSF	45
4.3. Absolute quantification of 87 putative CSF miRNAs in post-injury CSF	46
4.3.1. Standard curve for absolute quantification	46
4.3.2. Quantities of targeted miRNAs present in CSF differ up to a million-fold	47

4.3.3. The targeted 87 miRNAs likely derive from the blood and account for only a tiny proportion of miRNAs present in the CSF after severe traumatic brain injury	51
4.4. miRNA cargo of extracellular vesicles in post-TBI CSF.....	53
4.4.1. EVs are present in intracranial CSF after sTBI.....	53
4.4.2. miRNA is present at similar levels in both extracellular vesicles and free protein portions of cerebrospinal fluid	56
5. DISCUSSION	60
5.1. Study importance and main limitations	60
5.2. High haemolysis level affects miRNA isolation and quantification	62
5.3. Targeted 87 miRNAs are present in post-TBI CSF but constitute only a small fraction of the total cDNA.....	63
5.4. Extracellular vesicles as a potential cargo for an only small portion of targeted miRNAs	68
6. CONCLUSIONS	71
7. REFERENCES	72
ILLUSTRATIONS.....	87
List of figures.....	87
List of tables.....	88
CURRICULUM VITAE	94

1. INTRODUCTION AND LITERATURE REVIEW

1.1. Traumatic brain injury

Traumatic brain injury (TBI) refers to an acquired alteration of brain function caused by an external mechanical force. The injury results in permanent or temporary impairment of physical, cognitive, and psychological functions, with an altered state of consciousness [1]. After transferring the energy to the brain tissue at impact, initial or primary brain injury triggers a cascade of secondary pathophysiological events. Onwards, these trauma-initiated processes disturb brain physiology balance, causing further neuronal destruction and aggravating the injury impacts [2].

Due to the consequences of the mentioned brain changes, TBI remains one of the leading causes of morbidity with long-term implications for survivors and also mortality with complex, long-lasting, and expensive hospital treatment. The annual global incidence of TBI is estimated from 27 to 69 million people, representing a „silent epidemic“ of today and a global socioeconomic problem [2, 3].

Except for the injury type and demographic differences among patients suffering from TBI, our knowledge about complex, secondary mechanisms is incomplete. These events can last from hours to years, and there are still no readily available biomarkers to facilitate therapeutic management and neurorecovery of TBI patients. Extensive research has been directed at identifying and characterising different biochemical and cellular agents associated with these processes [1, 4].

1.1.1. Classification of brain injury severity

The early step in managing TBI towards therapeutic measures and prognosis is a classification of injury severity. Most classification systems are based on patient symptomatology, physical examination emphasizing neurological status, and imaging techniques during the early phase of the patient's assessment. Usually, these classifications do not include progressive secondary TBI events. Therefore, it has been suggested that repeated risk assessments should be used over time. The international Glasgow Coma Scale (GCS) total score has been the most widely used method for repetitive, objective, and rapid recording of the consciousness level in all types of trauma patients, including TBI patients, with application in pre-hospital, emergency department, and intensive care unit settings [5, 6, 7].

The GCS is scored based on 3 subscale scores with predefined points for eye-opening (from 1 to 4 points), verbal response (from 1 to 5 points), and motor response (from 1 to 6

points) (Table 1). Adding all together, the total sum of the score is a minimum of 3 points and a maximum of 15 points, reflecting the severity of TBI. In clinical terms, a score of 3 points indicates a comatose, severely injured patient, while a score of 15 points is a label for a completely alert and cooperative patient. When using the scale and assessing the TBI patient, the best response in all 3 components is always recorded. Therefore, the TBI severity classification is divided into mild TBI with a GCS score ranging from 13 to 15 points, moderate TBI with a GCS score from 8 to 12 points, and severe TBI (sTBI) with a GCS score of ≤ 8 points [8].

Table 1. The Glasgow Coma Scale (GCS) total score. Adapted from [8].

Parameter	Patient response	Score
Eye-opening response	Eyes open spontaneously	4
	Eyes open to sound	3
	Eyes open to pain and pressure	2
	No response	1
Verbal response	Oriented	5
	Confused	4
	Inappropriate words	3
	Incomprehensible sounds	2
	No response	1
Motor response	Obeys command	6
	Localizing the pain	5
	Normal flexion	4
	Abnormal flexion/decortication	3
	Extension/decerebration	2
	No response	1

The standardized Glasgow Outcome Scale (GOS) assesses the outcome after the injury. GOS scores of 4 and 5 are considered a good patient outcome, while GOS of 1 to 3 is considered a poor patient outcome, as shown in Table 2. The GCS poorly correlates with TBI outcomes, but at the moment of clinical assessment, the calculated GCS score is inversely proportional to the progression of the TBI. Hence, if a drop in the GCS is established in re-evaluation, it is likely due to the progression of the TBI.

Table 2. The Glasgow Outcome Scale (GOS) score.

GOS SCORE	CLINICAL MEANING
1	Death
2	Persistent vegetative state
3	Severe disability – neurological deficit limits the performance of daily activities independently
4	Moderate disability – minor neurological deficit with possibility of independent performance of daily activities
5	Good outcome – return to normal functional state

In conclusion, all the TBI patient's characteristics must be considered to correctly diagnose TBI severity (for example, consumption of addictive substances and drugs) and supported by neuroradiological imaging techniques such as computed tomography (CT) of the brain, which stands as a gold standard in emergency TBI diagnostics. Furthermore, new research is needed to improve prognostics and extend the knowledge in pathophysiological processes regarding TBI [6, 7, 8].

1.1.2. Epidemiology and demographics

A systematic review from 2021 included available studies from all of Europe and showed that the TBI incidence ranged from 47.3 to 849 cases per 100.000 population per year. This statistical data was compared with results from the previous analysis referring to European countries conducted in 2006, and the mean incidence rates remained the same [9,10]. The European results are comparable to the incidence rates in the United States, with 180-250 cases per 100.000 population per year. Interestingly, the highest global TBI incidence rate was noted in a population-based incidence study performed in New Zealand, with 790 cases per 100.000 population per year, corroborating the results of the global TBI incidence analysis showing the highest rates in Southern Asia and Western Pacific [3, 11, 12].

The most common mechanisms of the TBI are traffic-related accidents and falls. Traffic-related accidents are the leading TBI cause due to the broader use of motorized vehicles and machinery, especially in low-middle income countries, with nearly 3 times more TBI cases than in high-income countries. An increase in falls among older adults in high-income countries leads to a high second place on the injury mechanism scale [4, 9, 13]. Other injury causes include violence, sport-related injuries, accidents in the home or at work, suicides or suicide attempts.

TBI is related to age groups, and it shows a specific distribution. Falls are the most common cause of injury in early childhood from 0 to 4 years (839 per 100.000 per year) and in older adults aged 65 years and more, especially in the age group of ≥ 75 with 599 cases per 100.000 per year. Adolescents and young adults aged 15 to 24 have the highest incidence of motor vehicle accidents (236 per 100.000 per year) [8, 9]. There is a growing trend of falls as a cause of TBI, mainly in high-income countries, due to the ageing population, improved road infrastructure, and traffic discipline [14].

TBI is more common in males. Such an incidence pattern has been constantly present in all epidemiological TBI studies over the last few decades. This can be related to the fact that the male gender is much more represented as participants in traffic and sports activities, and also, a more significant number of them are involved in violence [8]. A recent study highlights the role of hormones in recovery after TBI, showing that woman, both of reproductive age and postmenopausal, may experience better outcomes compared to men of the same age group, suggesting a neuroprotective role of female sex hormones. [15].

Many TBI patients, primarily those suffering from moderate TBI and especially sTBI, have long-term neurological damage that significantly affects their quality of life. Furthermore, out of all traumatic deaths, sTBI is the primary cause in 1/3 to 1/2 cases resulting from external injury, with a note that about half of patients who suffer sTBI die at the scene of the accident. Therefore, prevention, diagnosis and targeted treatment of sTBI are critical components in reducing mortality among this population [11].

1.1.3. Biophysical aspects

TBI is generally defined as a result of an external force leading to brain tissue injury. The physical forces generated during the impact are transmitted to the brain tissue and lead to structural and biochemical changes in the brain. Several forces may contribute to TBI, including rotational (angular) and linear (translational) forces, leading to rising intracranial pressure gradients [16]. Therefore, shearing and strain forces are responsible for further neuronal and blood vessel tissue damage. As a result of force action, TBI can be divided into contact or impact loading when the head is struck or strikes an object and noncontact or inertial loading if there is a movement of the brain within the skull with significant acceleration-deceleration of the head (Figure 1) [17].

It is essential to understand the biophysical aspects of TBI since there is a correlation between the type of force action and pathoanatomical brain changes. For instance, if the shock waves

are created in the moment of impact loading, they will travel through the skull and brain, resulting primarily in focal injuries, for example, brain contusions, skull fractures, and some forms of intra- and extra-axial haematomas [17].

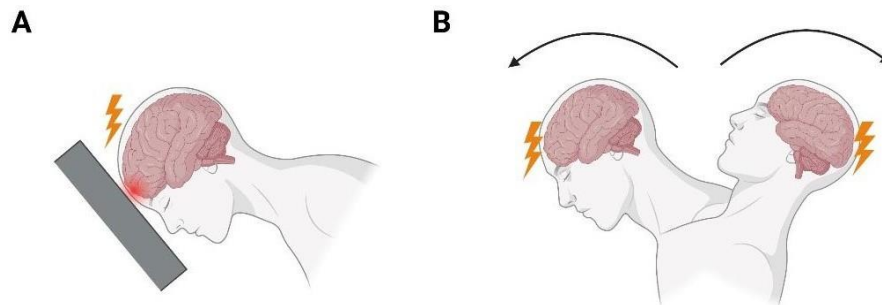


Figure 1. Most common types of biophysical forces during traumatic brain injury. (A) Contact or impact loading is when the head directly strikes an object. **(B)** Action of acceleration-deceleration forces during noncontact or inertial loading (Adapted from “BioRender.com (2023). Retrieved from <https://app.biorender.com/biorender-templates>, May 1st 2024).

On the other side, inertial loading causes more severe brain changes, such as diffuse injuries due to acceleration-deceleration movement. Diffuse brain injuries are often severe and include diffuse axonal injury (DAI) as one of the most common causes of TBI permanent disability and mortality. Impact on the skull is not essential to cause this type of injury. In conclusion, the most common cause of TBI is a combination of contact and acceleration-deceleration forces [17,18].

Lastly, brain damage can be located on the impact site, resulting in coup injury, or on the opposite side, known as contrecoup injury. Blunt head trauma in a non-moving position is associated with coup injuries. Inertial loading injuries with acceleration and deceleration of the head are associated with contrecoup injuries [16,19].

1.1.4. Pathoanatomical changes

During the initial assessment of a TBI patient in the emergency department, a neuroradiological diagnosis is essential for further medical treatment. In addition to the GCS total score and the patient’s physical examination, diagnostic imaging provides insight into the morphological events after the injury. A routinely used imaging method for TBI is brain CT without a contrast. This technique is fast, sensitive, and highly suitable, especially for sTBI, which usually requires emergent neurosurgical treatment. Based on anatomic location of lesions, the imaging findings are

divided as follows: intra-axial lesions with CT changes localized in the brain parenchyma; extra-axial lesions if changes are detected outside of brain tissue[20].

Intra-axial lesions include intracerebral haematoma, parenchymal contusions, diffuse axonal injury, and brain stem injury [20]. After the injury, blood vessels in the brain parenchyma suffer from shearing forces, resulting in intracerebral haematoma. Isolated intracerebral haematoma can have good treatment outcomes, but, unfortunately, it often results in the movement of brain tissue to the contralateral side, known as mass effect and also with diffuse axonal injury. Parenchymal contusions are a common form of damage in TBI. They are frequently associated with haemorrhagic foci, usually with multifocal and bilateral locations, and with the highest incidence in temporal (46%) and frontal (31%) lobes [21, 22]. Diffuse axonal injury occurs after the action of mainly rotational forces on the brain. Consequently, shearing leads to axonal swelling within 3-6 hours after the injury. Axotomy and axonal or Wallerian degeneration on the nerve distal end after the injury can be seen for 6-12 hours post-injury [20]. Furthermore, axons in sTBI can immediately suffer complete transection together with blood vessels. Persistent axonal changes lead to long-term neurological disability and high mortality, mainly if DAI is associated with brain swelling due to oedema and vascular congestion. Moreover, axonal injury is the most common type of brain stem injury, equal to the one described in the brain parenchyma. Other manifestations of brain stem injury are multifocal petechial haemorrhages and secondary (Duret) haemorrhages that are usually hardly detectable using brain CT imaging techniques. Taken together, described intra-axial lesions have a high potential for poor outcomes and often lethal prognosis [20, 21, 22].

Anatomically, epidural, subdural, and subarachnoid spaces are located extra-axially, with haemorrhage as the most common pathology after TBI. Bleeding in these spaces results from shearing and tearing forces impacting arteries and veins at the moment of injury. Bleeding origin and potential progression exert pressure on the brain (axial) tissue, resulting in life-threatening neurological changes. Epidural (EDH), subdural (SDH), subarachnoid (SAH), and intraventricular haematomas (IVH) can be formed, respectively [20, 22]. The most favourable outcome has EDH, a lenticular-shaped haematoma between the dura mater and the skull with arterial or venous origin. It results most commonly from middle meningeal artery disruption in the temporal or temporoparietal region. SDH forms due to the tearing of bridging veins that connect the dura and arachnoid mater. The underlying mechanism of SDH derives from the fact that the dural sinuses are fixed while the brain is in a mobile phase during the injury, so the mentioned veins get damaged [23]. SAH is the most common brain CT finding during sTBI patient assessment, and it is most often associated with other brain injuries, making the prognosis worse, including increased mortality. CT scans on admission show that 40% of sTBI patients suffer from SAH and exhibit lower GCS total scores [24]. Depending on the severity

of TBI, IVH has an incidence from 0.4 to 22% of patients, most commonly overlapping with SAH. Biophysical changes in IVH include tearing subependymal veins after exerting the rotational forces on the brain during the injury. [20]. Accompanying DAI in the corpus callosum is reported in 60% of patients with IVH, making the severity of injury more life-threatening. The same recent cohort study associated IVH with increased disability and mortality, regardless of other accompanying brain injuries [25].

1.1.5. Current strategies and challenges in acute treatment

Therapeutic management of sTBI relies on initial assessment and continuous evaluation, with the GCS total score being the most commonly used tool. Furthermore, a neuroradiological diagnosis is essential to determine potentially new or progressive pathoanatomical changes (described in subsection 1.1.4.). After the evaluation, this critical neurologic condition usually requires an emergent start of treatment. Unfortunately, due to the severity of the brain changes after suffering sTBI, it does not necessarily mean a good treatment outcome. Great attention is paid to the research in sTBI molecular diagnostic and implementation in clinical practice [26, 27].

A combination of intensive care and surgical treatment is life-saving therapeutic management for patients with sTBI. To prevent harmful effects of oxygen deficiency, as the most important substrate for brain survival, controlled protective mechanical ventilation is indicated with maintaining carbon dioxide target values by avoiding hyper- and hypocapnia. The procedure mentioned above requires patients' analgosedation to reduce the excitatory brain metabolism. The further goal is to provide a haemodynamic support and thereby to avoid hypotension and the consequent hypoxia. Haemodynamic support is achieved by maintaining the blood pressure thresholds of ≥ 100 mmHg and ≥ 110 mmHg for patients aged 50 to 69 years and 15 to 49 and >70 years, respectively. These target pressure values are necessary to ensure brain cerebral perfusion pressure (CPP) values from 60 to 70 mmHg. The targeted CPP ensures that the brain is supplied with vital nutrients and that the mortality risk is lowered [28]. Crucial aspects of further intensive care treatment are the avoidance of hyper- and hypoglycaemia, as well as the prevention of infections and deep vein thrombosis prophylaxis [28, 29].

Intracranial hypertension, defined as elevated intracranial pressure (ICP), was found to be highly associated with fatal outcomes. The mortality rate was 47% for values greater than 20 mmHg [30]. Therefore, current guidelines include ICP monitoring as a salvageable measure in the sTBI management. Additionally, ICP monitoring is indicated in all sTBI patients and with abnormal neuroradiological CT findings. However, even when the CT scans show no changes,

ICP monitoring is indicated if the patient is 40 years of age and older, has a unilateral or bilateral motor posture, or has systolic blood pressure <90 mmHg at admission. ICP monitoring facilitates the clinical management of sTBI patients. It indicates further fluid management and osmotherapy with mannitol as the first medication of choice in treating elevated ICP when the values are 22 mmHg and greater [28]. The gold standard for ICP monitoring is placing an external ventricular drain (EVD) by an attending neurosurgeon. EVD allows the monitoring and control of ICP by diverting cerebrospinal fluid (CSF). Values of ICP are used to assess CPP by subtracting the ICP value from the mean arterial pressure (MAP) value ($CPP = MAP - ICP$). These three values are defined by the Monroe-Kellie doctrine as a pressure-volume equilibrium between brain tissue (85%), blood (10%), and CSF (5%), respectively [31]. Equilibrium means that an increase in the volume of any component must be compensated by a decrease in the remaining two. Therefore, ICP monitoring is crucial for acquiring knowledge about a patient's brain equilibrium and further therapeutic management [28, 31].

Therapeutic measures established in the guidelines for treating sTBI patients facilitate clinical management. However, the mortality of sTBI patients at the global level is still high and prompts novel therapeutic strategies. Therefore, translational research has been initiated, focusing treatment on a broad spectrum of pathophysiological mechanisms. Trials are often limited at the clinical level by the heterogeneity of patient characteristics, pathoanatomical changes, different levels of intensive care, surgical approaches and rehabilitation among sTBI patients [32].

In addition to the standard medications that should be used as the first line of sTBI patient treatment, a recent review article described the attempts of extensive preclinical, randomized studies on progesterone and erythropoietin introduction in clinical treatment [33]. Unfortunately, no clinical effect to increase the patient's recovery was recorded. In rat studies, levetiracetam and glibenclamide have shown the most promise. The antiepileptic drug levetiracetam improved outcomes in 2 rat model injuries but still has insufficient evidence to be recommended in humans over phenytoin. On the other hand, glibenclamide, antagonist of sulfonylurea receptor 1 (SUR1), has been evaluated in several clinical studies and showed improved GCS score and Glasgow Outcome Score (GOS) used for evaluation of 3-months post-injury treatment outcome [32, 34]. There are also mitochondrial-target therapy studies since impaired energy metabolism is a potential target of TBI therapy [35].

On the other side, serum biomarkers have the potential to serve as early post-injury indicators of neurorecovery. Various studies sought to compare the efficacy of different serum biomarkers of TBI, mainly in sTBI, such as glial cell injury biomarkers, including glial fibrillary

acidic protein (GFAP) and S100 calcium-binding protein B (S100B), respectively [32, 36]. Neuron-specific enolase (NSE) as a neuronal cell injury biomarker has also been studied [36]. Although none showed superior sensitivity or specificity compared to the others, S100B protein is currently used for early control of mild and moderate TBI in Scandinavia since it can predict normal CT scans after TBI. The Scandinavian guidelines for head injury management use S100B protein to reduce unnecessary brain CT scans. Different axonal and inflammatory biomarkers have been identified with low sensitivity and specificity. The limitation of serum biomarkers is that they do not indicate precisely the event at the signalling pathophysiological pathway, but may serve more as an early predictor of overall therapeutic efficacy [32, 36, 37].

Due to their role in regulating almost all genes at the post-transcriptional level, microRNAs (miRNAs) have been recommended as biomarkers involved in primary and secondary molecular patterns in rat and human sTBI. Mechanisms of intercellular communication include extracellular vesicles (EVs) and their molecular cargo – miRNAs. Circulating miRNAs may be used as potential biomarkers within existing diagnostic and therapeutic approaches for better understanding of neurorecovery and prognosis following sTBI. [38, 39].

1.2. Molecular mechanisms of acute intracranial pathophysiology

The TBI mechanism during the initial event, biophysical properties, and the following pathoanatomical changes together form the primary brain injury. The primary injury is irreversible. Prevention can only be achieved by acting on TBI occurrence such as providing better road infrastructure and protective equipment in traffic, and increasing awareness of injury and safety measures for activities that can lead to falls. Formed intra- or/and extra-axial lesions result in brain vessel damage and metabolism dysregulation followed by neuronal death. Furthermore, a cascade of signalling pathways triggered in the brain leads to an indirect injury called secondary TBI that can be reversible. Depending on the severity of the primary TBI, secondary TBI can start from several hours to a few weeks or even months after the initial event. Therefore, with timely treatment and knowledge about underlying basic biomechanisms - a current focus of research for targeted therapeutic agents - secondary injury is preventable [21, 40].

The major biomechanisms of secondary injury are excitotoxicity, oxidative stress, mitochondrial dysfunction, neuroinflammation, apoptosis, and blood-brain barrier (BBB) dysfunction. Although these biomechanisms have been intensively studied, they are still not targeted in TBI treatment. More knowledge is required to elucidate how to prevent the progression of secondary injury and permanent neurological sequels with their effects on a global socioeconomic level [21, 41].

1.2.1. Excitotoxicity and calcium disbalance

One of the main and most detrimental processes in the post-TBI brain is the overabundance of excitatory neurotransmitters, mainly glutamate, and activation of ionotropic glutamate receptors, namely N-methyl-D-aspartate (NMDA) and α -amino-3-hydroxy-5-methyl-4-isoxazolepropionic acid (AMPA) receptors. This process is known as glutamate-dependent excitotoxicity, leading to loss of neuronal cells. Namely, increased synaptic release of glutamate causes the corresponding receptors to get overactivated, resulting in an excessive influx of sodium, potassium, and calcium ions into the cells [42]. NMDA receptors, more precisely, the extrasynaptic ones, are responsible for initiating excitotoxicity. Such a mediator of the excitotoxic response is GluN2B, consisting of seven subunits [40, 41, 42, 43].

The main initiator of the cellular response is calcium in extremely high intracellular concentrations. Inside the cell, calcium stimulates several downstream signaling pathways, mainly calcium/calmodulin-dependent protein kinase II, protein kinase C, mitogen-activated protein kinases (MAPK), and protein phosphates [42]. The most detrimental process for the neuron is the activation of self-digesting cytosolic apoptotic proteins such as calpain, calcineurin, and caspases directly responsible for neuronal cell death [42]. Calpains induce striatal-enriched protein tyrosine phosphatase (STEP), activating the p38 mitogen-activated protein kinase pathway, thereby initiating lysosomal membrane rupture, proteolysis and cell death [42]. On the other hand, action of caspases results in proteolysis of deoxyribonucleic acid (DNA)- repairing proteins and degradation of cytoskeletal proteins [42].

Excitotoxicity can also be triggered by a glutamate-independent mechanism in which the shearing and stretching forces in primary injury lead to stress activation of NMDA receptors [41]. This mechanosensitive response is mediated by the GluN2B subunit, which initiates the same cascade as the glutamate-dependent response, facilitating pro-death pathways. The resulting pores in the cell membrane inhibit the action potential generation, so calcium influx is obtained with further exacerbation of direct excitotoxicity [42, 43, 44]. Next to excitotoxic effects, calcium also leads to the generation of free radicals, inducing the development of mitochondrial dysfunction and oxidative stress, which are the most severe forms of secondary brain injury, as explained below [45].

1.2.2. Mitochondrial dysfunction and oxidative stress

Mitochondrial dysfunction and the previously described release of excitatory neurotransmitters are two of the first mechanisms in secondary brain injury leading to neuronal cell death. Increased concentration of calcium ions inside the neurons and consequent excessive mitochondrial

calcium uptake result in generating reactive species and depletion of adenosine triphosphate (ATP) as the main cellular energy source [35, 42]. Elevated levels of intracellular calcium cause the induction of enzymes such as nitric oxide synthase (NOS) and xanthine oxidase, which leads to the production of free radicals. The most common reactive oxygen species (ROS) are superoxide ($O_2^{\cdot-}$) and the hydroxyl (OH^{\cdot}) radical, as well as non-radical species such as hydrogen peroxide. ROS overproduction exceeds the cellular antioxidant capacity and promotes apoptosis by activating pro-apoptotic factors and caspases. Furthermore, the impairment of mitochondrial respiratory oxidative phosphorylation leads to respiration inhibition and aerobic metabolism failure [35, 46].

Conclusively, excitatory neurotransmitter overabundance and high cytosolic and mitochondrial calcium with consecutive release of ROS result in further brain oxygen loss and energy failure. The post-TBI brain is greatly susceptible to these events, due to its high metabolic demands. Mitochondria are the energy carriers of the brain, and their damage in TBI is a direct path to neuronal death, impairing neurological function in TBI patients and leading to long-term disability and morbidity [35, 46]. While emphasis is placed on ROS formation among post-traumatic events, reactive nitrogen species (RNS) also lead to severe, irreversible damage to neuronal cells. The free endogenous product of RNS is NO. In normal circumstances, the cellular antioxidant activity will eliminate reactive species. However, the oxidant-antioxidant balance is disturbed in the injured brain, resulting in oxidative stress [35, 40, 42, 46].

The endogenous antioxidant system consists of different enzymes such as glutathione, glutathione reductase (GR), glutathione peroxidase (GPx), glutathione-S-transferase (GST), catalase (CAT), and superoxide dismutase (SOD). Their main role is to neutralize the effects of ROS and RNS. Imbalance between oxidant-antioxidant effect contributes to increased membranous lipid peroxidation (LP), protein oxidation, DNA breakage, and mitochondrial phosphorylation dysfunction presented as respiratory inhibition. Oxidative stress ultimately results in neuronal cells undergoing apoptosis or necrosis [40, 45]. Peroxiredoxin 6 (PRDX6) is one of the key antioxidant enzymes involved in protecting the cell membrane. During LP, PRDX6 serves as a membrane restorer and stabilizer by activating GPx and acidic calcium-independent phospholipase A2 (PLA2) [47].

Polyunsaturated fatty acids are a part of neuronal, glial, and vascular cells and myelin membranes and, as such, are highly susceptible to peroxidation induced by the hydroxyl radical. The main consequence of LP is the disruption of the membrane ion gradient. The ion pumps are additionally activated to maintain the ion gradient, contributing to calcium cell influx with more energy and glucose consumption. Lastly, the mitochondria are destroyed, leaving

the cell lacking additional energy. A closed circuit of the secondary TBI signalling pathways is created, which is irreversible [41, 48].

1.2.3. Neuroinflammation

Neuroinflammation is mediated by inflammatory cells resident in the brain and immune cells from circulation. The resident inflammatory cells are microglia, which act as the main neuroinflammation initiators upon activation in the injured brain. Microglia represents the macrophages of the brain with the central immune role. On the other hand, circulating inflammatory cells are also recruited in the injured brain due to the primary brain injury and the forces that damage the BBB. These accumulated immune cells, primarily activated microglia, increase the synthesis of inflammatory mediators such as cytokines and chemotactic chemokines, including interleukin 1 beta (IL-1 β), interleukin 6 (IL-6), and tumour necrosis factor alpha (TNF- α) [40]. The released cytokines further contribute to BBB integrity disturbance by inducing the migration of leukocytes to the injury site and disrupting the BBB which additionally increases inflammation [40].

TNF- α activates caspases that induce apoptosis and are also activated by stimulated microglial cells. Furthermore, activated microglia continue to attract inflammatory cells and release various neurotoxic substances such as ROS and glutamate, closing the vicious circle [40, 41]. Chemokines, such as interleukin 8 (IL-8), have a described mechanism in recruiting the leukocytes to the injured tissue. The described cascade leads to cerebral oedema and intracranial hypertension, which are life-threatening conditions [40, 49]. The release of prostaglandins, notably prostaglandin E₂ (PGE₂), leukotrienes, and thromboxanes, which may exert vasoconstrictive effects, along with microvascular obliteration due to leukocyte and platelet adhesion, can further contribute to cerebral oedema and reduced blood flow to the injured brain [50].

1.2.4. Apoptosis

Programmed cell death or apoptosis, in the initial phase after the injury, helps to remove damaged cellular elements, thereby having a protective effect on the brain tissue. However, in pathological conditions of the brain, such as in sTBI, apoptosis can lead to the deterioration of the underlying pathophysiological mechanisms. The apoptosis can be initiated through two core pathways – intrinsic and extrinsic [51].

The primary apoptosis mediators are mitochondria, which initiate several signalling pathways called intrinsic pathways inside injured cells. Damaged mitochondria in sTBI lead to disturbance in signalling pathways, resulting in apoptosis of neural cells with a detrimental effect on the patient's condition [51]. The opening of the mitochondrial permeability transition pore, due to overabundant intracellular calcium accumulation, activates the mitochondrial-mediated pathways. As a result, cytochrome c is released – a pro-apoptotic protein that further interacts with apoptotic protease-activating factor-1 and forms apoptosome. Furthermore, activating a caspase gene family, specifically caspases 3 and 9, leads to DNA fragmentation and apoptosis [42, 49].

On the other hand, extrinsic pathways of apoptotic signalling start by engaging the extracellular ligands TNF and Fas and their attachment to extracellular domains of death receptors. The interaction of these compounds forms a death-inducing signalling complex. As a result, this pathway is also named the “death receptor pathway”, with primary activation of a caspases family as the main executioner of the apoptosis [51].

1.2.5. The brain-blood barrier dysfunction

The function of the BBB is being damaged by both the force action during the primary injury and the development of pathophysiological mechanisms of secondary brain injury. The resulting dysfunction encompasses two biological processes essential for BBB integrity. First, paracellular permeability is impaired due to a loss of tight junction proteins, and second, transcytosis of large molecules through damaged endothelial cells is deregulated. The damaged paracellular permeability results in the influx of immune cells, which usually are restricted from entering the brain and contribute to neuroinflammation. The dysregulated transcytosis results in the influx of larger molecules, such as serum proteins, primarily albumins. The described mechanisms favour the development of brain oedema, a pathological entity associated with high sTBI mortality [52].

Oedema is generated as a result of an increased water accumulation across the brain tissue. There are 2 types of brain oedema: vasogenic oedema following the disruption of the BBB, and cytotoxic oedema caused by ion channel activation with excessive water influx, leading to neuronal cell swelling and worsening the BBB dysfunction, respectively. Untreated brain oedema may result in intracranial hypertension, a life-threatening and usually irreversible condition with impaired CPP and cerebral blood flow (CBF) that contributes to brain herniation and patient death, as described in subsection 1.1.5. [52, 53, 54].

The brain uses oxygen and glucose to maintain its function. All pathophysiological mechanisms described in subsection 1.2. lead to the loss of these two vital supplements with the additional threat of impaired CPP and CBF. Inadequate oxygen supply results in conversion to anaerobic metabolism of the injured brain, further contributing to an increase in lactate level, acidosis, and lack of essential energy [35]. Timely treatment and recognition of these conditions is the only way to prevent the development and progression of the detrimental brain changes.

1.3. MicroRNA

MicroRNAs (miRNAs) are short, noncoding RNA molecules sizing from 22 to 25 nucleotides that regulate post-transcriptional silencing of target genes. They are located in introns of coding genes, noncoding genes or exons, and their location influences their expression. About 50% of miRNAs are transcribed from non-protein coding genes, and the remaining are coded in the introns of coding genes. In the mammalian genome, over 2200 miRNAs have been reported, with more than 1000 located in the human genome. Their activity is critical for normal developmental processes, such as metabolism changes, cell proliferation and programmed cell death, and for the functioning of various tissues and organs, including brain morphogenesis, muscle differentiation, and division of the stem cells. Besides normal physiological processes, the role of miRNAs has been recorded in various diseases. Moreover, miRNAs have been documented in different human cancers and cardiovascular diseases, including cardiac failure, inflammatory and autoimmune diseases, liver and skin conditions, and neurodevelopmental and neurodegenerative states. Among the diseases above, the most important role has been noted in the brain, where miRNAs regulate a substantial proportion of genes specific to neuronal tissue. In the context of complete human genome, microRNAs regulate 1/3 of all expressed genes [55].

1.3.1. Biogenesis of miRNA

MiRNA biogenesis starts with ribonucleic acid (RNA) polymerase II, which transcribes miRNA genes into stem-loop RNA transcripts. The process can be mediated by canonical and non-canonical pathways (Figure 2). RNA binding protein DiGeorge Syndrome Critical Region 8 (DGCR8) and Drosha, a ribonuclease III enzyme, comprise a microprocessor complex and cleave pri-miRNA to form precursor-miRNA (pre-miRNA).

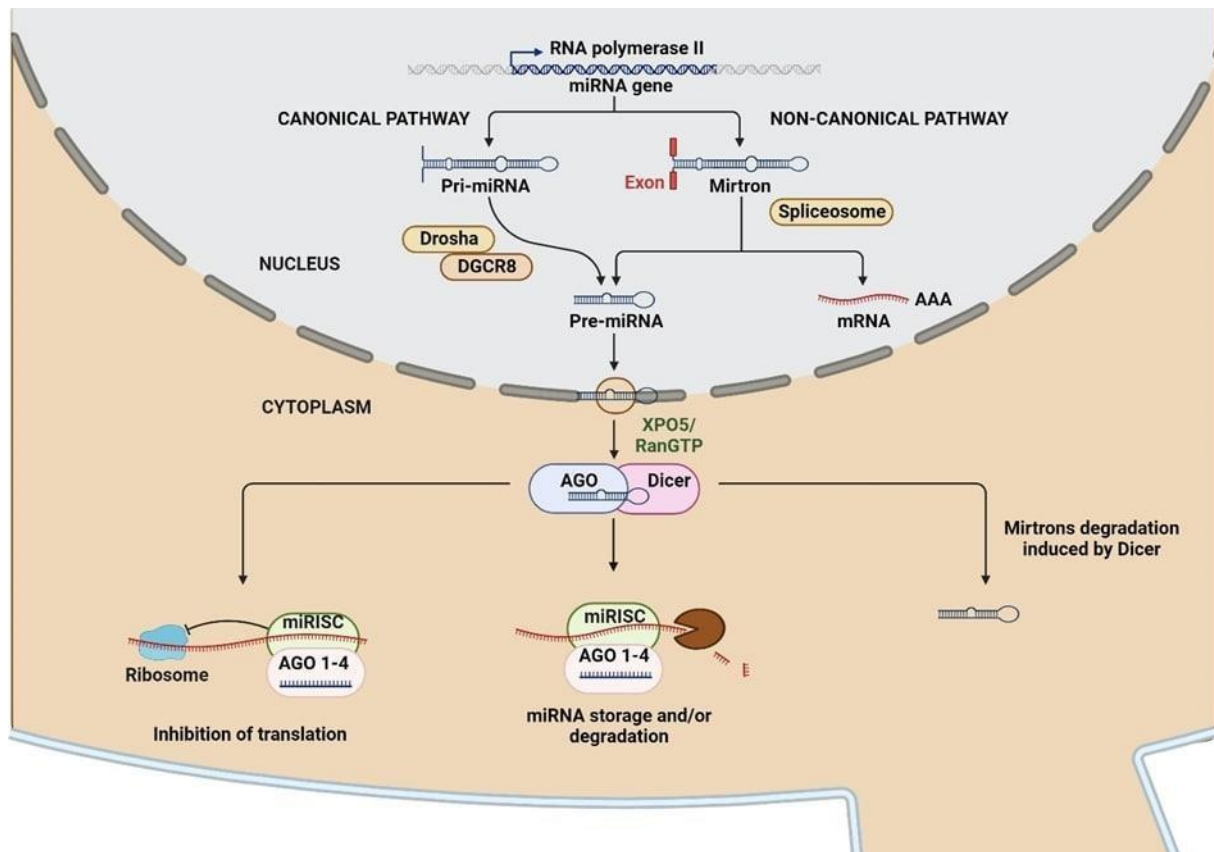


Figure 2. Schematic overview of microRNA (miRNA) biogenesis – Drosha-dependent / Dicer-dependent canonical pathway and Drosha-independent / Dicer-dependent noncanonical pathway. In canonical miRNA pathway, pri-miRNA transcripts are produced from miRNA genes and further processed by Drosha/DGCR8 into pre-miRNAs. In noncanonical pathway, pre-miRNAs are formed by splicing of short introns called mirtron. Pre-miRNAs generated by both pathways are exported to the cytoplasm in Exportin 5 (XPO5)/RanGTP manner and followed by Dicer cleavage. The resulting miRNA duplex is unwound by Argonaute protein family (AGO 1-4) and loaded onto the RNA-induced silencing complex (RISC) forming the miRISC complex. Finally, forming of the miRISC complex is followed by inhibition of translation and miRNA degradation in the cytoplasm. Adapted from “miRNA Processing Mechanisms in the Brain”, by BioRender.com (2023). Retrieved from <https://app.biorender.com/biorender-templates>, May 1st 2024.

After generating pre-miRNAs, this hairpin-shaped RNA is exported in an Exportin5 (XPO5)/RanGTP-dependent manner into the cytoplasm with further downstream exposition to RNase III endonuclease called Dicer. Dicer processes pre-miRNAs by removing the terminal loop and forming the mature 22-25 nucleotide miRNA duplex. From the 5' end, the 5p strand

is derived, and the 3p strand arises from the 3' end. Either the 5p or 3p strands of mature miRNA duplex are loaded into the Argonaute (AGO 1-4) family of proteins in an ATP-dependent manner. This highly conserved and ubiquitously expressed protein family is found in all higher eukaryotes, sharing their names with the band of heroes from Greek mythology, the Argonauts. AGOs can maintain genome integrity, contributing to protein synthesis control and RNA stability. Typically, the strand with lower 5' stability is loaded into AGO and considered a guide strand. After the strand loading, a miRNA-induced silencing complex (miRISC) is formed, and the other strand is usually degraded. The recruitment of AGOs to the miRISC complex gives them a key role in miRNA processing and function on transcriptional and post-transcriptional gene regulation levels as miRISC effector proteins mediating target silencing. On the other hand, overexpression of AGOs induces elevated levels of miRNAs, while low AGO expression reduces their levels. This regulation mechanism is owed to AGOs' protection of miRNAs 3' and 5' ends from exosomes and exonucleases, respectively. The role of mature miRNA is to facilitate the target miRNA cleavage and translational repression [56, 57, 58, 59, 60,61].

Non-classical or non-canonical pathways are less common routes of miRNA biogenesis, and they can be further grouped into Drosha/DGCR8-independent and Dicer-independent pathways. Drosha/DGCR9-independent pathway encompasses the synthesis of mirtrons, forms of pre-miRNAs produced from the introns during spliceosome-induced mRNA splicing [56, 57]. Mirtrons are exported using XPO5/RangGTP directly into the cytoplasm and subsequently cleaved by Dicer. Functional miRNAs are also produced in the Dicer-independent pathway. Such miRNAs originate from endogenous short hairpin RNA (shRNA) precursors, which undergo cleavage by the RNase III enzyme Drosha as part of the primary miRNA processing pathway. Without Dicer to complete the maturation, the pre-miRNAs are loaded into AGO with further slicing of the 3p strand and the final 3'-5' trimming of the 5p strand to complete the maturation. However, the Dicer-independent pathway is a novel pathway not fully elucidated [56].

1.3.2. Mode of action of miRNAs

MiRNAs can bind to a complementary sequence at the 3' untranslated region (UTR) of target mRNAs to induce translational repression or mRNA degradation. Binding to the 5' UTR or coding regions can also influence gene expression, typically through silencing mechanisms such as translational inhibition or destabilization of the mRNA. One miRNA can affect several mRNAs, making its effect potentially powerful. Furthermore, the same mRNA can be a target for different miRNAs, adding another layer of complexity to gene regulation. Moreover, miRNAs can indirectly modulate the expression of multiple genes if their targets are mRNAs encoding transcription

factors or other regulatory proteins [61].

After forming the miRISC and loading within the AGO family, only AGO2 has a dominant role in endonucleolytic cleavage and destruction of target mRNAs. The degree of complementarity between the miRISC complex and target mRNA defines the degree of silencing, called target-mediated miRNA protection. miRNA “seeds” are bases of 2-7 nucleotides in length responsible for the target specificity. The result of the miRISC binding to target mRNAs is destabilization and degradation of mRNA. In the process of inducing the mRNA degradation, the essential factor is the interaction between AGO2 and the GW182 protein family, which are crucial for miRNA-mediated silencing. GW182 directly recruits deadenylase complexes contributing to deadenylation and destabilization of targeted mRNAs [62, 63]. Previous knowledge associates the AGO2- and GW182-dependent recruitment of deadenylase complexes and induction of translational repression mechanism. The interaction of GW182 with poly(A)-binding protein (PABP) and complexes needed for deadenylation, such as Ccr4-NOT and PAN2-PAN3 complexes, is followed by decapping and subsequent mRNA degradation. Translational repression is under debate due to not fully elucidated mechanisms [57, 62, 63].

1.3.3. The role of microRNAs in brain function

The brain is a complex organ with an extensive communication network between neuronal and non-neuronal cells. The notable diversity of brain cells, coupled with the expression of roughly 70% of the known 2500 mammalian mature miRNAs in the human nervous system, indicates that miRNAs may have uniquely significant functions in the brain relative to other organs. Brain miRNAs participate in its development and affect the final neurological functions, including neuronal differentiation, adult neurogenesis and synaptic plasticity, which can be changed in neurological diseases, neurodegenerative disorders, and injuries [64, 65, 66, 67].

The essential function in governing neuronal genesis has been shown for let-7, miR-9, and miR-124 [67]. The synergistic action of miR-9 and miR-124 drives the *in vitro* conversion of adult fibroblasts into neuronal cells due to their interference with the neurogenic transcription factor NEUROD2. These two miRNAs are, therefore, called the master regulators of neuronal differentiation [67, 68]. The miR-9 expression is also associated with suppression of nuclear transcription receptor TLX, characteristically located in the neurogenic regions of the forebrain and retina, where it plays a significant role in balancing cellular processes, such as cell cycle and DNA replication. TLX suppression by miR-9 causes transcriptional repression of TLX downstream target genes and blocks the proliferation of neuronal stem cells. Similarly, to miR-9, Let-7 also controls the proliferation of neuronal stem cells through TLX signalling pathways.

Another miR-9 negative impact on neuronal stem cells is achieved by suppression of highly conserved Notch pathway, a major factor for maintaining neuronal stem cells starting from early embryonic brains. Therefore, miR-9 plays a vital role in brain development. On the other hand, miR-124 functions by downregulating the polypyrimidine tract-binding protein-1 (PTBP1) expression and, thus, regulates the non-canonical alternative pre-miRNA splicing during neuronal development [66, 67]. Furthermore, miR-124 is considered to be the most abundant miRNA in the brain [69].

Further miRNAs impacting neurogenesis and synaptic plasticity include miR-132, miR-134, and miR-138. MiR-132 exerts its neuronal maturation effect by inhibition of p250 GTPase-activating protein (p250GAP), which interacts with GluNR2B subunit of NMDA receptors and is involved in NMDA receptor activity-dependent actin reorganization in dendritic spines. Moreover, miR-132 stimulates NMDA receptors, leading to increased synaptic excitability and calcium influx [66]. By targeting the actin filament growth regulator LIM domain kinase 1 (LIMK1), miR-134 participates in neurogenesis [65, 66]. MiR-138 regulates dendritogenesis by inhibition of acyl protein thioesterase 1 (APT1) or the RNA-binding protein and translational repressor Pumilio 2 (Pum2) [66, 67].

MicroRNAs (miRNAs) are a class of highly conserved non-coding RNAs with 21–25 nucleotides in length and play an important role in regulating gene expression at the posttranscriptional level via base-pairing with complementary sequences of the 3'-untranslated region of the target gene mRNA, leading to either transcript degradation or translation inhibition. In addition to their roles in brain development and physiology, miRNAs have also been detected in neurological conditions, including neurotrauma, Down's syndrome, Alzheimer's disease, Huntington's disease, fragile X syndrome, schizophrenia, Rett syndrome, and autism spectrum disorders. However, the specific contribution of miRNAs to these brain disorders is yet to be elucidated [66, 67, 70].

Brain-enriched miRNAs act as versatile regulators of brain development and function, including neural lineage and subtype determination, neurogenesis, synapse formation and plasticity, neural stem cell proliferation and differentiation, and responses to insults. Herein, we summarize the current knowledge regarding the role of miRNAs in brain development and cerebrovascular pathophysiology. We review recent progress of the miRNA-based mechanisms in neuronal and cerebrovascular development as well as their role in hypoxic-ischemic brain injury. These findings hold great promise, not just for deeper understanding of basic brain biology but also for building new therapeutic strategies for prevention and treatment of pathologies such as cerebral ischemia [67, 68, 70].

1.3.4. Biomarker potential of microRNAs in traumatic brain injury

Circulating miRNAs can be detected in biological fluids, including cerebrospinal fluid, blood, saliva, urine, breast milk, tears, peritoneal fluid, bronchial lavage, seminal fluid, and ovarian follicular fluid. [38, 56]. Therefore, the great interest in miRNA biomarker potential is not surprising, especially in neurology, including TBI, considering that miRNAs regulate many genes in the brain and that a broad spectrum of pathophysiological events evolve during primary and secondary brain injury.

An extensive systematic review and meta-analysis of miRNAs from different human fluids after TBI encompassed 215 TBI patients, 152 controls, and, overall, 44 experiments and listed miRNAs detected in serum, plasma, saliva, brain tissue, blood and urine, albeit with different sensitivity and specificity across the sample types [71]. For example, miR-135b, as a potential sTBI biomarker has shown 75% specificity and 86% sensitivity when isolated post-mortem from cerebellar tissue, but when isolated from saliva, the corresponding percentages were 73% and 20% [71, 72, 73]. Furthermore, miRNA-16, miRNA-92a, and miRNA-765 plasma levels can have sTBI diagnostic power within the first 24 hours after the injury with 100% sensitivity and specificity for discriminating sTBI from healthy volunteers [74]. Elevated serum levels of miR-93, miRNA-191, and miRNA-499 were detected in patients with different TBI in comparison to healthy controls – the 3 miRNAs had higher levels in sTBI patients with poor outcome than in patients with moderate and mild TBI with good outcome [75]. Another study showed that serum levels of the following 6 miRNAs have high brain-specificity: miRNA-124-3p, miRNA-219a-5p, miRNA-9-5p, miRNA-9-3p, miRNA-137, and miRNA-128-3p [76]. Interestingly, these 6 miRNAs have brain-specific functions during neurological development, neurogenesis, and plasticity [66, 67].

Next to commonly analysed plasma and serum samples, human saliva is also easily accessible and was used for miRNA studies in TBI. However, differentially expressed saliva miRNAs of TBI patients greatly varied between studies due to several factors, including miRNA isolation techniques, different injury severity, and broad sampling window ranging from <30 minutes to 14 days post-injury, as recently reviewed [77]. CSF could be a more reliable human sample for brain biomarkers since CSF is in direct contact with the brain and contains molecules secreted from brain cells. However, CSF is accessed by an invasive method, either by sampling intracranial CSF from placed EVD or using the lumbar puncture method, making CSF studies less common. Due to the anatomical distance from the injury site, lumbar CSF might be a less precise source for brain biomarkers. In contrast to lumbar CSF, differential expression of miR-9 and miR-451 was observed in the intracranial CSF of sTBI patients [78]. Furthermore, miR-328, miR-362, miR-486, and miR-451 were significantly upregulated in lumbar CSF of sTBI patients compared to moderate and mild TBI and healthy controls [79]. A microarray-based study of lumbar CSF from sTBI patients detected upregulation of miR-141,

miR-572, miR-181a, miR-27b, miR-483- 5p, miR-30b, miR-1289, miR-431, miR-193b, and miR-499, and downregulation of miR-1297, miR-33b, miR-933 and miR-449b in comparison to healthy controls [80].

Taken together, the characterisation of sTBI biomarkers is challenging due to the colourful palette of pathophysiological mechanisms after sTBI and the heterogeneity of patients, and, on the other hand, due to differences in sample types and sampling time points. Furthermore, miRNAs can circulate in body fluids as free molecules or associated with nanoparticles, affecting the isolation method of choice [38, 78].

1.4. Extracellular vesicles

Extracellular vesicles (EVs) are a family of heterogeneous membrane-enclosed vesicles released by cells. These membranous nanoparticles range in diameter from 20 to 1000 nanometers (nm) with subdivision into small EVs (sEVs) and medium/large EVs (m/IEVs) of a size from 20 to 200 nm and more than 200 nm, respectively [81]. The release of EVs is an essential mediator of intercellular communication since they carry various surface or internalized cargo originating from the parent cell, such as proteins, nucleic acids, and lipids. The composition of EVs reflects the type and condition of the parent cell, with the ability to reprogram the target cell, which can be located very far from the cell of origin. They play critical roles in key physiological functions and are actively secreted during numerous pathological processes, significantly influencing disease progression and tissue response [81, 82].

1.4.1. Overview of extracellular vesicle biogenesis

Based on The Minimal Information for Studies of Extracellular Vesicles 2018 (MISEV 2018) update, EVs are categorized based on their biogenesis pathway into 3 biotypes: exosomes (EXOs), microvesicles (MVs), and apoptotic bodies (APOs) [83]. EXOs are sEVs released from cells in a process of vesicular secretion called exocytosis, which is similar to reverse endocytosis. The whole process is part of the endo-lysosomal system. It starts with forming an early endosome in the cell after the invagination of the cell plasma membrane. Early endosomes mature into late endosomes with intraluminal vesicles (ILVs), also called multivesicular bodies (MVBs). MVBs can fuse with lysosomes for degradation or make connections with plasma membrane to release ILVs into extracellular space known as EXOs (Figure 3).

Numerous proteins participate in the ILV secretion and transport, including endosomal sorting complex (ESCRT) and ESCRT core protein complexes 0, I-, II-, and III-, tumour

susceptibility gene 101 (TSG101), ALG-2 interacting protein X (Alix) and syntenin. Another group of transmembrane proteins, including tetraspanins, such as CD9, CD81, and CD63, mediate the vesicle adhesion. All these proteins, together with ubiquitously expressed membrane-associated proteins flotillin-1 and -2, make a list of over 100 proteins denoted as EXO biomarkers. A more precise classification of EXO protein markers enabling differing EV types still needs to be developed [81, 83, 84, 85, 86]. EXOs have been isolated from different body fluids, including blood, CSF, saliva, urine, breast milk, semen, and amniotic fluid. Owing to their specimen diversity, they have emerging importance in physiological and pathological processes in all human tissues as cargo carriers of different components, including miRNAs [85, 87].

In contrast to EXOs, MVs are shed by outward budding and pinching of the plasma membrane. They have irregular shape and range in size between 100 and 1000 nm.

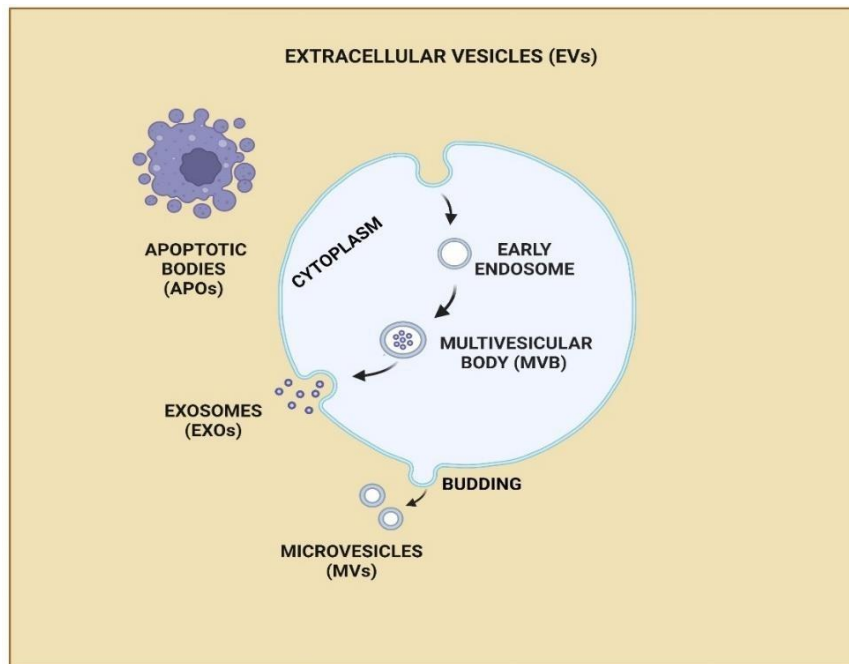


Figure 3. Biotypes of extracellular vesicles (EVs). Exosomes (EXOs) are formed within the endosomal network and released after the fusion of multivesicular bodies (MVBs) with the plasma membrane. Microvesicles (MVs) are produced by outward budding of the membrane. Apoptotic bodies (APOs) are the largest EVs formed by blebbing during the apoptosis.

The mechanism of MV formation has yet to be fully understood, but current knowledge indicates that MV biogenesis usually requires an intracellular calcium influx. Calcium activates the floppase protein family and scramblase enzyme family, resulting in the asymmetry of the plasma membrane as a critical factor for MV formation. Asymmetry is further stimulated by the action of calpain and disruption of membrane and cell cytoskeleton anchorages [81, 87].

The largest EVs are APOs, a group of subcellular membrane-bound vesicles generated during the programmed cell death. The APO formation starts with cell rounding and shrinkage accompanied by membrane detaching and blebbing, which results in membrane protrusions known as apoptopodia. They often contain different organelles and nuclear contents in their lumen, but biogenesis mechanisms are less known compared to EXOs and MVs [81]. During the process of apoptosis, phosphatidylserine is transported to the membrane surface, providing one of the APO characteristics. The translocated PS binds to Annexin V. Annexin V is defined as a phospholipid-binding protein and is primarily used as an APO biomarker. Next

to the translocation of PS, thrombospondin and the complement protein C3b are bound to the membrane and can also be used as APO biomarkers [88, 89].

1.4.2. Isolation, characterisation and quantification of extracellular vesicles (EVs) – what do the guidelines say?

EVs can be detected in numerous body fluids and have different biophysical characteristics, from size and density to cargo composition. The above defines them as a heterogeneous population that is challenging to separate from other particles and molecules. Further challenges derive from the fact that biological fluids differ in their content and EV concentration. For example, plasma and serum contain non-EV lipid structures, such as lipoproteins, that can interfere with EV separation. Other parameters with a significant effect on EV isolation include technical details in sampling such as volume of collected fluid, discarding of the first tube, type of container, choice of anticoagulant, storage and processing with the degree of haemolysis, and therefore, must be clearly defined before the sampling [83].

The most used methods for EV isolation are differential ultracentrifugation, density gradients, precipitations, filtration, size exclusion chromatography (SEC), and immunoisolation with the constant development of breakthrough techniques and modifications in this highly dynamic research field [83]. Each method is based on different physical and chemical properties, resulting in diverse quantity and quality of isolated EVs. SEC is increasingly recognised as an EV isolation method that can deliver total and well-preserved EVs [90]. However, the scientific community has yet to reach a consensus about EV isolation methods, making the results from different EV studies difficult to compare due to differences in protocols for EV isolation.

MISEV 2018 guidelines recommend characterizing EVs by at least three protein markers, of which at least one is a transmembrane protein such as tetraspanins (CD63, CD81, CD82), integrins, MHC class 1, or transferrin receptor, and one is a cytosolic protein such as TSG101, Alix, flotillins-1 and -2 or heat shock proteins. Next, one negative protein marker should be included, usually a lipoprotein abundant in plasma and serum (apolipoproteins A1/A1 and B or albumin). Western blot is the most commonly used method for EV protein characterization with increasing use of mass spectrometry [83]. Finding the protein suitable for EV isolation is demanding, as shown in the L1CAM example. The transmembrane protein L1CAM was believed to be the ideal candidate marker for neuron-derived EVs that can be detected in human plasma and CSF. However, a more careful study has shown that L1CAM is also present in the blood as a cleaved by-product not associated with EVs [91].

EV quantification is also achieved by various methods, whereby the most commonly used techniques are nanoparticle tracking analysis (NTA), standard flow cytometry for IEVs, high-resolution flow cytometry for sEVs, tunable resistive pulse sensing (TRPS) for a wide range of sizes or some other similar techniques [83]. Similarly, to EV isolation methods, EV quantification is based on different physical principles, resulting in various reproducibility and precision.

In conclusion, EVs offer a lot of information about physiological and pathological events in the human body, but their usage in diagnostics and prognostics is hampered by the demanding purification, characterization and quantification. Therefore, it is imperative to continue research in this area and gain new knowledge that can be implemented into the clinical practice of various medical branches.

1.4.3. Extracellular vesicles and severe traumatic brain injury

The BBB represents a selectively permeable membrane built by brain microvascular endothelial cells that form a dense brain vascular network and connect CNS with the peripheral circulatory system. EVs can pass through all biological barriers, including the BBB, and are considered as a precious source of information about brain events, especially in conditions with BBB failure such as sTBI due to many EV properties, including the ability to cross the BBB, the role as intercellular communication mediators, low immunogenicity, high stability, and a long half-life [92]. EVs can pass in both ways through the disrupted BBB; from CNS to the peripheral circulation and vice versa. The latter enables the detection of EVs in blood samples and, paves the way towards liquid biopsy for biomarker studies [93]. However, CSF stands out as a particularly suitable source of biomarkers due to its close connection to the injury side. EVs isolated from CSF can reflect changes during the sTBI and carry molecular cargo that could reveal biochemical brain changes [94].

Typical sTBI pathophysiology includes many detrimental events, such as neuroinflammation, axonal shredding, and neurodegeneration with long-term sequels. The current opinion is that all CNS cells can produce EVs and play a role in the sTBI processes mentioned above [95]. The studies of EV roles in sTBI were mainly conducted in animal (rat) models and only a few studies involved sTBI patients [93]. EVs can change in CSF after sTBI and their cargo includes miRNA molecules [78, 96]. Furthermore, CSF from sTBI patients contains inflammasomes with proteins that regulate the activation of caspase 1 and the maturation of the pro-inflammatory cytokines IL-1 β and IL-18 into their active form [97]. Our group has demonstrated that EVs isolated from CSF of sTBI patients change their size, number and protein composition during the acute phase of recovery [98].

Taken together, EVs in sTBI might derive from various cells and reflect different processes associated with pathophysiology or recovery.

1.4.4. MicroRNA as cargo of extracellular vesicles after severe traumatic brain injury

Different subpopulations of RNA, including miRNAs, can circulate as extracellular RNAs in biofluids, such as blood and CSF. While miRNAs act intracellularly, their extracellular forms are part of intercellular communication. The extracellular miRNAs are protected from enzymes as encapsulated cargo of EVs or by forming complexes with non-EV particles, such as AGO2 proteins or lipoproteins. Very little is known about the latter mechanism of cell-to-cell communication. Conclusively, a small fraction of extracellular miRNAs protected in EVs can be considered as potentially valuable biomarkers [99, 100].

Several studies have investigated the presence of miRNA in CSF-derived EVs after the sTBI. Brain EVs derived from sTBI rat models after the controlled cortical impact contained miR-146, miR-7a, miR-21, and miR-7b with the highest change of miR-21 leading to proposing miR-21 as a cargo of neuron-derived EVs since increased levels were simultaneously detected in neurons near the injury onset [101]. MiRNA sequencing of brain-derived GluR2+ EVs in rat and human TBI identified eight miRNAs (miR-150-5p, miR-669c-5p, miR-488-3p, miR-22-5p, miR-9-5p, miR-6236, miR-219a.2-3p and miR-351-3p) in rat and four miRNAs (miR-203b, miR-203a-3p, miR-206, and miR-185-5p) in humans with a biomarker potential [71, 102]. Another study of rat sTBI detected miR-124-3p in brain tissue-derived EVs from activated microglia cells [103]. Astrocyte-derived EVs extracted from the rat brain tissue after injury contained miR-873a-5p, also detected in patients with sTBI [104].

In conclusion, research of EV-associated miRNAs in sTBI is in its infancy, although several approaches have been applied, including animal models and post-mortem brain tissue samples. Indeed, the intracranial CSF accessible if EVD is indicated for patient management, represents one of the most promising approaches to detect miRNAs with biomarker potential. However, difficulties in obtaining these precious human samples and challenges in EV isolation and characterisation still slow the research. Therefore, standardization of sample processing is sought to improve the diagnosis, management and neurorecovery of sTBI patients by identifying reliable biomarkers with results that can be repeated in different clinical settings with high specificity and sensitivity [93].

2. RESEARCH OBJECTIVES

Despite occupying the attention of neuroscientists worldwide, a unique, sensitive, and specific marker of brain events during severe traumatic brain injury (sTBI) has not yet been elucidated. Our understanding about the brain events during the injury has broadened substantially, therefore microRNA (miRNA), showing significant expression in a brain-specific and brain-enriched manner, have been proposed as a potentially valuable biomarker.

The research is based on the hypothesis that extracellular miRNAs have the potential to convey valuable biological information regarding the biochemical events during the early phase of neurorecovery following sTBI. However, the isolation and characterization of EVs represents a challenging step during experimental work. Our group has explored alterations in EVs regarding size, concentration and protein composition in sTBI patients compared to healthy individuals, revealing the dynamics of the process with the role of EVs in the early phase of neurorecovery. Additionally, to implement new knowledge in the EVs purification process, the more effective size-exclusion chromatography (SEC) method was established using a Sepharose CL-6B column.

All of the aforementioned, along with the successes of our group's work so far, encouraged us to include miRNAs as potentially valuable biomarker of sTBI in further work, especially knowing the fact that sTBI is still a common cause of morbidity and mortality in the population.

To test our assumed hypothesis, further goals were set:

1. To detect and quantify miRNAs in CSF samples after creating the biobank;
2. To separate CSF into extracellular vesicle (EV) and free protein (FP) enriched fractions by SEC method;
3. To detect and quantify miRNAs in EV- and FP-enriched fractions;
4. To identify miRNAs with biomarker potential, define CSF collection time points, and establish optimal isolation method.

3. SUBJECTS AND METHODS

3.1. Subjects

The research included patients with severe traumatic brain injury (sTBI) treated at the Anaesthesiology, Intensive Medicine and Pain Treatment Clinic at Clinical Hospital Centre Rijeka or the Clinic for Anaesthesia, Reanimation, Intensive Care Medicine and Pain Treatment at Pula General Hospital, Croatia. The study was approved by Ethics Committee of Clinical Hospital Center Rijeka (class: 003-05/19-1/57, registry number: 2170-29-02/1-19-2), Ethics Committee of Pula General Hospital (registry number: 4943/19-1), and Ethics Committee for biomedical research at Faculty of Medicine, University of Rijeka (class: 007- 08/22-01/61, registry number: 2170-24-04-3/1-22-3). The sTBI patients were enrolled in the study after a family member or patient's legal representative signed the informed consent due to the patient's altered state of consciousness and intensivist treatment with analgosedation. The study team member explained all the details about the research goals, sampling procedure, and possible dangers of the study before signing the consent.

The study did not include patients older than 80 years, nor the population younger than 18 years of age. Patients with acute or chronic inflammatory, malignant, and autoimmune conditions were also excluded from a study.

The diagnosis of sTBI was established by a standard procedure that included a physical examination consisting of a neurological assessment of consciousness using the Glasgow Coma Scale (GCS) total score. According to GCS, brain injury was considered severe if the total score was ≤ 8 (Table 1). The diagnosis was confirmed by brain computed tomography (CT) as the standard neuroradiological method for emergency diagnosis [7, 8].

After the initial assessment and confirmation of the brain pathoanatomical changes using CT, sTBI patients were further treated using intensive measures according to the current guidelines and following the usual protocol for sTBI treatment [28]. If indicated, the attending neurosurgeon placed the external ventricular drain (EVD) under general, balanced anaesthesia. The EVD system enables the monitoring of the intracranial pressure (ICP) values in the brain ventricles, as well as CSF drainage if the ICP values are above those set by the guidelines, or if there are signs of patient's neurological deterioration after pupil examination.

Analgosedation was achieved using benzodiazepines, primarily midazolam and opioids, standardly sufentanyl with head raised by bed position at 30°. Before the surgical procedure, the patients were orotracheally intubated with an endotracheal tube and put on protective mechanical ventilation. Protective mechanical ventilation was maintained using ventilation machines, which were adjusted to inspiration volume from 4-8 mL/kg of the patient's predictive

body weight. Positive end-expiratory pressure was set at lower values from 4 to 6 kPa, along with maintaining the peak pressure in the airways lower than 30 cmH₂O. Normocarbica was maintained at values from 35 to 45 mmHg, saturation of peripheral arterial blood greater than 95% with inhaled oxygen of ≥ 0.4 . Central venous catheter and intra-arterial cannula were placed to enable volume optimization and monitor the value of the mean arterial pressure (MAP), respectively. The clinical procedure included infusion of intravenous crystalloids and haemodynamic medications, primarily noradrenaline, to achieve the target values of systolic blood pressure and MAP as set by the current guidelines. The main goal of target MAP values >100-110 mmHg was to maintain the cerebral perfusion pressure (CPP) within range of 60 and 70 mmHg [28]. Additionally, urinary catheter and an orogastric tube were placed.

Continuous 24-hour monitoring of vital functions included aforementioned monitoring and management of MAP and, furthermore, measurement of body temperature, diuresis, and ICP values with maintenance of normothermia as well as normoglycemia. An increase in ICP above 20 mmHg was treated with conventional methods such as additional sedation, mild hyperventilation, CSF drainage, and hyperosmolar medications - specifically mannitol to reduce brain oedema. According to the guidelines, patients also received antibiotic therapy and prophylaxis for deep vein thrombosis. Nutritional support was started within the first 5 days after injury onset.

3.2. Materials

3.2.1. Chemicals, cell culture and molecular biology reagents and materials

Chemicals and reagents used in this work are listed in Table 3.

Table 3. Chemicals and reagents used in the study.

Chemical/Reagent	Producer (Location)
2-Mercaptoethanol	Sigma-Aldrich, St. Louis, MO, USA
Acetic acid	Kemika, Zagreb, Croatia
Bovine serum albumin (BSA)	Cell Signaling Technology, Danvers, MA, USA
Bromophenol blue	Sigma-Aldrich, St. Louis, MO, USA
Ethanol (96–100%)	Sigma-Aldrich, St. Louis, MO, USA
Glycerol	Sigma-Aldrich, St. Louis, MO, USA
Glycine	Carl Roth, Karlsruhe, Germany

Hydrochloric acid (HCl)	Kemika, Zagreb, Croatia
Isopropyl alcohol (99.9%)	Kemika, Zagreb, Croatia
L-Glutamine	Gibco, Gaithersburg, MD, USA
Methanol	Kemika, Zagreb, Croatia
Polysorbate 20 (Tween® 20)	Sigma-Aldrich, St. Louis, MO, USA
Ponceau S	Sigma-Aldrich, St. Louis, MO, USA
Sodium dodecyl sulfate (SDS)	Sigma-Aldrich, St. Louis, MO, USA
Sodium chloride	Kemika, Zagreb, Croatia
Tris base	Sigma-Aldrich, St. Louis, MO, USA
Bisacryl-P (30%, 29:1)	Thermo Fisher Scientific, Kandel, Germany
Phosphate-buffered saline (PBS), sterile	Life Technologies, Grand Island, NY, USA
Nitrocellulose membrane, 0.2 µm	Global Life Sciences Solutions, Little Chalfont, UK
Prestained protein ladder (PageRuler™)	Thermo Scientific, Waltham, MA, USA
SignalFire™ Plus ECL Reagent	Cell Signaling Technology, Danvers, MA, USA
SignalFire™ Elite ECL Reagent	Cell Signaling Technology, Danvers, MA, USA
Sepharose CL-6B®	GE Healthcare Bio-Sciences AB, Uppsala, Sweden
Bio-Rad column	Bio-Rad Laboratories, Hercules, CA, USA
Blotting Grade Blocker (nonfat dry milk)	Santa Cruz Biotechnology, Dallas, TX, USA
Carboxylated polystyrene beads, 200 nm (CPC200®)	Izon Science, Christchurch, New Zealand
DMEM	Gibco, Thermo Fisher Scientific, Waltham, MA, USA
Fetal bovine serum (FBS Standard)	PAN-Biotech, Aidenbach, Germany
Penicillin-Streptomycin	PAN-Biotech, Aidenbach, Germany

3.2.2. Solutions

Solutions used in this work are listed below.

Laemmli buffer for SDS-PAGE (5x)

1M Tris HCl pH 6.8, 50% glycerol (v/v), 10% SDS (w/v), 0.05% bromophenol blue (w/v), 2-mercaptoethanol

Laemmli buffer for slot-blot analysis (5x)

1M Tris HCl pH 6.8, 10% SDS (w/v), 0.05% bromophenol blue (w/v), 2-mercaptoethanol

Running buffer for SDS-PAGE (1x)

25 mM Tris, 192 mM glycine, 0.1% SDS, pH 8.3

Transfer buffer for western blot (1x)

25 mM Tris, 192 mM glycine, 20% methanol

Tris buffered saline (TBS)

20 mM Tris, 150 mM NaCl

Antibody blocking solution

5% milk in TBS

TBS-T buffer

5% BSA, 0.1% Tween 20 in TBS

Ponceau S staining solution

0.1% Ponceaus S in 5% acetic acid

3.2.3. miRNA isolation and quantification kits and reagents

Commercial kits, buffers and other materials used in this study are listed in Table 4.

Table 4. Commercially available reagents and kits for miRNA profiling.

Reagent name	Producer
Norgen's Urine microRNA Purification Kit®	Norgen Biotek Corp., Thorold, ON, Canada
miRNeasy Serum/Plasma Advanced Kit®	Qiagen Sciences, Germantown, MD, USA

miRCURY Locked Nucleic Acid (LNA) RT Kit®	Qiagen Sciences, Germantown, MD, USA
RNA isolation spike-in mix (UniSp2®, UniSp4®, UniSp5®, cel-miR-39-3p®, Qiagen RNA Spike-In Kit, For RT®),	Qiagen Sciences, Germantown, MD, USA
miRCURY LNA SYBR Green PCR Kit®	Qiagen Sciences, Germantown, MD, USA
miRCURY microRNA QC PCR Panel®	Qiagen Sciences, Germantown, MD, USA
miRCURY LNA Human CSF Exosome Focus miRNA PCR Panel®	Qiagen Sciences, Germantown, MD, USA

3.2.4. Antibodies

All applied antibodies were manufactured by Cell Signalling Technology, Danvers, MA, USA with the exception of antibody for PRDX5. The antibody type and specificity are listed in Table 5.

Table 5. Antibodies applied in the study.

Antibody
mouse monoclonal antibody anti-human apolipoprotein A1
rabbit monoclonal antibody anti-human albumin
rabbit monoclonal antibody anti-human apolipoprotein E
rabbit monoclonal antibody anti-human CD9
rabbit monoclonal antibody anti-human CD81
rabbit monoclonal antibody anti-human Flotilin-1
rabbit monoclonal antibody anti-human Flotilin-2
rabbit monoclonal antibody anti-human TSG101
anti-mouse horseradish peroxidase-linked antibody
anti-rabbit horseradish peroxidase-linked antibody
rabbit monoclonal antibody anti-human PRDX1
rabbit monoclonal antibody anti-human PRDX2
rabbit monoclonal antibody anti-human PRDX6
rabbit monoclonal antibody anti-human PRDX5

3.3. Methods

3.3.1. CSF collection and pooling

Samples were collected according to bioethical standards, including protecting the confidential data of patients involved in the research to ensure medical privacy. The research was conducted according to the Nuremberg Code, the latest revision of the Declaration of Helsinki, and other internationally recognized ethical guidelines, resulting in adherence to all applicable ethical and bioethical principles – beneficence, non-maleficence, autonomy, and justice, as well as those derived from them (privacy and trust) [105, 106, 107] The CSF samples were obtained from an EVD system placed in the lateral chamber of the cerebral ventricular system. The external part of the EVD system contained two possible accesses for obtaining the CSF: 1) a valve positioned in the line proximally to the head and enabling CSF aspiration and 2) a distal sterile chamber for collecting freely drained CSF. When possible, samples of up to 1.5 ml were collected by direct and careful aspiration from the valve when there were no sampling-associated hurdles such as difficult aspiration or appearance of blood and the brain tissue. The remaining sample volume was collected from the sterile drainage chamber, which drained freely in 24 hours. Sampling was done every 24 hours for 12 days after the injury onset or while there was an indication for ICP management using EVD. After collection into the low-protein binding tubes (*Eppendorf*, Hamburg, Germany), samples were transported on ice and stored in freezers at -80°C until use.

Before the analysis, the individual CSF samples were thawed and combined in equal volumes to generate the predefined CSF pools. The CSF pools were designed based on collected individual samples and aimed to obtain successive CSF pools with a comparable number of individual samples. Individual CSF samples collected at indicated days (d) were combined into the following CSF pools to study temporal changes in CSF composition: d1-2, d3-4, d5-6, and d7-12 containing 10, 9, 8 and 9 individual samples from the indicated period, respectively.

3.3.2. Cell culture

The cell lines U-87 and SH-SY5Y were propagated in cell culture plastic dishes with a diameter of 100 mm and flasks with a surface of 25 cm², respectively. They were grown in a complete 10% DMEM medium at 37°C in humid conditions with 5% carbon dioxide and passaged every three days to maintain confluency up to 80%.

3.3.3. Western blot

An aliquot of 20 µl of CSF pool was combined with 5x Laemmli buffer, denatured at 95°C

for 10 minutes and loaded on 12% SDS polyacrylamide gel. Electrophoresis was run in 1x running buffer by using a mini electrophoresis chamber (MiniVE SE 300, Hoefer, Holliston, MA, USA) at 90 V for 30 minutes, at 150 V for approximately 1.5 hours. Separated proteins were transferred by wet transfer onto a nitrocellulose membrane (*Global Life Sciences Solutions Operations UK Ltd.*, Little Chalfont, UK). The transfer was carried out in the transfer buffer at 70 V for an hour and a half in a mini transfer system (Mini Trans-Blot® Cell, Bio-Rad, Hercules, California, USA) with cooling.

After the completion of protein transfer, the membrane was stained with the Ponceau S solution, incubated with the antibody-blocking solution for 15 minutes and washed with TBS buffer. Next, the membrane was incubated overnight with the primary antibody diluted 1:1000 in the TBS-T buffer at 4°C; these conditions were applied for all primary antibodies as per manufacturer's instructions. The membrane was washed three times for 5 minutes in TBS-T the next day and incubated with a horseradish peroxidase-labelled secondary antibody for 30 minutes at 4°C. After incubation, the membrane was washed in TBS-T buffer three times. Applying SignalFire Plus ECL Reagent® or SignalFire Elite ECL Reagent® to the membrane produced a chemiluminescence signal, and a charge-coupled device (CCD) ImageQuant LAS 500® (*GE Healthcare Bio-Sciences AB*, Uppsala, Sweden) was used to create the image.

3.3.4. Size-exclusion chromatography

The size-exclusion chromatography (SEC) was performed with CSF pools by using a 1.5 × 50 cm glass column (*Bio-Rad Laboratories*, Hercules, CA, USA) filled with Sepharose CL-6B (*GE Healthcare*, Uppsala, Sweden) and applying the gravity flow protocol previously established by our group [89]. Briefly, the column closed with a 30 µm frit at the bottom and equipped with a flow adaptor (*Bio-Rad Laboratories*, Hercules, CA, USA) at the top was packed with Sepharose CL-6B by applying distilled water and washed with a minimum of 3 bed volumes of sterile PBS before the first run.

The CSF pools were created by combining equal CSF volumes from five sTBI patients. The CSF pool of 4 mL was loaded onto the column using a 5 mL sterile plastic syringe. The SEC was conducted by a gravity flow using the sterile PBS positioned above the column at room temperature. From each run, 46 fractions of 1.5 mL were collected in low-protein binding tubes (*Eppendorf*, Hamburg, Germany). The column was washed at least with 2 bed volumes of PBS between each SEC run.

3.3.5. Slot blot

SEC fractions were mixed with 5x Laemmli buffer without glycerol and incubated at 95°C for 10 minutes to enable detection of targeted proteins. Nitrocellulose membrane (*GE Healthcare Life Science*, Uppsala, Sweden) previously soaked in distilled water was inserted into the slot blot device (*Hoefler Scientific Instruments*, San Francisco, CA, USA). A volume of 300 µL of SEC fractions per slot was applied using a vacuum pump. Each slot was rinsed three times with 1 mL of sterile PBS. After removing from the slot blot device, the membrane was stained with Ponceau S and incubated with 5% milk in TBS to block non-specific binding. The incubation with antibodies and detection of the chemiluminescence signal was performed as previously described for the western blot protocol.

3.3.6. Tunable resistive pulse sensing (TRPS)

Tunable resistive pulse sensing (TRPS) was used to measure the concentration and size of nanoparticles in the CD81+ pool of SEC fractions, as CD81 is a ubiquitous protein marker for EVs and has been shown in our previous studies to be commonly present in CSF after TBI, making it useful for detecting SEC fractions enriched in EVs [90]. Using a qNano Gold instrument, NP400 nanopores, and Control Suite v3.4 software, the measurement was performed according to the manufacturer (*Izon Science*, Christchurch, New Zealand). The nanopore was wetted, coated, and equilibrated using the Izon reagent kit. Calibration runs were conducted with 200 nm carboxylated polystyrene beads, diluted 500-fold in filtered electrolyte solution provided by the manufacturer. Nanopore stretch and voltage were adjusted to detect particles in the 100 to 420 nm diameter range with a constant 46.00 mm stretch and maintaining baseline current at approximately 125 nA. Fractions were diluted 2-fold in a filtered electrolyte solution and vortexed for 30 seconds before measurement in triplicates at 2 pressure steps of 2.5 and 5 mbar. The nanopore was washed with the provided electrolyte solution at a pressure of 20 mbar between each sample measurement to avoid cross-contamination between samples. At least 500 particles were detected during measurement at both pressure conditions after 5 minutes of recording and stated as TRPS-positive fractions. Recordings with less than 500 nanoparticles during 5 minutes were considered TRPS-negative fractions.

3.3.7. RNA isolation and quantification

In the optimization phase, a testing ribonucleic acid (RNA) isolation was performed to compare Quiagen's miRNeasy Serum/Plasma Advanced Kit® and Norgen's Urine microRNA Purification Kit®. These two manufacturers were chosen based on the comparative methodical study showing that the kits above have the highest efficiency in RNA isolation with the

possibility of using on CSF samples [104, 105]. RNA isolation was performed according to the manufacturer's instructions. Quantification determination of RNA concentration was performed using spectrophotometer (NanoPhotometer® P-330, Implen GmbH, Munich, Germany).

3.3.8. Synthesis of complementary DNA (cDNA)

Synthesis of complementary DNA (cDNA) was performed using MiRCURY Locked Nucleic Acid (LNA) RT Kit® according to the manufacturer's instructions. Briefly, the isolated RNA from CSF pools, EV- and FP- enriched SEC fractions in the amount of 20 ng, was reverse transcribed in 20 µL reactions with a thermal cycler (Applied Biosystems, Singapore, Singapore). Before the cDNA synthesis, the following miRNA spike-ins were added to reactions: UniSp2®, UniSp4®, Unisp5®, and cel-miR-39-3p® provided with miRNA spike-in kit, as well as UniSp6® provided by MiRCURY Locked Nucleic Acid (LNA) RT Kit®. All RNA spike-ins were added in amounts recommended by the producer to enable quality control and quantification of targeted miRNAs.

3.3.9. Real-time polymerase chain reaction (RT-PCR)

Each cDNA was first tested for quality using the polymerase chain reaction (PCR) - based quality control (QC) array (MiRCURY microRNA QC PCR Panel®) according to manufacturer's instructions. Briefly, an aliquot containing 1/10 of the total cDNA was applied on the above QC array based on a 96-well plate with 12-well strips. If the cDNA met the quality requirements, the rest was applied to quantify targeted miRNAs. MiRNA profiling and quantification were conducted using a 96-well plate PCR-based array (MiRCURY LNA Human CSF Exosome Focus miRNA PCR Panel®) and a real-time (RT) PCR machine (7300 real-time PCR system, *Applied Biosystems*, Singapore, Singapore). The Ct values of miRNA spike-ins were used to create a base curve from which amounts of targeted miRNAs were calculated.

3.3.10. Statistical analysis

Statistical analysis was conducted using GraphPad Prism 9 (version 9.5.1., *GraphPad software Inc.*, San Diego, CA, USA). Shapiro-Wilk test was performed to assess the normality of data distribution, after which a one-way ANOVA was applied for several independent groups using a post-hoc Tukey test. Values with $p < 0.05$ were considered as statistically significant.

3.3.11. Figures and tables

Figures were created using the BioRender application (<https://www.biorender.com> - BioRender.com) and Microsoft Excel (Microsoft Corporation, Redmond, WA, USA).

Tables were created using Microsoft Excel (Microsoft Corporation, Redmond, WA, USA).

4. RESULTS

4.1. Clinical characteristics of severe traumatic brain injury patients

The research included 5 patients who suffered from severe traumatic brain injury (sTBI) and whose initial treatment required placing the external ventricular drain (EVD) on the indication of attending neurosurgeon. The EVD was used to drain cerebrospinal fluid (CSF) drainage and manage intracranial pressure (ICP). Clinical diagnosis was established based on physical examination, neuroradiological diagnostics, and the Glasgow Coma Scale (GCS). The GCS upon admission in all patients was ≤ 8 , confirming the diagnosis of sTBI. CSF samples were obtained from four males and one female patient without assuming gender influence on treatment outcomes and research results. The age ranged from 19 to 49 years, with a median of 33 years. The outcome of the three-month treatment was monitored using the Glasgow Outcome Scale (GOS). All but one patient had satisfactory outcomes with a GOS score of 4 and 5 (Table 6).

Table 6. Characteristics of sTBI patients included in the study.

Patient	Gender	Age	Mechanism of injury	GCS ¹	Pathoanatomical characteristics of sTBI	GOS ²
1	M	44	Fall from height	5	Epidural haematoma	4
2	F	49	Motor vehicle accident	5	Intracerebral and subdural haematoma	4
3	M	33	Pedestrian in a traffic motor accident	3	Subdural haematoma, focal brain injury (frontal, temporal, occipital)	4
4	M	24	Motor vehicle accident	5	Diffuse axonal injury	5
5	M	19	Fall from height	3	Subdural haematoma, subarachnoid haemorrhage	1

GCS¹ – Glasgow Coma Scale score at admission, **GOS²** – Glasgow Outcome Scale score three months after discharge from hospital.

Structural changes and pathoanatomical characteristics of sTBI were determined based on neuroradiological findings. Traumatic subarachnoid haemorrhage (SAH) was present in three sTBI patients, thus making it the most common intracranial pathology. In two of three patients with SAH, the injury was combined with other structural brain changes. The remaining brain injuries included isolated diffuse axonal injury (DAI) in one patient, intracranial haemorrhage combined with SAH in 1 patient, subdural haemorrhage (SDH) combined with SAH in 1 patient, and isolated epidural haematoma (EDH) in 1 patient (Table 6).

4.2. Dynamics of intracranial CSF molecular content in acute phase of sTBI patient recovery

4.2.1. CSF biobank is created from samples collected during 12 days after the injury

To better understand the molecular profile 35 CSF samples were collected from 5 sTBI patients every 24 hours. The collection was carried out within 12 days from the injury occurrence and EVD placement (Figure 4A). Sampling was stopped after clinical indication for EVD removal or the patient's fatal outcome. To facilitate the analysis, CSF samples were organized into 4 pools – days (d) 1 and 2 (d1–2), which consisted of 10 individual samples; d3–4, which consisted of 9 individual samples; d5–6 with 7 individual samples; and finally, d7–12 with 9 individual samples (Figure 4B). Thus, each pool consisted of a comparable number of individual CSF samples but showed a decreasing amount of blood contamination (Figure 4C).

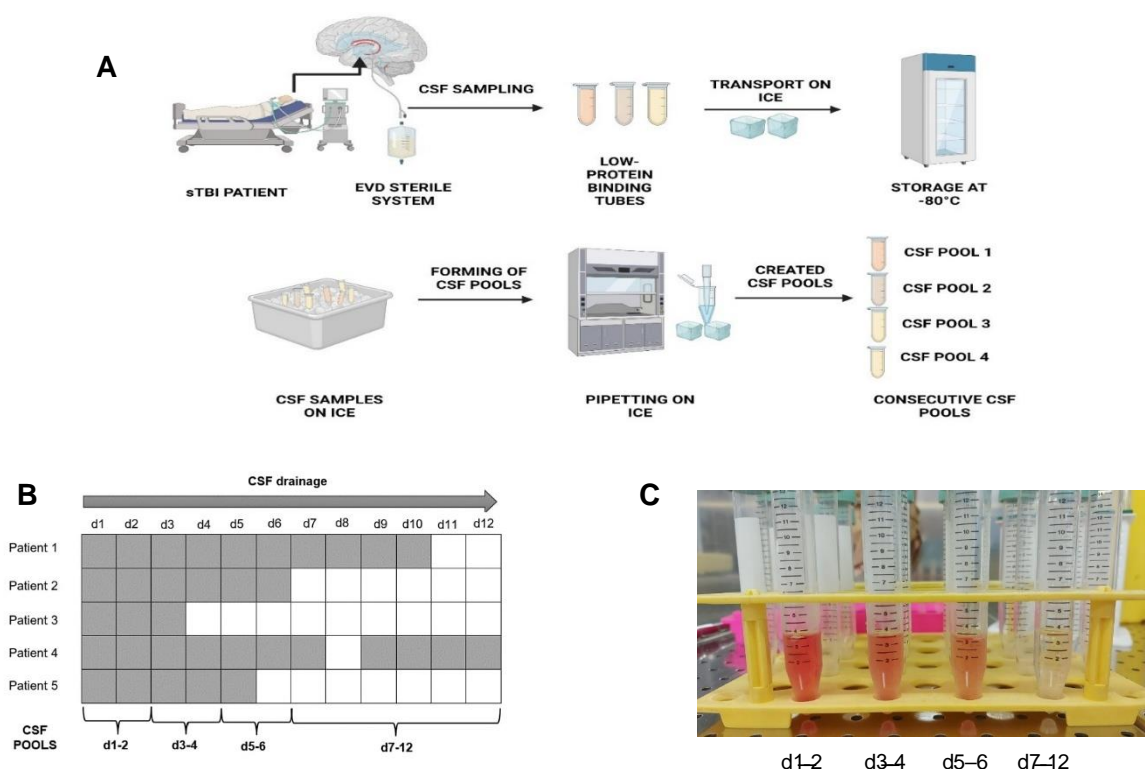


Figure 4. Creation of a CSF biobank from sTBI patients.

Following the collection of 35 cerebrospinal fluid (CSF) samples up to a maximum 12 days after the injury, four successive CSF pools were formed with macroscopically seen blood in the early stages following the injury. **(A)** An overview of the process of CSF sampling, storage, and pooling. **(B)** Grey coloured cubes mark the days (d) when individual CSF samples were collected from sTBI patients. Curly brackets indicate formed CSF pools based on individual samples. **(C)** Decreasing blood amount in formed CSF pools.

4.2.2. Plasma and cell protein levels in CSF are increased in the first 4 days after the injury

For a more detailed analysis of CSF pool composition, including the detection of blood (plasma) components, the first step was to perform a western blot analysis of albumin and apolipoproteins I and E (ApoI, ApoE). The results showed that the highest albumin levels were detected in the d1–2 and d3–4 CSF pools, with decreasing levels in the downstream pools. ApoI showed the same results as albumin but with a slightly lower intensity. ApoE, interestingly, was detected in higher levels in pools d5–6 and, especially, in d7–12. Western blot analysis also included peroxiredoxins (PRDX), ubiquitously expressed proteins in different cells, including erythrocytes and leukocytes, which could, therefore, indicate the presence of damaged cells in CSF pools. PRDX2 and 6 showed the strongest signal in the pool d1–2, with decreasing signal strength in subsequent pools and barely noticeable detection in d7–12. On the other side, PRDX 1 and 5 were weakly detected in d1–2, with no clear signal detection in the remaining pools (Figure 5). It is important to emphasize that the described protein variabilities across different post-TBI time points were observed in CSF samples loaded in equal volumes. The volume-based approach was chosen to account for the highly variable total protein amount in post-TBI CSF, which arises from the dynamic secondary injury processes, including changes in blood-brain barrier permeability and the release of cellular content from damaged tissues such as blood vessels and brain parenchyma. Due to the substantial variability in protein concentration—particularly the low protein content in CSF samples without significant blood contamination, such as those collected at later time points—this can create challenges when loading a small amount of total protein. Insufficient protein loading may hinder the detection of less abundant proteins and compromise the reliability of downstream analyses, necessitating careful consideration of normalization strategies and the sensitivity of detection methods.

Another challenge in analysing highly variable post-TBI CSFs is associated with standardizing loading controls for such samples. Unlike tissue or cell lysates, CSF lacks consistent and universally accepted housekeeping proteins for use as loading controls, with total protein being

proposed as a potential normalization strategy [108]. However, post-TBI CSF demonstrates not only variability in specific protein types but also significant fluctuations in total protein concentration due to evolving pathological processes such as inflammation, oedema, and cellular breakdown.

Taken together, these results emphasize the complex and variable composition of post-TBI CSF, characterized by fluctuating levels of cellular proteins (e.g., oxidative stress markers like peroxiredoxins) and plasma-derived components (e.g., albumin and lipoproteins), likely reflecting both cellular injury and blood-brain barrier compromise.

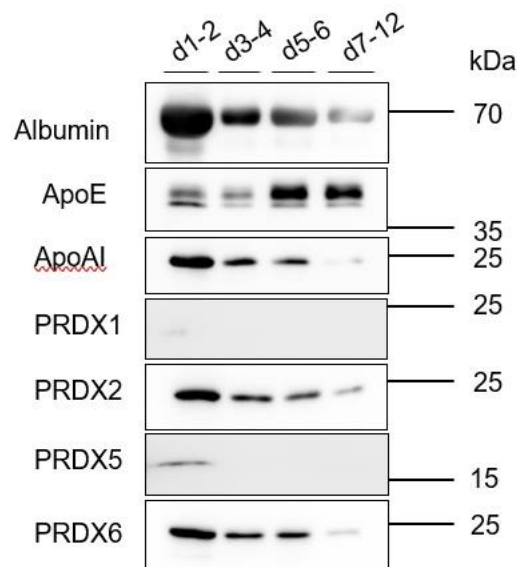


Figure 5. Common plasma and cell proteins in intracranial cerebrospinal fluid (CSF) after severe traumatic brain injury (sTBI). Post-sTBI CSF samples obtained on the indicated days (d) were combined with the Laemmli buffer and analysed by western blot. Shown are representative images of the depicted proteins with protein sizes expressed in kilodaltons (kDa).

4.2.3. miR451 quantification shows varying levels of haemolysis in post-TBI CSF

Considering that the macroscopic appearance and preliminary protein analyses of CSF pools revealed higher haemolysis levels, the subsequent step was to quantify the haemolysis in the CSF pools. The haemolysis level was assessed by performing reverse transcription and applying the cDNAs to a commercially available quality control (QC) PCR plate containing miR-451 and miR-23a-3p as haemolysis dependent and independent miRNAs, respectively (Figure 6). The difference in threshold cycles ($\Delta Ct = Ct(miR-451) - Ct(miR23a-3p)$) of 7 or more indicates a presence of haemolysis.

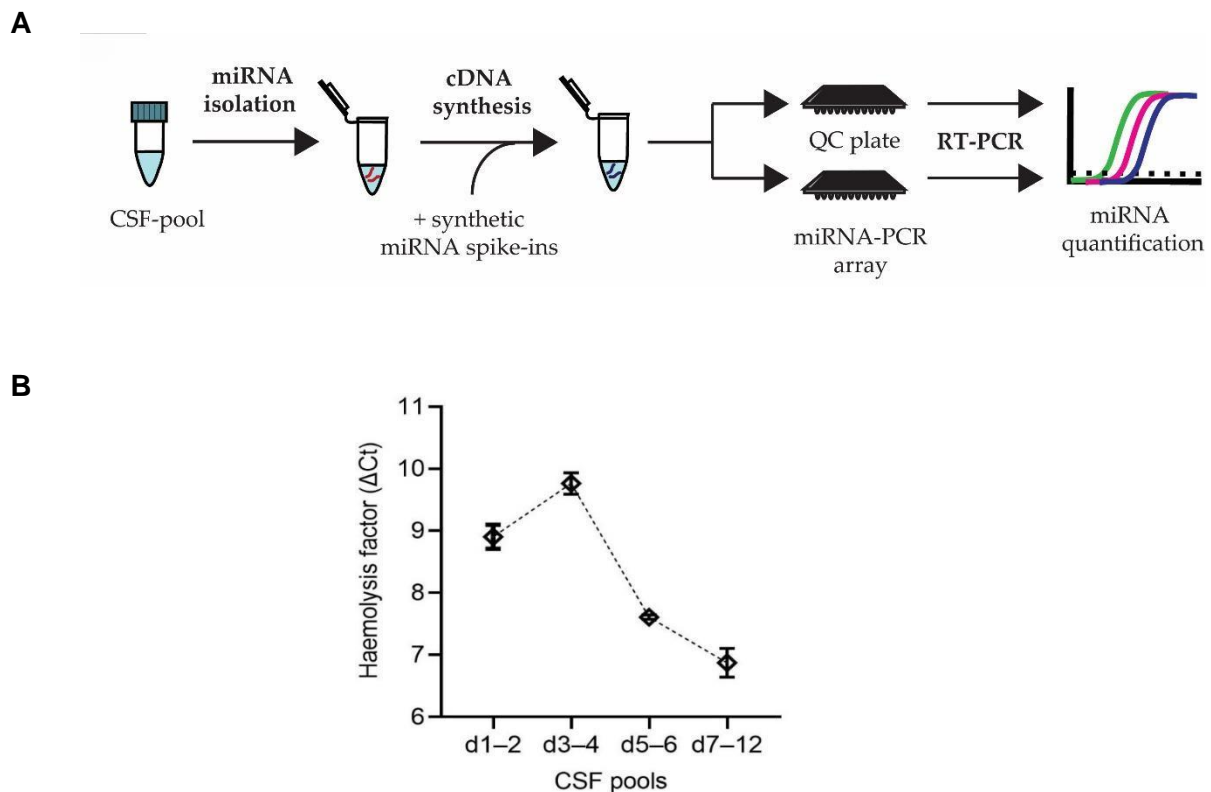


Figure 6. Assessment of haemolysis in CSF by miRNA quantification. (A) After miRNA isolation, the experimental protocol included adding of synthetic miRNA spike-ins before the complementary DNA (cDNA) synthesis. Real-time PCR served for miRNA quantification with arrays including 87 primers for targeted miRNAs (miRNA-PCR array) or miRNAs used for a quality control (QC) plate. **(B)** Haemolysis factor assessed as difference in threshold cycles (ΔCt) by using a formula: $\Delta Ct = Ct(miR-23a-3p) - Ct(miR451a)$. Shown are the mean values of three experiments with standard deviations.

The highest ΔCt values of 8.90 ± 0.19 and 9.76 ± 0.17 were found in d1–2 and d3–4, respectively, while in d5–6 and d7–12 were detected ΔCt values of 7.61 ± 0.04 and 6.87 ± 0.23 , respectively. These results indicate that d1–2 and d3–4 might be significantly more affected by haemolysis than d5–6 and d7–12.

4.3. Absolute quantification of 87 putative CSF miRNAs in post-injury CSF

After the initial characterization of CSF following sTBI, which revealed significant variability in protein content and haemolysis levels across the four analysed time points, the study's focus shifted to its primary goal: investigating whether extracellular miRNA levels are also impacted by sTBI. Quantification of extracellular miRNAs in CSF presents a significant challenge. Unlike intracellular RNA, extracellular miRNAs lack stable housekeeping genes for normalization, such as actin or GAPDH, which are commonly used in relative quantification of various mRNAs from cells and tissues [109]. The limitation of miRNA relative quantification is particularly pronounced in the context of post-TBI CSF, where variability in molecular content and haemolysis levels can further confound the results. To overcome this challenge, absolute quantification was chosen as a robust approach to determine the exact concentrations of multiple miRNAs in post-sTBI CSF.

4.3.1. Standard curve for absolute quantification

Absolute quantification of extracellular miRNAs was achieved using a commercial real-time PCR array, which included primers designed by the manufacturer for both synthetic miRNA sequences to generate the standard curve and for the targeted miRNAs of interest to be quantified. The PCR array was selected because each primer pair was unique and with incorporated Locked Nucleic Acid (LNA) technology to enhance binding affinity and provide specificity of amplicons [110].

The synthetic miRNA sequences included four miRNA spike-ins, named UniSp2, UniSp4, UniSp5, and cel-miR-39-3p, which were added in 100-fold incremental concentrations to represent a broad dynamic range and ensure robust amplification across multiple quantification cycles. These spike-ins were amplified simultaneously with the targeted miRNAs on the PCR array. The resulting cycle threshold (Ct) values were used to construct a standard curve (Figure 7), yielding an R-squared (R^2) value of 0.9877 and minimal deviations from the regression line (S value: 0.8808).

The 96-well format of the PCR array, with a predefined arrangement of unique primer pairs in each well, limited the analysis of each amplicon to a single well. Additionally, the spike-ins were commercially provided at fixed 100-fold incremental concentrations, making it

impractical to prepare reasonable serial dilutions for each amplicon. Despite these constraints, the strong linearity of the standard curve and minimal deviations from the regression line suggest that amplification efficiencies of the spike-ins were reliable across the tested range.

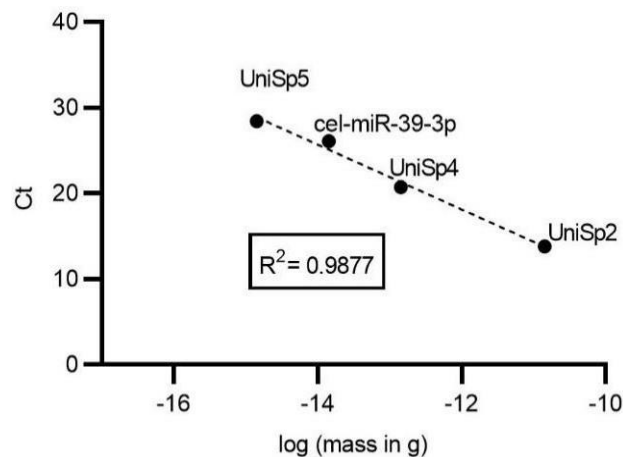


Figure 7. A standard curve for absolute quantification of miRNAs. The resulting cycle threshold (Ct) values were obtained using four RNA spike-ins in pre-defined concentrations, which were co-amplified with targeted miRNAs on a commercial PCR-array plate. The calculated R- squared (R^2) value is shown. Masses are expressed in grams (g).

4.3.2. Quantities of targeted miRNAs present in CSF differ up to a million-fold

A commercial PCR-array containing primers for 87 putative CSF miRNAs was chosen to analyse consecutive CSF pools after sTBI. All 87 miRNAs were detected and quantified using the previously described standard curve. The quantities of 87 miRNAs differed more than a million-fold. Using the Ct values, miRNAs were grouped into high (Ct <25), moderate (Ct 25 to <30), and low (Ct ≥30) abundance groups (Table 7). Their mass values expressed in picograms (pg) ranged from 2-16 pg, 1-4 pg, and <1 pg for high, moderate and low abundance group, respectively. The highest levels of miRNAs were detected in d1–2. Exceptions are miR- 25-3p, miR-486-5p, and miR-92a-3p (bold and underlined in Table 7) with the highest detection levels in d3–4. We could not detect miR-181c-5p and miR-182-5p in d5–6 and d7– 12, as well as miR-155-5p in d7–12 (bold and underlined in Table 7).

Table 7. Amounts of detected and quantified targeted 87 microRNAs (miRNAs) from cerebrospinal fluid (CSF) pools. After absolute quantification, amounts of 87 miRNAs from CSF pools were analysed and shown in femtograms (fg) as highly (A), medium (B) and low abundant (C) with the highest detection for majority of miRNAs in days (d) d1–2. Shown are

mean values of duplicates. ND (Not Detected) indicates values below the detection limit.

A

miRNA (d1–2, d3–4, d5–6, d7–12) mass in fg			
miR-451a (16010, 8426, 1524, 385)	miR-92a-3p (95, 213 , 3.8, 1.9)	miR-9-5p (23, 1.0, 0.4, 0.3)	miR-424-5p (11, 2.2, 3.3, 1.0)
miR-16-5p (2962, 2262, 38, 12)	miR-93-5p (80, 49, 1.8, 0.6)	miR-23a-3p (22, 8.4, 7.0, 3.4)	miR-181a-5p (10, 4.2, 0.5, 0.4)
miR-144-3p (764, 422, 66, 16)	miR-106b-5p (77, 39, 4.0, 1.2)	miR-27b-3p (20, 1.5, 0.3, 0.2)	miR-27a-3p (10, 1.3, 0.2, 0.1)
miR-20a-5p (549, 289, 69, 16)	let-7i-5p (67, 35, 4.8, 1.5)	let-7f-5p (18, 8.3, 2.2, 0.6)	miR-29a-3p (8.4, 0.7, 0.4, 0.3)
let-7b-5p (381, 144, 69, 13)	miR-125b-5p (61, 5.6, 0.7, 1.2)	miR-29c-3p (18, 3.3, 1.0, 0.4)	let-7d-5p (8.0, 4.1, 0.9, 0.2)
miR-15a-5p (304, 131, 23, 6.9)	miR-338-3p (59, 1.9, 1.1, 0.7)	let-7c-5p (16, 1.4, 0.6, 0.2)	miR-29b-3p (7.7, 1.4, 0.3, 0.1)
miR-21-5p (231, 101, 85, 45)	let-7g-5p (49, 29, 3.8, 1.0)	miR-148b-3p (16, 5.1, 1.7, 0.6)	miR-126-3p (7.6, 11, 0.1, 0.04)
miR-19b-3p (224, 135, 6.9, 2.1)	miR-142-3p (41, 28, 1.8, 0.3)	miR-32-5p (15, 8.0, 0.7, 0.3)	miR-204-5p (7.1, 6.3, 4.9, 2.3)
miR-223-3p (192, 73, 40, 9.3)	miR-26b-5p (39, 24, 1.3, 0.4)	miR-148a-3p (15, 8.0, 6.0, 1.5)	miR-18a-5p (1, 3.8, 0.1, 0.02)
miR-106a-5p (167, 97, 18, 5.2)	miR-103a-3p (39, 23, 1.4, 0.5)	miR-99a-5p (15, 0.9, 0.5, 0.2)	miR-425-5p (5.2, 6.0, 0.2, 0.1)
miR-15b-5p (147, 65, 21, 5.7)	let-7a-5p (38, 11, 3.7, 1.1)	miR-100-5p (14, 1.4, 0.6, 0.5)	miR-26a-5p (4.8, 3.5, 0.6, 0.3)
miR-25-3p (120, 142 , 2.0, 1.1)	miR-124-3p (30, 1.7, 0.3, 0.3)	miR-23b-3p (14, 2.8, 1.3, 0.8)	miR-194-5p (1, 5.4, 0.1, 0.04)

B

miR-101-3p (109, 64, 12, 2.9)	miR-107 (29, 17, 1.0, 0.4)	miR-24-3p (12, 3.6, 0.4, 0.3)	
miR-486-5p (107, 232 , 2.7, 0.8)	miR-320a (24, 21, 1.3, 0.5)	miR-191-5p (11, 9.1, 0.6, 0.3)	
let-7e-5p (4.1, 1.1, 0.5, 0.2)	miR-150-5p (2.1, 2.0, 1.0, 0.6)	miR-125a-5p (1.2, 0.2, 0.04, 0.1)	miR-146b-5p (0.7, 0.4, 0.03, 0.02)
miR-132-3p (4.0, 0.5, 0.2, 0.2)	miR-181b-5p (2.0, 0.2, 0.1, 0.1)	miR-128-3p (1.1, 0.6, 0.02, 0.03)	miR-30e-5p (0.7, 1.0, 0.1, 0.03)
miR-192-5p (3.9, 3.5, 0.2, 0.1)	miR-590-5p (1.8, 1.0, 0.1, 0.03)	miR-30b-5p (1.0, 1.6, 0.1, 0.1)	miR-145-5p (0.4, 0.2, 0.03, 0.02)
miR-142-5p (3.9, 2.6, 0.7, 0.3)	miR-143-3p (1.6, 0.5, 1.1, 0.3)	miR-532-5p (0.9, 0.7, 0.03, 0.01)	miR-92b-3p (0.3, 0.3, 0.01, 0.01)
miR-652-3p (3.8, 2.2, 0.5, 0.1)	miR-186-5p (1.5, 1.0, 0.1, 0.1)	miR-34a-5p (0.7, 0.1, 0.1, 0.1)	
miR-342-3p (3.1, 1.0, 0.4, 0.2)	miR-30c-5p (1.4, 2.5, 0.2, 0.1)	miR-138-5p (0.7, 0.04, 0.01, 0.01)	
miR-140-3p (3.1, 2.3, 0.1, 0.1)	miR-99b-5p (1.2, 0.1, 0.03, 0.04)	miR-378a-3p (0.7, 0.5, 0.1, 0.1)	

C

miR-197-3p (0.06,0.08,0.02, 0.01)	miR-181c-5p (0.03,0.01, ND , ND)	miR-155-5p (0.01,0.02,0.01, ND)	miR-182-5p (0.01,0.01, ND , ND)
miR-197-3p (0.06,0.08,0.02, 0.01)	miR-181c-5p (0.03,0.01, ND , ND)	miR-155-5p (0.01,0.02,0.01, ND)	miR-182-5p (0.01,0.01, ND , ND)

The following 10 miRNAs were the most prevalent across all 4 CSF pools: miR-451a, miR-16-5p, miR-144-3p, miR-20a-5p, let-7b-5p, miR-15a-5p, miR-21-5p, miR-223-3p, miR-106a-5p, and miR-15b-5p, each displaying a distinct expression pattern (Figure 8). Although all the depicted miRNAs were most abundant during the initial days (d1–2) following the injury, their quantities decreased at varying rates over time. The steepest declines, leading to the lowest concentrations by d7–12, were observed for miR-451a and especially miR-16-5p, both of which had the highest initial concentrations. In contrast, miR-21-5p exhibited the least steep slope, while the remaining miRNAs showed comparable patterns, maintaining elevated levels during the early days after the injury.

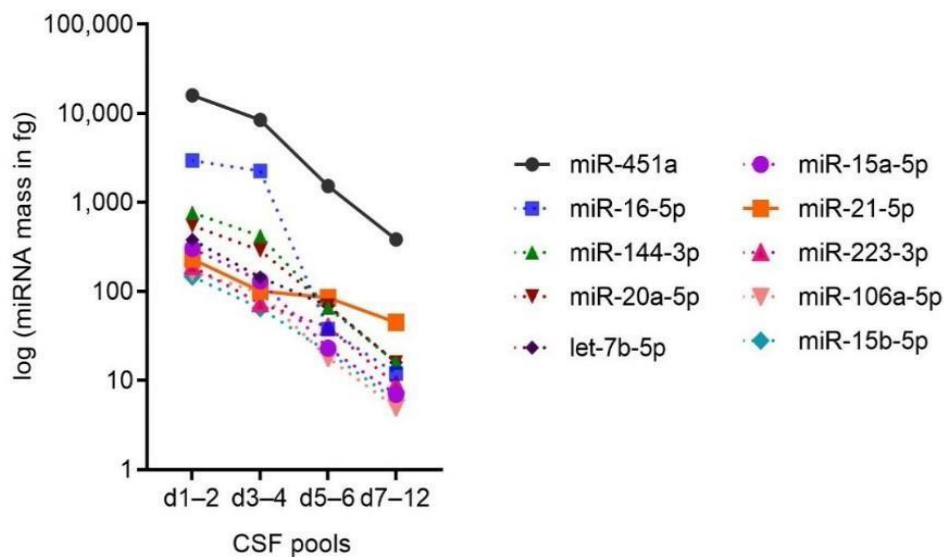


Figure 8. The highly abundant microRNAs (miRNAs) across cerebrospinal fluid (CSF) pools. A PCR array targeting 87 miRNAs was used to analyse spike-in containing cDNAs from cerebrospinal fluid (CSF) pools collected on specified days (d) after sTBI. The most abundant miRNAs are presented based on their quantification using spike-ins. Mean values from two independent experiments are shown.

These data indicate that targeted miRNAs could have a different cellular source and that not all are necessarily a direct product of the central nervous system (CNS). This conclusion is supported by the finding that miR-451a and miR-16-5p have been primarily isolated from blood samples, corroborating our results of high haemolysis levels in the first days after the injury [74, 106].

4.3.3. The targeted 87 miRNAs likely derive from the blood and account for only a tiny proportion of miRNAs present in the CSF after severe traumatic brain injury

To further investigate the overall changes of miRNA expression in post-TBI CSF, we quantified the total mass of targeted miRNAs across the four time points (d1–2, d3–4, d5–6, and d7–12). The total miRNA mass calculated in picograms (pg) across the CSF pools showed a decreasing trend (Figure 9A). The highest amount of 23.37 ± 1.03 pg was detected in d1–2, followed by 13.22 ± 1.29 pg, 2.05 ± 0.12 pg and 0.55 ± 0.05 pg for d3–4, d5–6 and d7–12, respectively. This quantification revealed that the targeted miRNAs represent only a small fraction of the total miRNA content.

To provide a clearer overview of miRNA dynamics in CSF during the acute phase of recovery, normalization was performed using CSF pool d5–6 as a reference due to its lower haemolysis levels compared to d1–2 and d3–4 (Figure 6D). The results of relative quantification are presented in a form of a heat map for the 87 targeted miRNAs across the CSF pools (Figure 9B). The heat map clearly showed that the highest levels of targeted miRNAs were present in d1–2, consistent with the trend in total miRNA mass observed earlier. In the subsequent CSF pools, a consistent decrease in miRNA levels was noted, with the exception of miR-181c-5p, miR-182-5p, and miR-155-5p which were undetectable in d5–6 (normalization reference) or at later time points. Taken together, these data suggest that the 87 targeted miRNAs, which represent putative CSF miRNAs, constitute only a minor fraction of the extracellular miRNAs in CSF after TBI. Moreover, the analysed miRNAs likely originate from the blood rather than being direct products of the CNS. This highlights the need for more comprehensive profiling to identify the majority of miRNAs that remain undetected in this analysis.

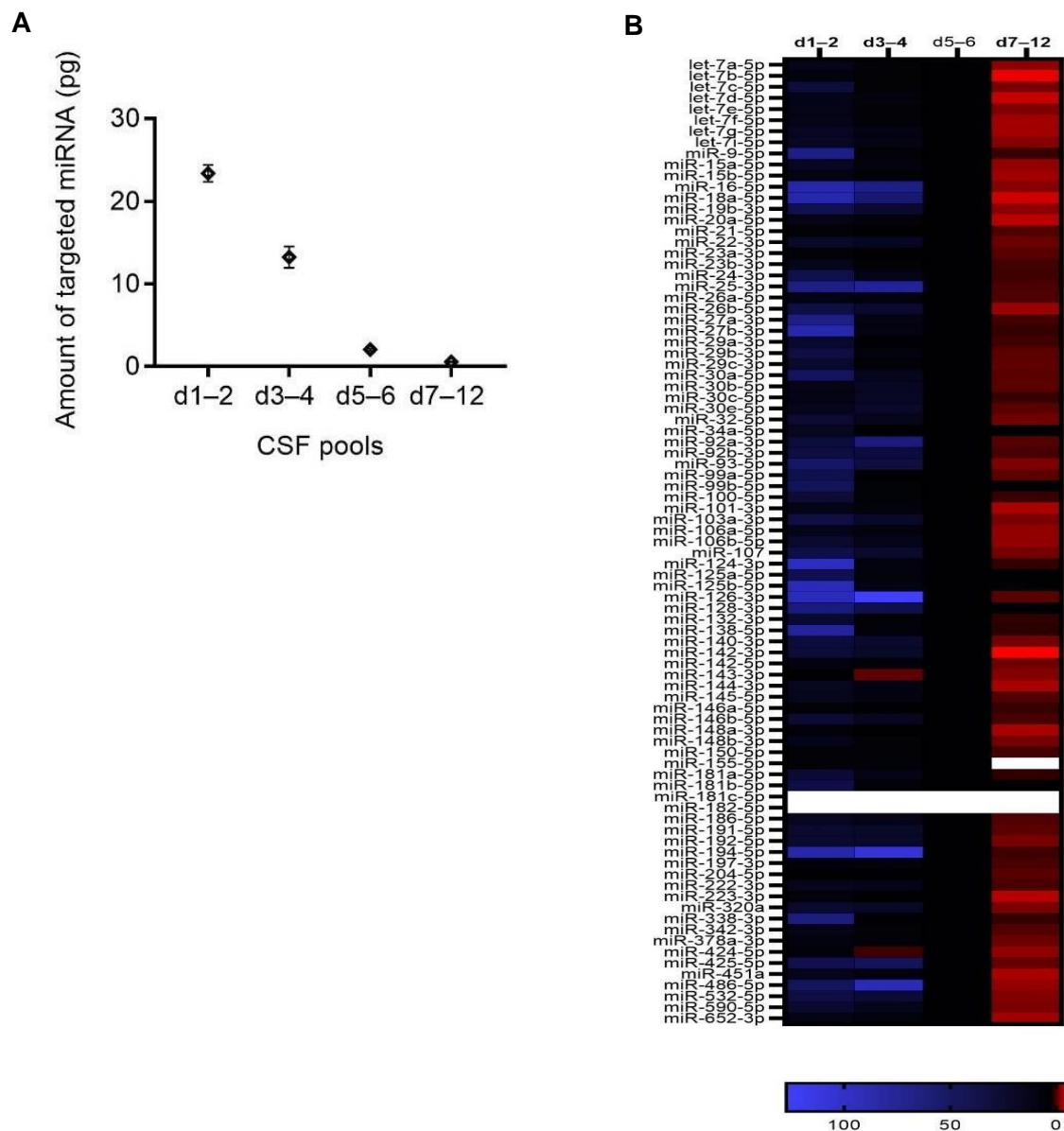


Figure 9. The targeted 87 miRNAs account for a minor portion of the miRNAs detected in the cerebrospinal fluid after severe traumatic brain injury and most likely derive from **the blood**. Quantities of targeted miRNAs, determined in cerebrospinal fluid by spike-in-based absolute quantification, are shown as the total sum for the indicated days (d) after severe traumatic brain injury (A) and as individual amounts normalised to d5–6, when haemolysis levels were low (B). The mean values from two independent experiments are presented, with standard deviations represented as error bars. White boxes denote miRNAs for which normalization was not possible due to undetected levels at d5–6 or other time points.

4.4. miRNA cargo of extracellular vesicles in post-TBI CSF

Following the results indicating the highest miRNA concentrations during the initial days post-injury, which coincided with elevated haemolysis levels in the CSF-samples, the next step was to investigate whether the targeted miRNAs are cargo of extracellular vesicles (EV) in the CSF. To address this, size-exclusion chromatography (SEC) was used to isolate EVs from post-TBI CSF, followed by miRNA isolation and quantification in the EV-enriched and EV-depleted fractions obtained through SEC.

4.4.1. EVs are present in intracranial CSF after sTBI

To investigate the EV content in CSF after sTBI, western blot analysis was performed on CSF samples using common protein markers for exosomes and apoptotic bodies, in line with the latest guidelines from Minimal information for studies of extracellular vesicles [111]. The markers analysed included flotillin-1 (Flot-1), flotillin-2 (Flot-2), tumour susceptibility gene 101 (TSG101), CD81, and CD9 for exosomes, as well as annexin-V for apoptotic bodies (Figure 10A). Similarly to extracellular RNA analysis where no housekeeping gene are available for normalisation, the analysis of CSF proteins faces a similar challenge in the context of sTBI, which is characterised by highly dynamic changes in CSF protein types and levels [78].

The highest levels of all analysed EV protein markers were observed during the first two days post-injury (d1-2). Flot- 1, Flot-2, and CD9 levels remained elevated at d3-4 before gradually declining in subsequent pools. This trend corresponded with the higher haemolysis levels detected in d1-2 and d3-4, suggesting a potential blood (plasma) origin for EVs carrying these markers. In contrast, TSG101 and CD81 showed a sharp decline in levels after d1-2, but their low levels remained comparable across d3-4, d5-6, and d7-12, indicating that blood is unlikely to be the source of EVs carrying these markers. Apoptotic bodies, identified using Annexin V, constituted only a small portion of the EV population at d1-2 and d7-12 and were barely detectable at d3-4 and d5-6.

Following the western blot results, which confirmed the presence of EVs in post-TBI CSF, SEC method was developed by our group [90] (Figure 10B). SEC separation resulted in 44 fractions per CSF pool, which were analysed by immunodetection for CD81 and albumin, widely accepted protein markers for EVs and free proteins (FP), respectively [82, 83, 84, 112]. SEC fractions with the highest detected signals spanned fractions 14-17 for CD81 (CD81+) and fractions 28 and later for albumin (Alb+), indicating that EVs were clearly separated from FPs in each CSF pool (Figure 10C). For subsequent analytical procedures, CD81+ fractions

and Alb+ fractions were pooled separately and designated as EV pools and FP pools, respectively.

To characterize the physical properties of EVs, their concentrations and sizes were measured in the EV pools using the tunable resistive pulse sensing (TRPS) method. The highest EV concentrations EVs were detected in d1–2, with a result of $(4.96 \pm 0.18) \times 10^9$ nanoparticles/mL, followed by $(0.52 \pm 0.15) \times 10^9$ in d3–4, $(1.32 \pm 0.19) \times 10^9$ in d5–6, and $(0.93 \pm 0.19) \times 10^9$ in d7–12 (Figure 10D).

Unlike the concentrations, the sizes of EVs were largest in d7–12, with a median diameter of 175 nm (interquartile range [IQR]: 151-218 nm). In the remaining CSF pools, smaller and comparable sizes were measured: 162 nm (IQR: 137-202 nm) for d1–2, 160 nm (IQR: 151-218 nm) for d3–4, and 160 nm (IQR: 135-197 nm) for d5–6 (Figure 10E).

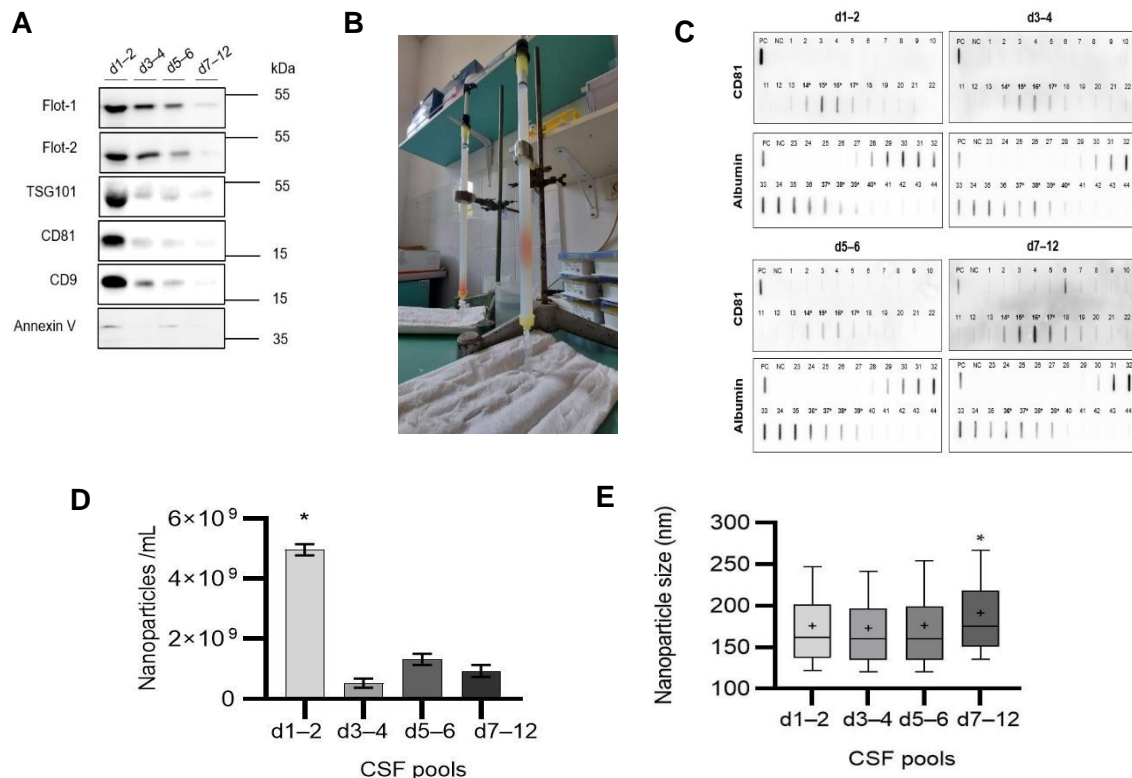


Figure 10. Extracellular vesicles (EVs) are present in intracranial cerebrospinal fluid (CSF) during 12 days after severe traumatic brain injury (sTBI) and can be separated from free proteins (FP) by size-exclusion chromatography (SEC). (A) Western blot and immunodetection of depicted proteins with indicated sizes expressed in kilodaltons (kDa) were used to analyse listed CSF pools. Shown are representative blots. **(B)** In-house developed SEC method based on glass column filled with Sepharose CL-6B **(C)** SEC fractions obtained from the separation of CSF pools were combined with loading buffer and applied to nitrocellulose membranes using a slot-blot technique, followed by immunodetection of CD81 and

albumin. Positive controls (PC) consisted of lysed corresponding CSF pools, while negative controls (NC) used phosphate-buffered saline (the SEC mobile phase). Numbers indicate individual SEC fractions, and asterisks mark the SEC fractions pooled for further analysis. **(D)** Tunable resistive pulse sensing (TRPS) method was used to measure EV concentrations in the pool of CD81+ SEC fractions. Performed were 3 measurements for each pool at 2 pressure conditions. Shown results are mean values with standard deviations. * $p < 0.001$ for d1–2 in comparison to other CSF pools - the result after performing one-way ANOVA with Tukey's test for multiple comparison. **(E)** Nanoparticle diameter was measured by TRPS in pooled CD81+ fractions. Performed were 3 measurements at 2 pressure conditions for each sample. Values are shown as box plots with marked median (bar), 25th, and 75th percentiles (box) as well as the 10th and 90th percentiles (whiskers), and mean value indicated as "+". * $p < 0.001$ in CSF pool d7–12 after the non-parametric ANOVA (Kruskal-Wallis test) with Dunn's test for multiple comparisons.

4.4.2. miRNA is present at similar levels in both extracellular vesicles and free protein portions of cerebrospinal fluid

The previously described separation of cerebrospinal fluid (CSF) into EV- and FP-enriched fractions enabled further study of intracranial extracellular miRNAs in sTBI. The first step in this follow-up characterisation was to determine whether miRNA is present in EV- and FP-enriched fractions. To address this, miRNAs were isolated from CD81+ and Alb+ SEC fractions representing EV- and FP-enriched fractions (Figure 10C), respectively, which were separately pooled across all four CSF time points (d1–2, d3–4, d5–6, and d7–12). The resulting eight samples of miRNAs ranged in concentration from 4.6 to 8.0 ng/ μ L in both EV and FP pools at all time points (Figure 1), meeting the minimal concentration required for cDNA synthesis and thus enabling miRNA analysis by real-time PCR.

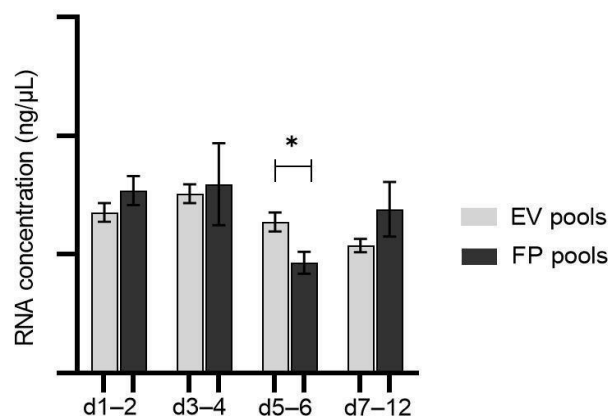


Figure 11. Extracellular vesicle (EV) and free protein (FP) enriched fractions of cerebrospinal fluid after (CSF) severe traumatic brain injury (sTBI) contain comparable levels of miRNA. miRNA was isolated from CSF samples collected at indicated days (d) post-TBI after separation by size exclusion chromatography (SEC) into EV and FP pools, represented by CD81+ and albumin+ SEC fractions, respectively. RNA concentrations were determined using spectrophotometric measurements. Mean values and standard deviations from two measurements for each sample are shown. *unpaired *t*-test resulted in $p=0.008$.

4.4.3. Targeted miRNAs are predominantly associated with free proteins rather than extracellular vesicles

To determine whether targeted miRNAs in post-TBI CSF are contained within EVs, miRNA isolated from SEC fractions was used for cDNA synthesis, followed by real-time PCR array and spike-in-based quantification. The resulting miRNA quantities for both EV and FP

pools at each of the four time points (d1–2, d3–4, d5–6, and d7–12) ranged from approximately 2.2 pg to less than 0.01 fg, with levels generally lower in the EV pool compared to the FP pool for the corresponding time point. The highest miRNA levels were observed in FP-pools at d1–2 and 3–4. Only 20 miRNAs were quantifiable at all four time points, and only in FP pools, while the majority of miRNA levels at d5–6 and d7–12 were below detectable limits [113].

To assess the enrichment of quantifiable miRNAs in FP and EV pools, corresponding ratios were calculated for the available quantities, considering only ratios that differed by at least fivefold (Table 8). The majority of enriched miRNAs were found in FP pools. In d1-2 and d3-4, the FP pools contained 59 and 35 of the targeted miRNAs, enriched up to approximately >200-fold and >300-fold, respectively. In d5–6 and d7–12, groups of 3 miRNAs were enriched up to 12-fold and 14-fold in FP pools, respectively.

EV pools contained far fewer enriched miRNAs, with 2, 3, 17 and 1 miRNAs enriched in d1-2, d3-4, d5-6, and d7-12, respectively. Notably, the majority of EV-enriched miRNAs were also found to be enriched in the FP pool at other time points (underlined in Table 8). Only seven miRNAs were specifically enriched in the EV pool. These uniquely EV-enriched miRNAs include miR-30b-5p (9-fold in d1–2), miR-92b-3p (5-fold in d1–2), miR-204-5p (55-fold in d3–4 and 42-fold in d5–6), miR-22-3p (6-fold in d3–4 and 8-fold in d5–6), miR-223-3p (26-fold in d5–6 and 16-fold in d7–12), miR-142-3p (54-fold in d5–6), and miR-125b-5p (9-fold in d5–6).

Table 8. Targeted microRNAs (miRNAs) enriched in extracellular vesicle (EV) and free protein (FP) pools on the depicted days (d). Underlined are miRNAs with cross-enrichment in both EV and FP pools. Numbers in brackets are fold enrichment.

Pool	EV enriched (fold)	FP enriched (fold)		
d1–2	miR-30b-5p (9)	miR-20a-5p (269)	miR-100-5p (33)	miR-124-3p (14)
	miR-92b-3p (5)	miR-29b-3p (253)	miR-132-3p (32)	<u>miR-27b-3p</u> (14)
		miR-424-5p (196)	miR-26b-5p (31)	let-7f-5p (13)
		miR-451a (179)	miR-32-5p (29)	<u>miR-338-3p</u> (13)
		miR-106a-5p (166)	miR-107 (29)	miR-146b-5p (13)
		miR-148a-3p (159)	let-7g-5p (28)	miR-34a-5p (13)
		let-7i-5p (139)	miR-15b-5p (28)	<u>miR-16-5p</u> (12)
		let-7b-5p (110)	miR-23a-3p (27)	<u>miR-19b-3p</u> (10)
		miR-93-5p (96)	miR-143-3p (23)	<u>miR-99a-5p</u> (10)
		miR-144-3p (82)	<u>miR-103a-3p</u> (22)	miR-590-5p (10)
		miR-106b-5p (81)	let-7d-5p (22)	<u>miR-27a-3p</u> (9)
		miR-101-3p (80)	miR-142-5p (22)	<u>let-7c-5p</u> (9)
		miR-148b-3p (71)	miR-21-5p (22)	let-7a-5p (9)
		miR-29c-3p (67)	miR-532-5p (22)	miR-23b-3p (9)
		miR-652-3p (65)	let-7e-5p (20)	miR-222-3p (9)
		miR-18a-5p (64)	miR-425-5p (18)	miR-146a-5p (7)
		miR-29a-3p (53)	miR-9-5p (18)	miR-140-3p (6)
		miR-15a-5p (40)	<u>miR-25-3p</u> (16)	miR-126-3p (6)
		miR-194-5p (40)	miR-99b-5p (16)	miR-486-5p (5)
		miR-192-5p (36)	miR-320a (14)	
d3–4	miR-204-5p (55)	let-7b-5p (336)	<u>miR-103a-3p</u> (27)	<u>miR-25-3p</u> (14)
	miR-22-3p (6)	miR-20a-5p (181)	let-7a-5p (25)	miR-32-5p (12)
	<u>miR-99a-5p</u> (5)	miR-106a-5p (123)	let-7i-5p (22)	<u>miR-92a-3p</u> (12)
		miR-451a (56)	miR-148b-3p (20)	miR-320a (11)
		let-7g-5p (51)	<u>miR-486-5p</u> (19)	miR-144-3p (10)
		miR-101-3p (49)	let-7d-5p (18)	<u>miR-191-5p</u> (9)
		miR-148a-3p (44)	miR-15b-5p (18)	miR-26a-5p (9)
		miR-93-5p (39)	miR-425-5p (16)	miR-15a-5p (7)
		miR-26b-5p (39)	miR-142-5p (15)	<u>let-7c-5p</u> (7)
		miR-107 (36)	miR-23a-3p (15)	miR-192-5p (7)
		let-7f-5p (35)	<u>miR-16-5p</u> (15)	miR-140-3p (5)
		miR-106b-5p (28)	miR-18a-5p (14)	
d5–6	miR-142-3p (54)	<u>miR-20a-5p</u> (12)		
	miR-204-5p (42)	<u>let-7b-5p</u> (11)		
	miR-223-3p (26)	<u>miR-106a-5p</u> (6)		
	<u>miR-92a-3p</u> (22)			
	<u>miR-338-3p</u> (18)			
	<u>miR-103a-3p</u> (11)			
	<u>miR-486-5p</u> (11)			
	miR-125b-5p (9)			

	miR-25-3p (9)		
	miR-124-3p (9)		
	miR-22-3p (8)		
	miR-16-5p (7)		
	let-7c-5p (7)		
	miR-19b-3p (7)		
	miR-27a-3p (6)		
	miR-27b-3p (6)		
	miR-191-5p (6)		
d7–12	miR-223-3p (16)	let-7b-5p (14)	
		miR-20a-5p (11)	
		miR-106a-5p (8)	

Ultimately, the results revealed intriguing findings. Several facts point to two possibilities: whether EV fractions in the first few days after the sTBI are rich in miRNAs from the blood; and whether miRNAs found in small but similar amounts in the last days (specifically in the pool d7-12) are the ones to look for because they come from the purest pool with the lowest haemolysis levels. Clearly, this undoubtedly necessitates additional research on a larger number of sTBI patients.

Severe traumatic brain injury (sTBI) represents a today's silent epidemic. As the leading cause of traumatic deaths with half of patients dying during the accident, sTBI is one of the world's leading causes of morbidity with long-term consequences for survivors and high-costs of hospital treatment [2, 3, 11]. Our understanding of complex, secondary mechanisms is not totally clear. These mechanisms, unlike the primary injury, can be timely treated and reversible, but further knowledge is needed. Here we provide analysis of miRNA from intracranial CSF of sTBI patients and show dynamic changes in CSF molecular content during the 12 days after the injury.

5. DISCUSSION

5.1. Study importance and main limitations

This study presents novel data regarding the temporal dynamics of the CSF molecular profile in sTBI and highlights significant methodological challenges that warrant future investigation in a larger sample. The research included 5 sTBI patients with admission Glasgow Coma Scale (GCS) ≤ 8 , whose initial treatment required placing the EVD and thus enabled CSF sampling after the injury (Table 1 in section 1.1., subsection 1.1.1.). The main injury mechanisms were traffic accidents and falls, consistent with the world's leading causes of sTBI in low-middle-income countries [4, 9]. The most common intracranial pathologies were different forms of haemorrhages, that are the leading brain pathoanatomical changes after the sTBI [20, 22]. Given that 80% of the study's participants are male, the findings align with contemporary statistics indicating that males predominantly suffer from sTBI, attributable to their greater involvement in traffic and sports activities [8]. The study included 1 female, but role of female gonadal hormones in neuroprotection is still insufficiently clarified [15, 114]. The recruited patients from the younger and middle-aged demographics exhibit a lower susceptibility to neurodegeneration and a greater likelihood of favourable outcomes [9, 14]. The standardized Glasgow Outcome Scale (GOS) was used to assess the 6-month outcome after the sTBI (Table 2 in section 1.1., subsection 1.1.1.). Consequently, 4 sTBI patients had moderate and good outcomes, as indicated by scores of 4 and 5, whereas 1 patient's GOS score was 1 due to a fatal outcome during intensive care unit (ICU) treatment. Judging by the favourable patient's treatment outcome, we can conclude that the obtained data of our study are relevant for the early neurorecovery, but the limiting factor is certainly the small number of subjects included in study.

A total of 35 samples were collected from 5 sTBI patients (Figure 4A, 4B in section 4.2., subsection 4.2.1.). Sampling was stopped when the EVD was removed, in accordance with the decision of the attending neurosurgeon based on diagnostic imaging and the clinical treatment course, with a fatal outcome in one patient during ICU treatment (Patient 5, Figure 4B in section 4.2., subsection 4.2.1.). Samples were collected during the 12 days following injury onset, with a 24-hour gap between collection time points to ensure that the expression of potentially valuable biomarkers at specific time points would not be overlooked. Larger intervals between sampling time points have been recorded in previous studies and identified as a major limitation, so we consider frequent sampling as a strength of our study [77]. Samples were preserved in low-protein binding tubes and promptly transferred to a freezer for storage at -80°C . However, no RNase inhibitors or other specific reagents to preserve RNA integrity were used, and thus, miRNA degradation cannot be excluded. This limitation may have

contributed to partial miRNA loss, potentially leading to incomplete results.

Another limitation of this study is that analyses were not performed on individual CSF samples but on CSF samples combined into pools resulting in the dilution of the original samples. Pools day (d) 1–2, d3–4, and d5–6 provided average miRNA amounts for 2 included days, while pool d7–12 provided average miRNA amounts for the 6 days. CSF samples were pooled to minimize the total number of samples analysed, given the available resources and the complexity of the workflow. Each individual sample underwent size exclusion chromatography (SEC), generating 38 SEC fractions per sample, all of which required further analysis by slot blot for immunodetection of EV and free protein content. To streamline the process, selected SEC fractions were pooled based on protein analysis and, together with the corresponding CSF pool, analysed using a miRNA array. The initial rationale behind this approach was to obtain a screening result that would guide subsequent single miRNA analyses. However, our findings revealed that the targeted 87 miRNAs originate from blood rather than the brain, which altered the direction of further analyses. Pooling was conducted while considering the distribution of subjects; as the number of individuals was higher in the initial post-injury days compared to later time points due to the duration of EVD placement (Figure 4B in section 4.2., subsection 4.2.1.). To minimize the risk of inconsistency and potential bias in the results, each pool was designed to include a comparable number of individual CSF samples.

Cerebrospinal fluid (CSF) represents the most reliable biological sampling fluid in the vicinity of the brain injury. The CSF sampling is a demanding process, owing to the fact that the only way to obtain a sample of intracranial CSF is placement of external ventricular drain using surgical approach to the frontal horn of the lateral ventricle. This procedure is performed at the indication of attending neurosurgeon following the admission management and diagnostic of sTBI [31]. Accumulated evidence shows that there is a difference between CSF sampled from EVD and CSF obtained by lumbar puncture. Lumbar CSF is thus not a reliable source for obtaining biological information about sTBI. Furthermore, the EVD placement procedure itself is associated with a lower rate of bleeding than the lumbar puncture [115]. On the other hand, due to the nature of the injury, sTBI carries a higher risk of blood contamination in CSF. Blood presence and potential haemolysis are important factors in CSF processing and analysis, as discussed in the following section.

In conclusion, for a thorough analysis of molecular changes in the acute phase of sTBI, it is crucial to use a sampling approach that captures the dynamic nature of the injury. CSF obtained from an EVD provides a unique opportunity for frequent sampling in close proximity to the injury site. Given the limited knowledge about molecular changes in the acute phase, more frequent CSF sampling may help provide a better temporal resolution of these processes.

Following sTBI, molecular insights can be gained through miRNAs that are either actively secreted or passively released from affected brain cells.

5.2. High haemolysis level affects miRNA isolation and quantification

Clinical CSF samples, particularly after sTBI, often contain blood, either visibly or microscopically. This results from both the invasive sampling procedure and the injury itself, which disrupts brain blood vessels, as previously discussed. Blood therefore enters CSF and significantly alters its EV and protein content [52, 92]. Ruptured cell membranes may reassemble into spherical structures resembling authentic EVs, making it harder to detect brain-derived molecules and EVs, which are typically present at low levels [93, 95].

Erythrocyte remnants, the most abundant blood cells, are the main source of blood-derived content in CSF, and haemolysis can be detected visually as red discoloration or at the molecular level by detecting erythrocyte-specific markers [92, 93]. Significantly, haemolysis signifies the existence of additional blood cells, notably leukocytes, whose quantity escalates due to the onset of inflammation in the later stages of sTBI. These factors affect the identification of brain-derived miRNA, highlighting the need for careful interpretation of haemolysis-related interference [52, 78].

MiRNAs play a crucial role in brain development, influencing neurological functions that may be altered in neurological diseases, neurodegenerative disorders, and neurotrauma. Although their roles in pathology remain incompletely understood, miRNAs regulate various cellular pathways, including the cell cycle, metabolism, apoptosis, and immune responses, making them promising biomarkers of brain (patho)physiological processes. Their biomarker potential in brain development, cerebrovascular pathophysiology, and TBI diagnosis has been explored in several studies using CSF, blood, or saliva samples, yet no miRNA candidate has achieved clinical relevance [66, 67, 71, 77, 78, 79, 80].

In this study, out of four consecutive CSF pools, the highest total miRNA concentrations were detected in pools d5–6 and d7–12, the last time point measured. The increase in total miRNA concentrations at later time points is unexpected, given that blood content - a likely miRNA source, is higher in the first days post-injury, as previously discussed and supported by our real-time PCR quantification of haemolysis levels (Figure 6B in section 4.2., subsection 4.2.3.). While miRNAs released from damaged blood and brain cells can significantly contribute to the total miRNA amount in CSF following TBI, other cellular components may hinder downstream miRNA analysis. Namely, heme - a by-product of haemolysis, along with immunoglobulins and whole blood, has been shown to inhibit PCR-based detection and quantification by interfering with polymerase activity and disrupting reaction conditions [116]. This underscores the importance of sample quality when analysing extracellular miRNAs relevant for the brain's response [117]. Detailed step-by-step protocols are available to

minimize cellular content in body fluids and optimize downstream analyses of extracellular components [118].

To address blood-associated challenges in PCR-based analysis of extracellular miRNAs, a purification step can be introduced. In this study, we applied size exclusion chromatography to separate miRNAs associated with EVs from those bound to free proteins, as extracellular miRNAs have been shown to exist in both forms [38, 78, 93, 95, 117]. However, EV-associated miRNAs may have greater biomarker potential, as their encapsulation within EVs protects them from enzymatic degradation [119].

5.3. Targeted 87 miRNAs are present in post-TBI CSF but constitute only a small fraction of the total cDNA

In this study, a commercial PCR-array with 87 targeted miRNAs was analysed. All 87 targeted miRNAs were detected and quantified across all 4 CSF pools. However, the CSF from later days contained enlarged EVs carrying RNA which is yet to be characterized. Results showed that miRNA quantities varied by more than a million-fold between the most and least abundant miRNAs, with the highest miRNA levels detected in CSF pools d1–2 and d3–4 (Table 7, section 4.3., subsection 4.3.2.). Moreover, the results indicate significant sample contamination in the early post-traumatic days (Figure 6B in section 4.2., subsection 4.2.3.), suggesting that the discovered miRNAs are primarily derived from blood, specifically erythrocytes. Targeted miRNAs were chosen as commonly present in CSF with, globally, central nervous system (CNS) specificity. So, the detected miRNAs with highest levels in earliest days after the sTBI were miR-451a, miR-16-5p, miR-144-3p, miR-20a-5p, let-7b-5p, miR-15a-5p, miR-21-5p, miR-223-3p, miR-106a-5p, and miR-15b-5p.

Among those mentioned, miRNA-451a, stands out the most. Except the fact that it has the highest detected amounts among other detected miRNAs in d1–2 and d3–4, accumulated data showed that it is highly expressed in erythrocytes. Also, it can be packed into the erythrocytes EVs and pass easily through the compromised BBB [120]. Along with the role in erythropoiesis, study in animals showed that miRNA-451a can have an important role in neuronal growth and differentiation with inhibitory effect on cell proliferation [121]. Further experimental evidence provided the role of miRNA-451a in promoting apoptosis by activation of machinery in neurons affected with flaviviral infection [122]. Immunological role of miRNA-451 can also be seen through improving the function of circulating NK cells after acute ischemic stroke [123]. Aside from the experimental models, expression of miR-451a was detected in EVs that were characterized in EVD derived CSF sample of sTBI patients [78]. Patz et al. approached the data with caution, considering the lengthy 2-year sampling period and the inclusion of participants with injuries to various body areas in the study. The role of miRNA-451a in gene expression during brain events certainly emerges but, owing to the numerous technical

limitations of our and other studies, it is questionable whether it is really a brain-specific of blood-derived miRNA.

Our study found miR-16-5p as the second most prevalent among the discovered miRNAs. In the context of sTBI, the study demonstrated that downregulation of miR-16-5p isolated from plasma samples, was observed within the first 24 hours post-injury, corroborating our findings [74]. Authors claimed their assay had 100% sensitivity and specificity for discriminating sTBI from healthy volunteers. A separate study examined serum samples from patients with mild TBI and concurrent skull fractures [124]. The results indicated that the downregulation of miR-16-5p using antagomir-16-5p enhanced fracture healing by boosting osteoblast proliferation and blocking their apoptosis in patients with skull fractures associated with TBI. Conversely, in Alzheimer's disease, results of plasma samples investigations showed that miR-16-5p can provoke neuronal death by direct inhibition of BCL-2 genes [125]. Moreover, together with miR-15a, it can promote endothelial BBB dysregulation in ischemic stroke as it was described in recent experimental study in mouse [126]. The role of miR-15a/16-5p cluster was also described in ischemic mouse brain model where, after miR-15a/16-5p cluster suppression, vascular regeneration was promoted [127]. Furthermore, vascular endothelial receptors and fibroblast growth factors with associated receptors have been described as a main target of named cluster. Considering abovementioned fact, it is not surprising that the cluster has a stronger expression in non-brain tissue with primarily spleen enrichment. Furthermore, considering research that investigated miR-16-5p using blood-derived samples, caution in results interpretation is needed due to the potential release from

erythrocytes and other stress-induced cells of the haematopoietic system. To conduct a more precise analysis of samples, it is essential to consider the specificity of miRNAs' extensive function in gene expression under various situations, including haematopoietic system diseases. It is important to promptly eliminate sTBI patients from future research, similar to patients with leukemia, where miR-16-15p and miR-15a/b-5p function as both tumour suppressors and oncogenes [128].

The third most abundant miRNA in our study was miR-144-3-p. Previously conducted animal study suggested blood origin of named miRNA, showing that miR-144-3p can contribute to secondary brain injury after intracerebral haemorrhage (ICH). High amounts of miRNA have been quantified using real time PCR of the perihematoma region [129]. The intended target is downregulation of the formyl peptide receptor (FPR2) which subsequently contributes to neuronal death and the progression of brain damage. Consequently, miR-144-3p can induce neuronal death and cerebral damage by targeting and downregulating FPR2 through the stimulation of the PI3K/AKT signalling pathway, which is crucial for cell cycle regulation. The activation of the specified mechanism facilitates neuronal apoptosis. Authors proposed miRNA-

144-3p as potential biomarker for revealing ICH outcome, but with need for further studies. Dominantly, cellular activity of miRNA-144-3p has been associated with impaired cognitive function after aggravating neuronal death in hippocampus. This role has been investigated in an *in vivo* and *in vitro* models of mild, moderate, and sTBI through 7 days after the injury [130, 131]. Recent study described another role of miRNA-144-3p in hippocampal region. In mouse Alzheimer's disease models, miR-144-3p has been associated with cholinergic neuron degeneration characterized by synaptic disorders and memory damage after the nerve growth factor (NGF) maturation disturbance impairment [132]. Considering the findings of our study indicating a potential blood origin of the proposed miRNA, and due to the various technical limitations present in our and other research, it remains uncertain whether this miRNA is truly brain-specific or merely blood-derived as is suggested for other highly abundant miRNAs. Another highly abundant miRNA detected in this study, miRNA-20a-5p belongs to the miRNA-17~92 family. The described effect in CNS of this family is increased proliferation, accelerated neuronal differentiation, and apoptosis inhibition. Lastly, they are a key regulator of adult neurogenesis [133]. Function of named family is accomplished by targeting anti-neural and anti-proliferative genes, including tensin homolog (PTEN), Tp53, p21, and p27. Specifically, miRNA-20a-5p ameliorates neurite growth during the development of cortical and hippocampal neurons. Moreover, it has been detected that miR-20a-5p plays a crucial role in recovery after CNS injuries, mainly spinal cord injury where this miRNA facilitates axon regeneration. Related to the early detection in TBI, previous study detected the upregulation of miRNA-20a-5p in serum and CSF of mild, moderate and severe TBI patients 2 days after the injury [79]. Another study performed on the mild TBI patients and non-TBI patients showed the possibility to distinguish these groups using miRNA-20a-5p [134]. Also, research showed that using saliva, several miRNAs including miR-20a-5p, can help distinguish mild TBI athletes from non-injured athletes in first 3 days after the injury [73]. Even if it is not univocally expressed in CNS, miR-20a-5p definitely merits a further investigation as a potential biomarker during sTBI events.

Brain-specific pattern and function in inhibiting the proliferation of neuronal stem cell with a consecutive effect on neuronal differentiation has been proposed for let-7b-5p [66]. Moreover, let-7b-5p was singled out as miRNA with high expression in the brain tissue, arachnoid sheath and spinal cord [135]. Interestingly, high levels of saliva let-7b-5p have been detected 4 weeks after the injury in a study with mild TBI paediatric patients that suffered from post-traumatic fatigue and prolonged concussion syndrome [136]. On the other hand, in CSF samples individuals with Alzheimer's disease, let-7b-5p showed the possibility to induce neurodegeneration by activating RNA-sensing Toll-like receptor (TLR) 7 expressed on microglia cells abundantly across the CNS [137]. The opposite impacts of the same miRNA across various age groups stem from its biological diversity in gene expression, particularly within the context of distinct cellular activities in numerous brain pathological situations.

Therefore, adequate selection of patients is very important to prevent the “mask effect” of multi-target miRNA effects on gene expression.

Literature supports a neuroprotective role of another highly expressed miRNA in earliest days after the injury, miR-21-5p. The first report of named miRNA, showed that miR-21-5p have the highest increase in EVs of the controlled cortical impact (CCI)-induced sTBI mouse brain model, located in neurons near reactive microglia. Authors propose that the specified miRNA is of neuronal origin, evidenced by its elevated expression in neurons next to the damage site, potentially implicating it in neuron-glia signaling [101]. The limitation of the study comparing to our result is a rare sampling period for isolation and characterization of EVs performed 7 days after the injury. However, the interesting fact is that miRNA-21-5p levels in our results were higher, except in d1–2 and d3–4, also in CSF pools d5–6 and d7–12 when comparing to the remaining 8 isolated miRNAs. The only exception is the previously described miRNA-451a with quantitative dominance in all consecutive CSF pools. Notably, mice without brain injury did not exhibit elevated levels of miR-21 within the first 12 hours, suggesting that its upregulation may be injury-specific. [138]. Further experimental study conducted on adult (5-6 months) and aged (22-24 months) mice brains following CCI, detected increased levels of miRNA-21-5p in 1, 3, and 7 post-injury days at adult brains using real-time PCR that can be comparable with ours. The maximum increase was detected in first 24 hours after the injury. In brain of aging animals, miR-21-5p, interestingly, showed no injury response with continuous up-regulation in post-injury period. Authors proposed that up-regulation of miR-21-5p can be useful in the elderly following TBI [139]. Related to the aforementioned, in our study patient's median age was 33 years, classifying patients to the adult population. Therefore, we can possibly expect higher levels of miR-21-5 at sampling points in 1, 3, and 7 post-injury days as detected in samples of adult patients, but further studies on higher number of patients are well needed. In a series of described neuroprotective effects of miR-21-5p, its role in reducing of apoptosis in an *in vitro* model of TBI was also suggested, as well as suppressed Rab11a-mediated neuronal autophagy [140]. Lastly, proposed neuroprotective role of miR-21-5p in TBI, with highlight on apoptosis and inflammatory processes, are certainly worth further researches [141].

Except miR-21-5p, miR-223-3p showed pronounced role in brain TBI inflammatory processes with significant alteration in hippocampal cytoplasm and mitochondria as described in a study on CCI-mouse severe TBI models [142]. Moreover, miR-223-3p has been previously shown to be elevated in experimental models of hippocampal tissue and in cerebral cortex at different time points with last measured 72 hours after the sTBI [143, 144,145]. In a recent *in vitro* study, after cell injury, authors demonstrated the apoptosis inhibition in brain microvascular endothelial cells (BMCEs) induced by miR-223-3p. Based on these results, authors proposed the protective role of miR-223-3p on the BBB integrity and maintenance of

CNS microenvironment balance. The highest levels were 3 hours after injury [146]. Additionally, it was found that miR-223-3p inhibits inflammatory response in a mouse model of ICH that can lead to reduced brain oedema and better neurological outcome [147].

Very little is known about the role of miR-106a-5p in sTBI, but its levels were recorded in our study. So far, its role has been described in ICH mouse models treated with agent called baicalein - flavonoid and herbal antioxidant. It has been stated that baicalein can inhibit oxidative stress and slow progression of brain injury after ICH by activation of antioxidant pathway called Nrf2/ARE using miR-106a-5p [148].

Taken together, currently available data suggest that our 10 most abundantly detected miRNAs in CSF pools, could originate from different cells and have various effects on brain recovery. The primary source of miRNA in cerebrospinal fluid following sTBI is likely blood and potentially damaged cells due to the injury, including secondary injury when immune cells penetrate the brain via disrupted BBB. The blood content in CSF was further supported by detection of albumin and apolipoproteins across all CSF samples (Figure 5) [149, 150]. Additionally, this trend is most clearly illustrated in Figure 8C, where all 10 highly abundant miRNAs from our study exhibit a decline at varying rates. Although all 87 targeted miRNAs showed decreasing trend in downstream CSF pools with accompanying decline of haemolysis, depicted miRNAs showed different slopes. For example, miR-451a, described in the literature overview as most likely of blood origin, has shown the most pronounced decline in CSF pools, accompanied by a haemolysis decline. On the other hand, miR-21-5p which, based on the earlier description and literature review was promoted as a potentially neuroprotective brain-specific miRNA, has the least pronounced decline across the CSF pools. A more detailed analysis of miRNA origins with refined patient criteria is needed in future studies. We suggest the inclusion of only those patients who suffered diffuse axonal injury (DAI) to reduce mainly blood contamination as a consequence of various intracranial haemorrhages described as the most common pathoanatomical forms of sTBI which agrees with our study [20, 22]. DAI accounts for more than 30% of all sTBI pathologies and it is a leading cause of long-term vegetative state and morbidity among this group of patients. Due to a progressive course and brain changes that are primarily consequence of axons tearing and derangement, accompanying bleedings are mainly minor and focal. Therefore, brain magnetic resonance imaging is usually required to confirm the diagnosis [151]. Isolated DAI is certainly suggestive for an adequate patient's selection to be included in the study, which would greatly facilitate the CSF analysis.

What we can conclude so far is that in the first days after the injury, pathophysiological mechanisms of secondary injury are pronounced, including oxidative stress. Our results suggest that the total amount of targeted miRNAs has made up only a small portion of miRNAs applied in cDNA synthesis (Figure 8A, 8B in section 4.3., subsection 4.3.2.). The majority of detected miRNAs from our study suggest a blood origin. Moreover, we assumed that, despite the elevated haemolysis levels in CSF pools, the lowest levels were observed in the d5–6 and d7–12, suggesting that some miRNAs may not necessarily originate from blood. Certainly, all miRNAs achieve specific effects in the brain during a secondary injury with positive or negative effects on sTBI treatment outcomes. Considering the actuality of the topic and the need for early intervention during the sTBI treatment, further research is necessary.

5.4. Extracellular vesicles as a potential cargo for an only small portion of targeted miRNAs

The accepted knowledge that EVs carry miRNAs as their cargo, imposes the fact that EVs mediate intercellular communication with the presence of miRNAs as known regulators of gene expression. Many researches aim to understand the role of EVs miRNAs in the pathophysiology of sTBI, but with isolation and characterization remain major limitations [38, 39, 83, 101, 102, 103, 104]. The aforementioned limitations were not an exception even in our study, but progress was made by our group so far to facilitate laboratory techniques of EVs purification and characterization [90, 98].

To obtain more biological information, we decided to perform size-exclusion chromatography (SEC) on total CSF pools. The main aim was to detect and quantify miRNAs that are potential cargo of EVs following immunodetection of CD81, as well as albumin for free proteins (FP). Promising information was that both EVs and FPs can be carriers of miRNAs, with important highlight on EVs. EVs, with molecular components including miRNAs, enable stable cargo transport with protein and lipid surface content which enables interaction with target cell. There is a growing number of studies that support the fact that even EVs originating from the same cell type do not always have the same content and function [82].

Our previous work has shown that EVs can be successfully separated by size-exclusion chromatography (SEC) using Sepharose CL-6B column [90]. The efficiency of this SEC was further confirmed in current study since RNA concentrations in EV and FP fractions were sufficient for cDNA analysis. Interestingly, the sizes of EVs were comparable in all pools, except for the d7–12 where the largest EVs have been detected (Figure 11E, in section 4.4., subsection 4.4.1.). The EV concentrations showed decline with a pool's decrease in haemolysis level (Figure 11D, in section 4.4., subsection 4.4.1.). In addition to our findings, further, isolation and quantification of 87 targeted miRNAs from EVs and FPs fractions was performed.

The amounts of miRNAs in fractions were too low to ensure the significance and comparability of the results; however, given the previously mentioned neuroprotective effect of miR-21-5p, further investigations with a larger number of study participants are warranted. An intriguing subject for further clarification is whether the miRNAs are connected with FPs from lysed cells or if they originate from secretion by intact cells. Certain miRNAs were identified as prevalent in both EV and FP fractions. This can be attributed to 2 possibilities: firstly, incomplete separation, and secondly, the assumption that identical miRNAs may exist in both fractions, originating from the same cells. In this step of elucidating these questions, Next-Generation Sequencing (NGS) can help to profile expression of known miRNAs and detecting unknown miRNAs. Named technique has already been included in the study of miRNAs in the central nervous system [152].

The recent discovery that specific miRNAs in subsequent pools may derive from uncontaminated sources indicates that miR-142-3p, miR-204-5p, and miR-223-3p, previously identified as among the ten most abundant miRNAs in overall CSF pools, are uniquely and strongly enriched in the intriguing d5–6 and d7–12 pools. This enrichment is attributed to the minimal levels of haemolysis in these pools, suggesting the presence of miRNAs potentially not originating from blood. (Table 8 in section 4.4., subsection 4.4.3.). Along with the aforementioned and described role of miR-223-3p in the TBI that is definitely worth further investigations, miR-142-3p was described in earlier research as miRNA enriched in brain mitochondria under normal conditions, but after the TBI, levels were significantly decreased 12 hours after the injury. That could suggest that secondary brain injury and mitochondrial stress can also alter the mitochondrial association with certain miRNAs, including miR-142-3p [153]. Interesting recent study showed that miR-142 was increased in CCI- mouse induced sTBI model and in human post-TBI cortex 2 weeks after the injury [154]. After characterization, results show >200-fold higher expression for miR-142-3p than for miR-142-5p with miR-142-3p enriched predominantly in EVs. Overexpression was associated with potential promotion of brain inflammation via astrocyte activation. Except astrocyte activation, miR-142-3p was associated with myeloid and lymphoid cells also included in brain inflammation. This study can possibly match our result due to later enrichment of miR-142-3p in EVs fraction with possible damaging role after the sTBI. Role in regulation of immune system was also described in one study [155]. Considering the results of a study performed on patients with ischemic stroke and on mouse-induced ischemic stroke models, miR-204-5p promoted neuronal viability with an *in vitro* reduced apoptosis. Upregulation reduced infarct volume and neurological impairment in ischemia and reperfusion-induced neuronal damage [156]. Due to missing studies on human TBI models for miR-204-5p, CSF and blood samples were compared in patients with spontaneous intracerebral haemorrhage. The heat map showed highly expressed miR-204-5p in CSF that was associated with the regulation of matrix metalloproteinase-9 (MMP-9). The

levels of MMP-9 were decreased in CSF and increased in plasma 24 hours after the intracranial event. Elevated levels of MMP-9 in plasma during the acute phase have described role in increased BBB damage, haematoma growth, and worsening of perihematoma oedema. The potential neuroprotective role of miR-204-5p during acute injury may be suggested, but further investigations on sTBI patients are definitely needed to confirm given information's [157]. One of the latest studies performed on non-human models showed that downregulation of miR-204-5p can ameliorate cognitive impairment and hippocampal pathology by inhibiting neuronal autophagy and apoptosis [158].

Taken all together, our results showed high dynamic nature of sTBI. While targeted miRNAs are present in varying levels in CSF mostly as free protein-bound molecules rather than EV-enriched cargo, EVs containing miRNAs fluctuate after sTBI and likely originate from damaged cells, highlighting the complexity of miRNA dynamics in post-injury CSF. Main study limitation was the insufficient patient sample size and the significant influence of haemolysis on the quantity of 87 targeted miRNAs in the analysed pools. It is important to note that all CSF quantifications for sTBI patients reflect mean values for the specified days post-injury, as they represent the entire volume of discharged CSF. It is possible that dynamic changes occur during the mentioned time intervals that could not be detected by protocol used in this study. Analysis of CSF on individual samples would certainly provide more information and should be pursued, especially due to study results showing that CSF in later days contained larger EVs with RNA cargo than other CSF pools, and 10 detected miRNAs with highest levels have to be yet characterized due to their potential neuro-recovery signals.

6. CONCLUSIONS

Severe traumatic brain injury (sTBI) is a life-threatening intracranial injury with a complex pathophysiology. Released cerebrospinal fluid (CSF) might provide much needed biological information about brain events during sTBI, as well as in early neurorecovery. This study demonstrates dynamic changes during sTBI, potentially leading to the discovery of valuable sTBI biomarkers. Our objective was to investigate information regarding microRNA (miRNA) occurrences in the context of sTBI. Obtained are quantities of 87 putative CSF-origin miRNAs in patients with sTBI during the 12 days after the injury.

Summarized main findings are:

- All targeted 87 miRNAs were detected in different levels in CSF, suggesting a complex and dynamic regulatory environment in response to sTBI indicating their potential as biomarkers of recovery after the injury.
- The amounts of targeted miRNAs represent only a small portion of total miRNA content in CSF, indicating that many other, possibly uncharacterized miRNAs may play important roles in the post-injury period and should be explored in future studies.
- Extracellular vesicles (EVs) carrying miRNAs were found in all analysed CSF pools; however, their concentrations and sizes are changing daily following sTBI with significant challenge for reliable characterization, which remains a current limitation in field.
- The majority of targeted miRNAs were found to be in free protein-bound form, with only a small count of miRNAs enriched in EVs – likely reflecting current limitations in EV isolation and characterization methods, and underscoring the need for larger, more comprehensive studies to accurately assess their distribution.
- MiRNAs described as cargo of CSF-EVs most likely originate from lysed erythrocytes or other damaged/immune cells, suggesting that their presence may reflect secondary injury processes such as cell damage or neuroinflammation with improved sample quality and handling in future studies.

Unlike our study, new research should use more frequent sampling intervals for individual CSF samples, along with improved selection criteria for a larger patient cohort. Undoubtedly, the application of electron microscopy and next-generation sequencing techniques should yield more detailed profiles of extracellular vesicles (EVs) and miRNA. Moreover, incorporation of clinical markers that offer supplementary information could enhance the comprehension of intracranial processes following sTBI.

7. REFERENCES

1. Ng SY, Lee AYW. Traumatic Brain Injuries: Pathophysiology and Potential Therapeutic Targets. *Front Cell Neurosci.* 2019 Nov 27;13:528.
2. Bellander BM, Olafsson IH, Ghatan PH, Bro Skejo HP, Hansson LO, Wanecek M, et al. Secondary insults following traumatic brain injury enhance complement activation in the human brain and release of the tissue damage marker S100B. *Acta Neurochir (Wien).* 2011 Jan;153(1):90–100.
3. Dewan MC, Rattani A, Gupta S, Baticulon RE, Hung YC, Punchak M, et al. Estimating the global incidence of traumatic brain injury. *J Neurosurg.* 2019 Apr;130(4):1080–97.
4. Haarbauer-Krupa J, Pugh MJ, Prager EM, Harmon N, Wolfe J, Yaffe K. Epidemiology of Chronic Effects of Traumatic Brain Injury. *J Neurotrauma.* 2021 Dec 1;38(23):3235–47.
5. Tenovuo O, Diaz-Arrastia R, Goldstein LE, Sharp DJ, van der Naalt J, Zasler ND. Assessing the Severity of Traumatic Brain Injury—Time for a Change? *J Clin Med.* 2021 Jan 4;10(1):148.
6. Hawryluk GWJ, Manley GT. Classification of traumatic brain injury. In: *Handbook of Clinical Neurology* [Internet]. Elsevier; 2015 [cited 2025 Mar 6]. p. 15–21. Available from: <https://linkinghub.elsevier.com/retrieve/pii/B9780444528926000027>
7. Foreman BP, Caesar RR, Parks J, Madden C, Gentilello LM, Shafi S, et al. Usefulness of the Abbreviated Injury Score and the Injury Severity Score in Comparison to the Glasgow Coma Scale in Predicting Outcome After Traumatic Brain Injury. *J Trauma Inj Infect Crit Care.* 2007 Apr;62(4):946–50.
8. Bodien YG, Barra A, Temkin NR, Barber J, Foreman B, Vassar M, et al. Diagnosing Level of Consciousness: The Limits of the Glasgow Coma Scale Total Score. *J Neurotrauma.* 2021 Dec 1;38(23):3295–305.
9. Brazinova A, Rehorcikova V, Taylor MS, Buckova V, Majdan M, Psota M, et al. Epidemiology of Traumatic Brain Injury in Europe: A Living Systematic Review. *J Neurotrauma.* 2021 May 15;38(10):1411–40.
10. Tagliaferri F, Compagnone C, Korsic M, Servadei F, Kraus J. A systematic review of brain injury epidemiology in Europe. *Acta Neurochir (Wien).* 2006 Mar;148(3):255–68.

11. Bruns J, Hauser WA. The Epidemiology of Traumatic Brain Injury: A Review. *Epilepsia*. 2003 Oct;44(s10):2–10.
12. Feigin VL, Theadom A, Barker-Collo S, Starkey NJ, McPherson K, Kahan M, et al. Incidence of traumatic brain injury in New Zealand: a population-based study. *Lancet Neurol*. 2013 Jan;12(1):53–64.
13. Jha S, Ghewade P. Management and Treatment of Traumatic Brain Injuries. *Cureus* [Internet]. 2022 Oct 23 [cited 2025 Mar 6]; Available from: <https://www.cureus.com/articles/109082-management-and-treatment-of-traumatic-brain-injuries>
14. Roozenbeek B, Maas AIR, Menon DK. Changing patterns in the epidemiology of traumatic brain injury. *Nat Rev Neurol*. 2013 Apr;9(4):231–6.
15. Biegon A. Considering Biological Sex in Traumatic Brain Injury. *Front Neurol*. 2021 Feb 10;12:576366.
16. Blennow K, Brody DL, Kochanek PM, Levin H, McKee A, Ribbers GM, et al. Traumatic brain injuries. *Nat Rev Dis Primer*. 2016 Nov 17;2(1):16084.
17. Hardman JM, Manoukian A. Pathology of head trauma. *Neuroimaging Clin N Am*. 2002 May;12(2):175–87.
18. Saatman KE, Duhaime AC, Bullock R, Maas AIR, Valadka A, Manley GT. Classification of Traumatic Brain Injury for Targeted Therapies. *J Neurotrauma*. 2008 Jul;25(7):719–38.
19. Morrison AL, King TM, Korell MA, Smialek JE, Troncoso JC. Acceleration-Deceleration Injuries to the Brain in Blunt Force Trauma: *Am J Forensic Med Pathol*. 1998 Jun;19(2):109–12.
20. Mutch CA, Talbott JF, Gean A. Imaging Evaluation of Acute Traumatic Brain Injury. *Neurosurg Clin N Am*. 2016 Oct;27(4):409–39.
21. Mckee AC, Daneshvar DH. The neuropathology of traumatic brain injury. In: *Handbook of Clinical Neurology* [Internet]. Elsevier; 2015 [cited 2025 Mar 6]. p. 45–66. Available from: <https://linkinghub.elsevier.com/retrieve/pii/B9780444528926000040>
22. Lolli V, Pezzullo M, Delpierre I, Sadeghi N. MDCT imaging of traumatic brain injury. *Br J Radiol*. 2016 May;89(1061):20150849.
23. Aromatario M, Torsello A, D’Errico S, Bertozzi G, Sessa F, Cipolloni L, et al. Traumatic

Epidural and Subdural Hematoma: Epidemiology, Outcome, and Dating. *Medicina (Mex)*. 2021 Feb 1;57(2):125.

24. Servadei F, Murray GD, Teasdale GM, Dearden M, Iannotti F, Lapierre F, et al. Traumatic Subarachnoid Hemorrhage: Demographic and Clinical Study of 750 Patients from the European Brain Injury Consortium Survey of Head Injuries. *Neurosurgery*. 2002 Feb 1;50(2):261–9.
25. Li CY, Chuang CC, Chen CC, Tu PH, Wang YC, Yeap MC, et al. The Role of Intraventricular Hemorrhage in Traumatic Brain Injury: A Novel Scoring System. *J Clin Med*. 2022 Apr 11;11(8):2127.
26. Veenith T, Goon SS, Burnstein RM. Molecular mechanisms of traumatic brain injury: the missing link in management. *World J Emerg Surg*. 2009 Dec;4(1):7.
27. Narayan RK, Michel ME, Ansell B, Baethmann A, Biegon A, Bracken MB, et al. Clinical Trials in Head Injury. *J Neurotrauma*. 2002 May;19(5):503–57.
28. Hawryluk GWJ, Rubiano AM, Totten AM, O'Reilly C, Ullman JS, Bratton SL, et al. Guidelines for the Management of Severe Traumatic Brain Injury: 2020 Update of the Decompressive Craniectomy Recommendations. *Neurosurgery*. 2020 Sep;87(3):427–34.
29. Dash HH, Chavali S. Management of traumatic brain injury patients. *Korean J Anesthesiol*. 2018;71(1):12.
30. Balestreri M, Czosnyka M, Hutchinson P, Steiner LA, Hiler M, Smielewski P, et al. Impact of Intracranial Pressure and Cerebral Perfusion Pressure on Severe Disability and Mortality After Head Injury. *Neurocrit Care*. 2006;4(1):008–13.
31. Chau CYC, Craven CL, Rubiano AM, Adams H, Tülü S, Czosnyka M, et al. The Evolution of the Role of External Ventricular Drainage in Traumatic Brain Injury. *J Clin Med*. 2019 Sep 10;8(9):1422.
32. Kochanek PM, Jackson TC, Jha RM, Clark RSB, Okonkwo DO, Bayir H, et al. Paths to Successful Translation of New Therapies for Severe Traumatic Brain Injury in the Golden Age of Traumatic Brain Injury Research: A Pittsburgh Vision. *J Neurotrauma*. 2020 Nov 15;37(22):2353–71.
33. Wright DW, Kellermann AL, Hertzberg VS, Clark PL, Frankel M, Goldstein FC, et al. ProTECT: A Randomized Clinical Trial of Progesterone for Acute Traumatic Brain Injury. *Ann Emerg Med*. 2007 Apr;49(4):391-402.e2.

34. Tani J, Wen YT, Hu CJ, Sung JY. Current and Potential Pharmacologic Therapies for Traumatic Brain Injury. *Pharmaceuticals*. 2022 Jul 6;15(7):838.
35. Cheng G, Kong R hua, Zhang L ming, Zhang J ning. Mitochondria in traumatic brain injury and mitochondrial-targeted multipotential therapeutic strategies: Mitochondria in traumatic brain injury. *Br J Pharmacol*. 2012 Oct;167(4):699–719.
36. Mozaffari K, Dejam D, Duong C, Ding K, French A, Ng E, et al. Systematic Review of Serum Biomarkers in Traumatic Brain Injury. *Cureus* [Internet]. 2021 Aug 10 [cited 2025 Mar 6]; Available from: <https://www.cureus.com/articles/66204-systematic-review-of-serum-biomarkers-in-traumatic-brain-injury>
37. Ingebrigtsen T, Romner B, Kock-Jensen C. Scandinavian Guidelines for Initial Management of Minimal, Mild, and Moderate Head Injuries: *J Trauma Inj Infect Crit Care*. 2000 Apr;48(4):760–6.
38. Pinchi E, Luigi C, Paola S, Gianpietro V, Raoul T, Mauro A, et al. MicroRNAs: The New Challenge for Traumatic Brain Injury Diagnosis. *Curr Neuropharmacol*. 2020 Mar 20;18(4):319–31.
39. Guedes VA, Devoto C, Leete J, Sass D, Acott JD, Mithani S, et al. Extracellular Vesicle Proteins and MicroRNAs as Biomarkers for Traumatic Brain Injury. *Front Neurol*. 2020 Jul 16;11:663.
40. Bramlett HM, Dietrich WD. Long-Term Consequences of Traumatic Brain Injury: Current Status of Potential Mechanisms of Injury and Neurological Outcomes. *J Neurotrauma*. 2015 Dec;32(23):1834–48.
41. Jarrahi A, Braun M, Ahluwalia M, Gupta RV, Wilson M, Munie S, et al. Revisiting Traumatic Brain Injury: From Molecular Mechanisms to Therapeutic Interventions. *Biomedicines*. 2020 Sep 29;8(10):389.
42. Thapa K, Khan H, Singh TG, Kaur A. Traumatic Brain Injury: Mechanistic Insight on Pathophysiology and Potential Therapeutic Targets. *J Mol Neurosci*. 2021 Sep;71(9):1725–42.
43. Wyllie DJA, Livesey MR, Hardingham GE. Influence of GluN2 subunit identity on NMDA receptor function. *Neuropharmacology*. 2013 Nov;74:4–17.
44. Tehse J, Taghibiglou C. The Overlooked Aspect of Excitotoxicity: Glutamate-Independent Excitotoxicity in Traumatic Brain Injuries. *Eur J Neurosci*. 2018 Dec 16;ejn.14307.

45. Liao R, Wood TR, Nance E. Nanotherapeutic modulation of excitotoxicity and oxidative stress in acute brain injury. *Nanobiomedicine*. 2020 Jan 1;7:184954352097081.
46. Hiebert JB, Shen Q, Thimmesch AR, Pierce JD. Traumatic Brain Injury and Mitochondrial Dysfunction. *Am J Med Sci*. 2015 Aug;350(2):132–8.
47. Manevich Y, Hutchens S, Halushka PV, Tew KD, Townsend DM, Jauch EC, et al. Peroxiredoxin VI oxidation in cerebrospinal fluid correlates with traumatic brain injury outcome. *Free Radic Biol Med*. 2014 Jul;72:210–21.
48. Ismail H, Shakkour Z, Tabet M, Abdelhady S, Kobaisi A, Abedi R, et al. Traumatic Brain Injury: Oxidative Stress and Novel Anti-Oxidants Such as Mitoquinone and Edaravone. *Antioxidants*. 2020 Oct 1;9(10):943.
49. Tran LV. Understanding the Pathophysiology of Traumatic Brain Injury and the Mechanisms of Action of Neuroprotective Interventions. *J Trauma Nurs*. 2014 Jan;21(1):30–5.
50. Harrison J, Rowe R, Lifshitz J. Lipid mediators of inflammation in neurological injury: shifting the balance toward resolution. *Neural Regen Res*. 2016;11(1):77.
51. Akamatsu Y, Hanafy KA. Cell Death and Recovery in Traumatic Brain Injury. *Neurotherapeutics*. 2020 Apr;17(2):446–56.
52. Cash A, Theus MH. Mechanisms of Blood–Brain Barrier Dysfunction in Traumatic Brain Injury. *Int J Mol Sci*. 2020 May 8;21(9):3344.
53. Jha RM, Kochanek PM, Simard JM. Pathophysiology and treatment of cerebral edema in traumatic brain injury. *Neuropharmacology*. 2019 Feb;145:230–46.
54. Ghaith HS, Nawar AA, Gabra MD, Abdelrahman ME, Nafady MH, Bahbah EI, et al. A Literature Review of Traumatic Brain Injury Biomarkers. *Mol Neurobiol*. 2022 Jul;59(7):4141–58.
55. Ardekani AM, Naeini MM. The Role of MicroRNAs in Human Diseases. *Avicenna J Med Biotechnol*. 2010 Oct;2(4):161–79.
56. O'Brien J, Hayder H, Zayed Y, Peng C. Overview of MicroRNA Biogenesis, Mechanisms of Actions, and Circulation. *Front Endocrinol*. 2018 Aug 3;9:402.
57. Shukla GC, Singh J, Barik S. MicroRNAs: Processing, Maturation, Target Recognition and Regulatory Functions. *Mol Cell Pharmacol*. 2011;3(3):83–92.

58. Winter J, Diederichs S. Argonaute proteins regulate microRNA stability: Increased microRNA abundance by Argonaute proteins is due to microRNA stabilization. *RNA Biol.* 2011 Nov;8(6):1149–57.
59. Hutvagner G, Simard MJ. Argonaute proteins: key players in RNA silencing. *Nat Rev Mol Cell Biol.* 2008 Jan;9(1):22–32.
60. Smibert P, Yang JS, Azzam G, Liu JL, Lai EC. Homeostatic control of Argonaute stability by microRNA availability. *Nat Struct Mol Biol.* 2013 Jul;20(7):789–95.
61. Mauro M, Berretta M, Palermo G, Cavalieri V, La Rocca G. The Multiplicity of Argonaute Complexes in Mammalian Cells. *J Pharmacol Exp Ther.* 2023 Jan;384(1):1–9.
62. Wilczynska A, Bushell M. The complexity of miRNA-mediated repression. *Cell Death Differ.* 2015 Jan;22(1):22–33.
63. O'Carroll D, Schaefer A. General Principles of miRNA Biogenesis and Regulation in the Brain. *Neuropsychopharmacology.* 2013 Jan;38(1):39–54.
64. Prodromidou K, Matsas R. Species-Specific miRNAs in Human Brain Development and Disease. *Front Cell Neurosci.* 2019 Dec 18;13:559.
65. Adlakha YK, Saini N. Brain microRNAs and insights into biological functions and therapeutic potential of brain enriched miRNA-128. *Mol Cancer.* 2014;13(1):33.
66. Nowak JS, Michlewski G. miRNAs in development and pathogenesis of the nervous system. *Biochem Soc Trans.* 2013 Aug 1;41(4):815–20.
67. Ma Q, Zhang L, Pearce WJ. MicroRNAs in brain development and cerebrovascular pathophysiology. *Am J Physiol-Cell Physiol.* 2019 Jul 1;317(1):C3–19.
68. Yoo AS, Sun AX, Li L, Shcheglovitov A, Portmann T, Li Y, et al. MicroRNA-mediated conversion of human fibroblasts to neurons. *Nature.* 2011 Aug;476(7359):228–31.
69. Sun Y, Luo ZM, Guo XM, Su DF, Liu X. An updated role of microRNA-124 in central nervous system disorders: a review. *Front Cell Neurosci* [Internet]. 2015 May 20 [cited 2025 Mar 6];9. Available from: http://www.frontiersin.org/Cellular_Neuroscience/10.3389/fncel.2015.00193/abstract
70. Wang H, Taguchi YH, Liu X. Editorial: miRNAs and Neurological Diseases. *Front Neurol.* 2021 Apr 20;12:662373.

71. Zhou Q, Yin J, Wang Y, Zhuang X, He Z, Chen Z, et al. MicroRNAs as potential biomarkers for the diagnosis of Traumatic Brain Injury: A systematic review and meta-analysis. *Int J Med Sci.* 2021;18(1):128–36.
72. Schober K, Ondruschka B, Dreßler J, Abend M. Detection of hypoxia markers in the cerebellum after a traumatic frontal cortex injury: a human postmortem gene expression analysis. *Int J Legal Med.* 2015 Jul;129(4):701–7.
73. Di Pietro V, Porto E, Ragusa M, Barbagallo C, Davies D, Forcione M, et al. Salivary MicroRNAs: Diagnostic Markers of Mild Traumatic Brain Injury in Contact-Sport. *Front Mol Neurosci.* 2018 Aug 20;11:290.
74. Redell JB, Moore AN, Ward NH, Hergenroeder GW, Dash PK. Human Traumatic Brain Injury Alters Plasma microRNA Levels. *J Neurotrauma.* 2010 Dec;27(12):2147–56.
75. Yang T, Song J, Bu X, Wang C, Wu J, Cai J, et al. Elevated serum miR-93, miR-191, and miR-499 are noninvasive biomarkers for the presence and progression of traumatic brain injury. *J Neurochem.* 2016 Apr;137(1):122–9.
76. O'Connell GC, Smothers CG, Winkelman C. Bioinformatic analysis of brain-specific miRNAs for identification of candidate traumatic brain injury blood biomarkers. *Brain Inj.* 2020 Jun 6;34(7):965–74.
77. Hiskens MI, Mengistu TS, Li KM, Fenning AS. Systematic Review of the Diagnostic and Clinical Utility of Salivary microRNAs in Traumatic Brain Injury (TBI). *Int J Mol Sci.* 2022 Oct 29;23(21):13160.
78. Patz S, Tractnig C, Grünbacher G, Ebner B, Güllly C, Novak A, et al. More than Cell Dust: Microparticles Isolated from Cerebrospinal Fluid of Brain Injured Patients Are Messengers Carrying mRNAs, miRNAs, and Proteins. *J Neurotrauma.* 2013 Jul 15;30(14):1232–42.
79. Bhomia M, Balakathiresan NS, Wang KK, Papa L, Maheshwari RK. A Panel of Serum MiRNA Biomarkers for the Diagnosis of Severe to Mild Traumatic Brain Injury in Humans. *Sci Rep.* 2016 Jun 24;6(1):28148.
80. You WD, Tang QL, Wang L, Lei J, Feng JF, Mao Q, et al. Alteration of microRNA expression in cerebrospinal fluid of unconscious patients after traumatic brain injury and a bioinformatic analysis of related single nucleotide polymorphisms. *Chin J Traumatol.* 2016 Feb;19(1):11–5.
81. Phillips W, Willms E, Hill AF. Understanding extracellular vesicle and nanoparticle heterogeneity: Novel methods and considerations. *PROTEOMICS.* 2021 Jul;21(13–

14):2000118.

82. Abels ER, Breakefield XO. Introduction to Extracellular Vesicles: Biogenesis, RNA Cargo Selection, Content, Release, and Uptake. *Cell Mol Neurobiol*. 2016 Apr;36(3):301–12.
83. Théry C, Witwer KW, Aikawa E, Alcaraz MJ, Anderson JD, Andriantsitohaina R, et al. Minimal information for studies of extracellular vesicles 2018 (MISEV2018): a position statement of the International Society for Extracellular Vesicles and update of the MISEV2014 guidelines. *J Extracell Vesicles*. 2018 Dec;7(1):1535750.
84. Gurung S, Perocheau D, Touramanidou L, Baruteau J. The exosome journey: from biogenesis to uptake and intracellular signalling. *Cell Commun Signal*. 2021 Apr 23;19(1):47.
85. Nederveen JP, Warnier G, Di Carlo A, Nilsson MI, Tarnopolsky MA. Extracellular Vesicles and Exosomes: Insights From Exercise Science. *Front Physiol*. 2021 Feb 1;11:604274.
86. Huda MN, Nafiujjaman M, Deaguero IG, Okonkwo J, Hill ML, Kim T, et al. Potential Use of Exosomes as Diagnostic Biomarkers and in Targeted Drug Delivery: Progress in Clinical and Preclinical Applications. *ACS Biomater Sci Eng*. 2021 Jun 14;7(6):2106–49.
87. Valadi H, Ekström K, Bossios A, Sjöstrand M, Lee JJ, Lötvall JO. Exosome-mediated transfer of mRNAs and microRNAs is a novel mechanism of genetic exchange between cells. *Nat Cell Biol*. 2007 Jun;9(6):654–9.
88. Clancy JW, Schmidtman M, D'Souza-Schorey C. The ins and outs of microvesicles. *FASEB BioAdvances*. 2021 Jun;3(6):399–406.
89. Li M, Liao L, Tian W. Extracellular Vesicles Derived From Apoptotic Cells: An Essential Link Between Death and Regeneration. *Front Cell Dev Biol*. 2020 Oct 2;8:573511.
90. Krušić Alić V, Malenica M, Biberić M, Zrna S, Valenčić L, Šuput A, et al. Extracellular Vesicles from Human Cerebrospinal Fluid Are Effectively Separated by Sepharose CL-6B—Comparison of Four Gravity-Flow Size Exclusion Chromatography Methods. *Biomedicines*. 2022 Mar 27;10(4):785.
91. Norman M, Ter-Ovanesyan D, Trieu W, Lazarovits R, Kowal EJK, Lee JH, et al. L1CAM is not associated with extracellular vesicles in human cerebrospinal fluid or plasma. *Nat Methods*. 2021 Jun;18(6):631–4.
92. Busatto S, Morad G, Guo P, Moses MA. The role of extracellular vesicles in the physiological and pathological regulation of the blood–brain barrier. *FASEB BioAdvances*. 2021 Sep;3(9):665–75.

93. Khan NA, Asim M, El-Menyar A, Biswas KH, Rizoli S, Al-Thani H. The evolving role of extracellular vesicles (exosomes) as biomarkers in traumatic brain injury: Clinical perspectives and therapeutic implications. *Front Aging Neurosci.* 2022 Oct 6;14:933434.
94. Sjoqvist S, Otake K, Hirozane Y. Analysis of Cerebrospinal Fluid Extracellular Vesicles by Proximity Extension Assay: A Comparative Study of Four Isolation Kits. *Int J Mol Sci.* 2020 Dec 10;21(24):9425.
95. Wu P, Zhang B, Ocansey DKW, Xu W, Qian H. Extracellular vesicles: A bright star of nanomedicine. *Biomaterials.* 2021 Feb;269:120467.
96. Nekludov M, Bellander BM, Gryth D, Wallen H, Mobarrez F. Brain-Derived Microparticles in Patients with Severe Isolated TBI. *Brain Inj.* 2017 Dec 6;31(13–14):1856–62.
97. de Rivero Vaccari JP, Brand F, Adamczak S, Lee SW, Perez-Barcena J, Wang MY, et al. Exosome-mediated inflammasome signaling after central nervous system injury. *J Neurochem.* 2016 Jan;136(S1):39–48.
98. Kuharić J, Grabušić K, Tokmadžić VS, Štifter S, Tulić K, Shevchuk O, et al. Severe Traumatic Brain Injury Induces Early Changes in the Physical Properties and Protein Composition of Intracranial Extracellular Vesicles. *J Neurotrauma.* 2019 Jan 15;36(2):190–200.
99. Sadik N, Cruz L, Gurtner A, Rodosthenous RS, Dusoswa SA, Ziegler O, et al. Extracellular RNAs: A New Awareness of Old Perspectives. In: Patel T, editor. *Extracellular RNA* [Internet]. New York, NY: Springer New York; 2018 [cited 2025 Mar 6]. p. 1–15. (Methods in Molecular Biology; vol. 1740). Available from: http://link.springer.com/10.1007/978-1-4939-7652-2_1
100. Albanese M, Chen YFA, Hüls C, Gärtner K, Tagawa T, Mejias-Perez E, et al. MicroRNAs are minor constituents of extracellular vesicles that are rarely delivered to target cells. He L, editor. *PLOS Genet.* 2021 Dec 6;17(12):e1009951.
101. Harrison EB, Hochfelder CG, Lamberty BG, Meays BM, Morsey BM, Kelso ML, et al. Traumatic brain injury increases levels of miR-21 in extracellular vesicles: implications for neuroinflammation. *FEBS Open Bio.* 2016 Aug;6(8):835–46.
102. Ko J, Hemphill M, Yang Z, Beard K, Sewell E, Shallcross J, et al. Multi-Dimensional Mapping of Brain-Derived Extracellular Vesicle MicroRNA Biomarker for Traumatic Brain Injury Diagnostics. *J Neurotrauma.* 2020 Nov 15;37(22):2424–34.
103. Huang S, Ge X, Yu J, Han Z, Yin Z, Li Y, et al. Increased miR-124-3p in microglial

exosomes following traumatic brain injury inhibits neuronal inflammation and contributes to neurite outgrowth *via* their transfer into neurons. *FASEB J.* 2018 Jan;32(1):512–28.

104. Long X, Yao X, Jiang Q, Yang Y, He X, Tian W, et al. Astrocyte-derived exosomes enriched with miR-873a-5p inhibit neuroinflammation via microglia phenotype modulation after traumatic brain injury. *J Neuroinflammation.* 2020 Dec;17(1):89.
105. The Nuremberg Code (1947). *BMJ.* 1996 Dec 7;313(7070):1448–1448.
106. World Medical Association Declaration of Helsinki: Ethical Principles for Medical Research Involving Human Subjects. *JAMA.* 2013 Nov 27;310(20):2191.
107. Beauchamp T, Childress J. *Principles of Biomedical Ethics*: Marking Its Fortieth Anniversary. *Am J Bioeth.* 2019 Nov 2;19(11):9–12.
108. Collins MA, An J, Peller D, Bowser R. Total protein is an effective loading control for cerebrospinal fluid western blots. *J Neurosci Methods.* 2015 Aug;251:72–82.
109. Moldovan L, Batte KE, Trgovcich J, Wisler J, Marsh CB, Piper M. Methodological challenges in utilizing miRNA s as circulating biomarkers. *J Cell Mol Med.* 2014 Mar;18(3):371–90.
110. Obika S, Nanbu D, Hari Y, Morio K ichiro, In Y, Ishida T, et al. Synthesis of 2'-O,4'-C-methyleneuridine and -cytidine. Novel bicyclic nucleosides having a fixed C3, -endo sugar puckering. *Tetrahedron Lett.* 1997 Dec;38(50):8735–8.
111. Welsh JA, Goberdhan DCI, O'Driscoll L, Buzas EI, Blenkiron C, Bussolati B, et al. Minimal information for studies of extracellular vesicles (MISEV2023): From basic to advanced approaches. *J Extracell Vesicles.* 2024 Feb;13(2):e12404.
112. De Simone G, di Masi A, Ascenzi P. Serum Albumin: A Multifaced Enzyme. *Int J Mol Sci.* 2021 Sep 18;22(18):10086.
113. Seršić LV, Alić VK, Biberić M, Zrna S, Jagoić T, Tarčuković J, et al. Real-Time PCR Quantification of 87 miRNAs from Cerebrospinal Fluid: miRNA Dynamics and Association with Extracellular Vesicles after Severe Traumatic Brain Injury. *Int J Mol Sci.* 2023 Mar 1;24(5):4751.
114. Mollayeva T, Mollayeva S, Pacheco N, Colantonio A. Systematic Review of Sex and Gender Effects in Traumatic Brain Injury: Equity in Clinical and Functional Outcomes. *Front Neurol.* 2021 Sep 10;12:678971.

115. Podkovik S, Kashyap S, Wiginton J, Kang C, Mo K, Goodrich M, et al. Comparison of Ventricular and Lumbar Cerebrospinal Fluid Composition. *Cureus* [Internet]. 2020 Jul 21 [cited 2025 Mar 6]; Available from: <https://www.cureus.com/articles/33859-comparison-of-ventricular-and-lumbar-cerebrospinal-fluid-composition>
116. Sidstedt M, Hedman J, Romsos EL, Waitara L, Wadsö L, Steffen CR, et al. Inhibition mechanisms of hemoglobin, immunoglobulin G, and whole blood in digital and real-time PCR. *Anal Bioanal Chem*. 2018 Apr;410(10):2569–83.
117. Blondal T, Jensby Nielsen S, Baker A, Andreasen D, Mouritzen P, Wrang Teilum M, et al. Assessing sample and miRNA profile quality in serum and plasma or other biofluids. *Methods*. 2013 Jan;59(1):S1–6.
118. Nieuwland R, Siljander PR. A beginner's guide to study extracellular vesicles in human blood plasma and serum. *J Extracell Vesicles*. 2024 Jan;13(1):e12400.
119. Atif H, Hicks SD. A Review of MicroRNA Biomarkers in Traumatic Brain Injury. *J Exp Neurosci*. 2019 Jan;13:117906951983228.
120. Koopaei NN, Chowdhury EA, Jiang J, Noorani B, da Silva L, Bulut G, et al. Enrichment of the erythrocyte miR-451a in brain extracellular vesicles following impairment of the blood-brain barrier. *Neurosci Lett*. 2021 Apr;751:135829.
121. Trattinig C, Üçal M, Tam-Amersdorfer C, Bucko A, Zefferer U, Grünbacher G, et al. MicroRNA-451a overexpression induces accelerated neuronal differentiation of Ntera2/D1 cells and ablation affects neurogenesis in microRNA-451a^{-/-} mice. Klymkowsky M, editor. *PLOS ONE*. 2018 Nov 21;13(11):e0207575.
122. Chakraborty S, Basu A. miR-451a Regulates Neuronal Apoptosis by Modulating 14-3-3ζ-JNK Axis upon Flaviviral Infection. Lee B, editor. *mSphere*. 2022 Aug 31;7(4):e00208-22.
123. Kong Y, Li S, Cheng X, Ren H, Zhang B, Ma H, et al. Brain Ischemia Significantly Alters microRNA Expression in Human Peripheral Blood Natural Killer Cells. *Front Immunol*. 2020 May 14;11:759.
124. Kim YJ, Kim SH, Park Y, Park J, Lee JH, Kim BC, et al. miR-16-5p is upregulated by amyloid β deposition in Alzheimer's disease models and induces neuronal cell apoptosis through direct targeting and suppression of BCL-2. *Exp Gerontol*. 2020 Jul;136:110954.
125. Sun Y, Xiong Y, Yan C, Chen L, Chen D, Mi B, et al. Downregulation of microRNA-16-5p accelerates fracture healing by promoting proliferation and inhibiting apoptosis of osteoblasts

in patients with traumatic brain injury. *Am J Transl Res*. 2019;11(8):4746–60.

126. Sun P, Zhang K, Hassan SH, Zhang X, Tang X, Pu H, et al. Endothelium-Targeted Deletion of microRNA-15a/16-1 Promotes Poststroke Angiogenesis and Improves Long-Term Neurological Recovery. *Circ Res*. 2020 Apr 10;126(8):1040–57.
127. Wang WX, Danaher RJ, Miller CS, Berger JR, Nubia VG, Wilfred BS, et al. Expression of miR-15/107 Family MicroRNAs in Human Tissues and Cultured Rat Brain Cells. *Genomics Proteomics Bioinformatics*. 2014 Feb 1;12(1):19–30.
128. Mardani R, Jafari Najaf Abadi MH, Motieian M, Taghizadeh-Boroujeni S, Bayat A, Farsinezhad A, et al. MicroRNA in leukemia: Tumor suppressors and oncogenes with prognostic potential. *J Cell Physiol*. 2019 Jun;234(6):8465–86.
129. Fan W, Li X, Zhang D, Li H, Shen H, Liu Y, et al. Detrimental Role of miRNA-144-3p in Intracerebral Hemorrhage Induced Secondary Brain Injury is Mediated by Formyl Peptide Receptor 2 Downregulation Both *In Vivo* and *In Vitro*. *Cell Transplant*. 2019 Jun;28(6):723–38.
130. Sun L, Zhao M, Zhang J, Liu A, Ji W, Li Y, et al. MiR-144 promotes β -amyloid accumulation-induced cognitive impairments by targeting ADAM10 following traumatic brain injury. *Oncotarget*. 2017 Aug 29;8(35):59181–203.
131. Liu L, Sun T, Liu Z, Chen X, Zhao L, Qu G, et al. Traumatic Brain Injury Dysregulates MicroRNAs to Modulate Cell Signaling in Rat Hippocampus. Scavone C, editor. *PLoS ONE*. 2014 Aug 4;9(8):e103948.
132. Zhou LT, Zhang J, Tan L, Huang HZ, Zhou Y, Liu ZQ, et al. Elevated Levels of miR-144-3p Induce Cholinergic Degeneration by Impairing the Maturation of NGF in Alzheimer's Disease. *Front Cell Dev Biol*. 2021 Apr 9;9:667412.
133. Arzhanov I, Sintakova K, Romanyuk N. The Role of miR-20 in Health and Disease of the Central Nervous System. *Cells*. 2022 May 3;11(9):1525.
134. Di Pietro V, Yakoub KM, Scarpa U, Di Pietro C, Belli A. MicroRNA Signature of Traumatic Brain Injury: From the Biomarker Discovery to the Point-of-Care. *Front Neurol*. 2018 Jun 14;9:429.
135. Ludwig N, Leidinger P, Becker K, Backes C, Fehlmann T, Pallasch C, et al. Distribution of miRNA expression across human tissues. *Nucleic Acids Res*. 2016 May 5;44(8):3865–77.
136. Johnson JJ, Loeffert AC, Stokes J, Olympia RP, Bramley H, Hicks SD. Association of

Salivary MicroRNA Changes With Prolonged Concussion Symptoms. *JAMA Pediatr.* 2018 Jan 1;172(1):65.

137. Lehmann SM, Krüger C, Park B, Derkow K, Rosenberger K, Baumgart J, et al. An unconventional role for miRNA: let-7 activates Toll-like receptor 7 and causes neurodegeneration. *Nat Neurosci.* 2012 Jun;15(6):827–35.
138. Meissner L, Gallozzi M, Balbi M, Schwarzmaier S, Tiedt S, Terpolilli NA, et al. Temporal Profile of MicroRNA Expression in Contused Cortex after Traumatic Brain Injury in Mice. *J Neurotrauma.* 2016 Apr 15;33(8):713–20.
139. Sandhir R, Gregory E, Berman NEJ. Differential response of miRNA-21 and its targets after traumatic brain injury in aging mice. *Neurochem Int.* 2014 Dec;78:117–21.
140. Han Z, Chen F, Ge X, Tan J, Lei P, Zhang J. miR-21 alleviated apoptosis of cortical neurons through promoting PTEN-Akt signaling pathway in vitro after experimental traumatic brain injury. *Brain Res.* 2014 Sep;1582:12–20.
141. Li D, Huang S, Zhu J, Hu T, Han Z, Zhang S, et al. Exosomes from MiR-21-5p-Increased Neurons Play a Role in Neuroprotection by Suppressing Rab11a-Mediated Neuronal Autophagy In Vitro After Traumatic Brain Injury. *Med Sci Monit.* 2019 Mar 12;25:1871–85.
142. Bai X, Bian Z. MicroRNA-21 Is a Versatile Regulator and Potential Treatment Target in Central Nervous System Disorders. *Front Mol Neurosci.* 2022 Jan 31;15:842288.
143. Wang WX, Visavadiya NP, Pandya JD, Nelson PT, Sullivan PG, Springer JE. Mitochondria-associated microRNAs in rat hippocampus following traumatic brain injury. *Exp Neurol.* 2015 Mar;265:84–93.
144. Lei P, Li Y, Chen X, Yang S, Zhang J. Microarray based analysis of microRNA expression in rat cerebral cortex after traumatic brain injury. *Brain Res.* 2009 Aug;1284:191–201.
145. Redell JB, Liu Y, Dash PK. Traumatic brain injury alters expression of hippocampal microRNAs: Potential regulators of multiple pathophysiological processes. *J Neurosci Res.* 2009 May;87(6):1435–48.
146. Liu Y, Li W, Liu Y, Jiang Y, Wang Y, Xu Z, et al. MicroRNA-223 Attenuates Stretch-Injury-Induced Apoptosis in Brain Microvascular Endothelial Cells by Regulating RhoB Expression. *Brain Sci.* 2022 Aug 30;12(9):1157.
147. Yang Z, Zhong L, Xian R, Yuan B. MicroRNA-223 regulates inflammation and brain injury via feedback to NLRP3 inflammasome after intracerebral hemorrhage. *Mol Immunol.* 2015

Jun;65(2):267–76.

148. Tang J, Yan B, Tang Y, Zhou X, Ji Z, Xu F. Baicalein ameliorates oxidative stress and brain injury after intracerebral hemorrhage by activating the Nrf2/ARE pathway via miR-106a-5p/PHLPP2 axis. *Int J Neurosci*. 2023 Dec 2;133(12):1380–93.
149. Michell DL, Vickers KC. Lipoprotein carriers of microRNAs. *Biochim Biophys Acta BBA - Mol Cell Biol Lipids*. 2016 Dec;1861(12):2069–74.
150. Ashby J, Flack K, Jimenez LA, Duan Y, Khatib AK, Somlo G, et al. Distribution Profiling of Circulating MicroRNAs in Serum. *Anal Chem*. 2014 Sep 16;86(18):9343–9.
151. Ma J, Zhang K, Wang Z, Chen G. Progress of Research on Diffuse Axonal Injury after Traumatic Brain Injury. *Neural Plast*. 2016;2016:1–7.
152. Liu J, Jennings SF, Tong W, Hong H. Next generation sequencing for profiling expression of miRNAs: technical progress and applications in drug development. *J Biomed Sci Eng*. 2011;04(10):666–76.
153. Wang WX, Sullivan PG, Springer JE. Mitochondria and microRNA crosstalk in traumatic brain injury. *Prog Neuropsychopharmacol Biol Psychiatry*. 2017 Feb;73:104–8.
154. Korotkov A, Puhakka N, Gupta SD, Vuokila N, Broekaart DWM, Anink JJ, et al. Increased expression of miR142 and miR155 in glial and immune cells after traumatic brain injury may contribute to neuroinflammation via astrocyte activation. *Brain Pathol*. 2020 Sep;30(5):897–912.
155. Chen CZ, Li L, Lodish HF, Bartel DP. MicroRNAs Modulate Hematopoietic Lineage Differentiation. *Science*. 2004 Jan 2;303(5654):83–6.
156. Xiang P, Hu J, Wang H, Luo Y, Gu C, Tan X, et al. miR-204-5p is sponged by TUG1 to aggravate neuron damage induced by focal cerebral ischemia and reperfusion injury through upregulating COX2. *Cell Death Discov*. 2022 Feb 28;8(1):89.
157. Iwuchukwu I, Nguyen D, Sulaiman W. Micro RNA Profile in Cerebrospinal Fluid and Plasma of Patients with Spontaneous Intracerebral Hemorrhage. *CNS Neurosci Ther*. 2016 Dec;22(12):1015–8.
158. Wang L, Zhang H, Xie C. Down-regulation of miR-204-5p ameliorates sevoflurane-induced brain injury in neonatal rats through targeting VCAM1. *Toxicol Mech Methods*. 2023 May 4;33(4):307–15.

ILLUSTRATIONS

List of figures

Figure 1. Most common types of biophysical forces during traumatic brain injury.....	9
Figure 2. Schematic overview of microRNA (miRNA) biogenesis – Drosha-dependent / Dicer-dependent canonical pathway and Drosha-independent / Dicer-dependent noncanonical pathway.....	19
Figure 3. Biotypes of extracellular vesicles (EVs).....	26
Figure 4. Creation of a CSF biobank from sTBI patients.....	42
Figure 5. Common plasma and cell proteins in intracranial cerebrospinal fluid (CSF) after severe traumatic brain injury (sTBI).....	44
Figure 6. Assessment of hemolysis in CSF by miRNA quantification.....	45
Figure 7. A standard curve for absolute quantification of miRNAs.....	47
Figure 8. The highly abundant microRNAs (miRNAs) across cerebrospinal fluid (CSF) pools.....	50
Figure 9. The targeted 87 miRNAs account for a minor portion of the miRNAs detected in the cerebrospinal fluid after severe traumatic brain injury and most likely derive from the blood.....	52
Figure 10. Extracellular vesicles (EVs) are present in intracranial cerebrospinal fluid (CSF) during 12 days after severe traumatic brain injury (sTBI) and can be separated from free proteins (FP) by size-exclusion chromatography (SEC).....	54
Figure 11. Extracellular vesicle (EV) and free protein (FP) enriched fractions of cerebrospinal fluid after (CSF) severe traumatic brain injury (sTBI) contain comparable levels of miRNA.....	56

List of tables

Table 1. The Glasgow Coma Scale total score.....	6
Table 2. The Glasgow Outcome Scale (GOS) score	7
Table 3. Chemicals and reagents used in the study.....	32
Table 4. Commercially available reagents and kits for miRNA profiling	34
Table 5. Antibodies applied in the study.....	36
Table 6. Characteristics of sTBI patients included in the study	41
Table 7. Amounts of detected and quantified targeted 87 microRNAs (miRNAs) from cerebrospinal fluid (CSF) pools	48
Table 8. Targeted microRNAs (miRNAs) enriched in extracellular vesicle (EV) and free protein (FP) pools of the depicted days (d).....	58

LIST OF ABBREVIATIONS

AGO	Argonaute protein family
ALIX	ALG-2-interacting protein X
AMPA	α -amino-3-hydroxy-5-methyl-4-isoxazolepropionic acid
ATCC	American Type Cell Collection
APOs	Apoptotic bodies
APT1	Acyl protein thioesterase 1
ATP	Adenosine triphosphate
BBB	Brain-blood barrier
BSA	Bovine serum albumin
CAT	Catalase
CBF	Cerebral blood flow
CCD	Charge-coupled device
CCI	Controlled cortical impact
cDNA	Complementary deoxyribonucleic acid
CNS	Central nervous system
CSF	Cerebrospinal fluid
CT	Computed tomography
Ct	Cycle threshold
CPP	Cerebral perfusion pressure
DAI	Diffuse axonal injury
DGCR8	DiGeorge Syndrome Critical Region 8
DISC	Death-inducing signalling complex

DNA	Deoxyribonucleic acid
EDH	Epidural haematoma
ESCRT	Endosomal sorting complexes required for transport
EVD	External ventricular drain
EVs	Extracellular vesicles
EXOs	Exosomes
FGF8	Fibroblast growth factor 8
GCS	Glasgow Coma Scale
GFAP	Glial fibrillary acidic protein
GOS	Glasgow Outcome Scale
GPx	Glutathione peroxidase
GR	Glutathione reductase
GST	Glutathione S-transferase
IL-1 β	Interleukin 1 beta
IL-6	Interleukin 6
IL-8	Interleukin 8
IL-18	Interleukin 18
ICH	Intracerebral haemorrhage
ICP	Intracranial pressure
ILVs	Intraluminal vesicles
ISEV	International Society for Extracellular Vesicles
IVH	Intraventricular haemorrhage

L-EVs	Long extracellular vesicles
LIMK1	Lim kinase 1
LP	Lipid peroxidation
MAP	Mean arterial pressure
MAPK	Mitogen-activated protein kinase
MiRISC	MiRNA-induced silencing complex
MISEV 2018	Minimal information for studies of extracellular vesicles 2018
MMP-9	Matrix metalloproteinase-9
MVs	Microvesicles
MVB	Multivesicular body
NMDA	N-methyl-D-aspartate
NO	Nitric oxide
NSE	Neuron-specific enolase
NTA	Nanoparticle tracking analysis
PABP	Poly(A)-binding protein
PBS	Phosphate buffered saline
PCR	Polymerase chain reaction
PGE2	Prostaglandin E2
PLA2	Phospholipase A2
PRDX	Peroxiredoxin protein family
PS	Phosphatidylserine
PTBP1	Polypyrimidine tract-binding protein 1
PUM1	Pumilio 1

PUM2	Pumilio 2
p250GAP RISC	p250 - GTPase-activating protein RNA-induced silencing complex
RNA	Ribonucleic acid
RNS	Reactive nitrogen species
RPM	Revolutions per minute
ROS	Reactive oxygen species
RT-PCR	Real time – polymerase chain reaction
S-EVs	Short extracellular vesicles
SAH	Subarachnoid haemorrhage
SDH	Subdural haemorrhage
SEC	Size-exclusion chromatography
shRNA	Small hairpin RNA
sTBI	Severe traumatic brain injury
STEP	Striatal-enriched protein tyrosine phosphatase
SOD	Superoxide dismutase
SUR1	Sulfonylurea receptor-1
S100B	S100 Calcium binding protein B
TBI	Traumatic brain injury
TBS	Tris buffered saline
TNF- α	Tumour necrosis factor alpha
TRPS	Tunable resistive pulse sensing
TSG101	Tumour susceptibility gene 101 protein

UTR	Untranslated region
QC array	Quality control array
XPO5	Exportin 5

CURRICULUM VITAE

PERSONAL INFORMATION

Name: Lara Valenčić Seršić

Date and place of birth: February 26th, 1991, Rijeka, Croatia

Nationality: Croatian

E-mail: lara.valencic@uniri.hr

Scientist identification number: 368534

WORK EXPERIENCE

- **June 2025 – Current** – Specialist in Anaesthesiology, Resuscitation and Intensive Care Medicine, Anaesthesiology, Intensive Medicine and Pain Treatment Clinic, Clinical Hospital Centre Rijeka
- **April 2018 - Current** – Research assistant at the Department of Anaesthesiology, Resuscitation, Emergency and Intensive Care Medicine, Faculty of Medicine, University of Rijeka
- **June 2018 - June 2025** – Resident in Anaesthesiology, Resuscitation and Intensive Care Medicine, Anaesthesiology, Intensive Medicine and Pain Treatment Clinic, Clinical Hospital Centre Rijeka
- **2016 – 2018** – Doctor of medicine, Institute of emergency medicine of Istrian County, Umag
- **2015 – 2016** – Internship, Clinical Hospital Centre Rijeka

EDUCATION

- **2018 - 2024** – Postgraduate student at University Doctoral Study of Biomedicine and Health, Faculty of Medicine, University of Rijeka
- **2021 – 2023** – Postgraduate Specialist Study of Anaesthesiology, Resuscitation and Intensive Care Medicine, Faculty of Medicine, University of Rijeka
- **2009 – 2015** – Integrated Undergraduate and Graduate University Study of Medicine, Faculty of Medicine, University of Rijeka
- **2005 – 2009** – Medical School in Rijeka, physiotherapy technician
- **1997 – 2005** – Elementary School “Klana”

TRAINING

- Focused Assessed Transthoracic Echocardiography (FATE) course, Skill's Lab Simulation Centre Faculty of Medicine, University of Rijeka, March 2025
- European Trauma Course (ETC), course of European Resuscitation Council (ERC), 1st category, March 2025
- Annual Flow Cytometry Course 2019, Srebrnjak Children's Hospital, Centre of Competence for Translational Medicine, Zagreb, December 2019
- Ultrasound guided Regional Anaesthesia, course of 1st category, November 2019
- Rapid Sequence Intubation – RSI course, October 2019
- Advanced Life Support (ALS), course of European Resuscitation Council (ERC), 1st category, June 2017
- Ultrasound Life Support (USLS BL1P COURSE), Clinical Hospital Centre Zagreb, March 2017

PERSONAL SKILLS AND COMPETENCIES

- Ultrasound guided Regional Anaesthesia provider (from November 2019)
- Rapid Sequence Intubation provider (from November 2019)
- ALS provider (from June 2017)
- Ultrasound Life Support (USLS BL1P COURSE) provider (from March 2017)

MOTHER TONGUE

- Croatian

OTHER LANGUAGES

- English

RESEARCH SKILLS AND COMPETENCES

- Collaborator on Croatian Science Foundation project "Identification of circulating biomarkers for neuro-recovery of brain-injured patients" (IP-2019-04-1511), led by Assoc. Prof. Kristina Grabušić, PhD (project duration: January 1st 2020 – December 31st 2023)
- Collaborator on the project "Strengthening capacities for higher education of pain medicine in western Balkan countries – HEPMP" (585927-EPP-1-2017-1-RS-EPPKA2-CBHE-JP), Erasmus + project (project duration: October 15th 2017 – October 15th 2020)

Scientific work from doctoral dissertation topic:

Valenčić Seršić L, Krušić Alić V, Biberić M, Zrna S, Jagoić T, Tarčuković J, Grabušić K. Real-Time PCR Quantification of 87 miRNAs from Cerebrospinal Fluid: miRNA Dynamics and Association with Extracellular Vesicles after Severe Traumatic Brain Injury. *Int J Mol Sci.* 2023;24(5):4751.

Other original research articles:

Knežević D, Batičić L, Curko-Cofek B, Batinac T, Ljubačev A, **Valenčić Seršić L**, Laškarin G, Zdravković M, Šoštarić M, Sotošek V. The Effect of Coronary Artery Bypass Surgery on Interleukin-18 Concentration and Biomarkers Related to Vascular Endothelial Glycocalyx Degradation. *Int. J. Mol. Sci.* 2025;26(12):5453.

Krušić Alić V, Malenica M, Biberić M, Zrna S, **Valenčić L**, Šuput A, Kalagac Fabris L, Wechtersbach K, Kojc N, Kurtjak M, Kučić N, Grabušić K. Extracellular Vesicles from Human Cerebrospinal Fluid Are Effectively Separated by Sepharose CL-6B - Comparison of Four Gravity-Flow Size Exclusion Chromatography Methods. *Biomedicines.* 2022;10(4):785.

Tarčuković J, **Valenčić L**, Polonijo Ž, Fućak A, Dangubić B, Grubješić I. Acute Liver Failure as the Leading Manifestation of Spontaneous Tumour Lysis Syndrome in a Patient with NonHodgkin Lymphoma: Do Current Diagnostic Criteria of Tumour Lysis Syndrome Need Re-Evaluation? *Case Rep Crit Care.* 2019;2019:2358562.

Glavaš S, **Valenčić L**, Trbojević N, Tomašić A-M, Turčić N, Tibauth S, Ružić A. Erectile function in cardiovascular patients: its significance and a quick assessment using a visual-scale questionnaire. *Acta Cardiol.* 2015;70(6):712-9.

Grebic D, Tomašić A-M, **Valenčić L**, Trbojević N, Grbas H. The Incidence and Characteristics of Chronic Postoperative Groin Pain after Inguinal Hernia Repair with Different Types of Prolene Mesh. *The West Indian Medical Journal.* 2017;66(1):46-49.

Valenčić L, Sotošek Tokmadžić V, Tarčuković J, Šustić A. The incidence of nosocomial infections in patients with isolated severe traumatic brain injury. *Sanamed.* 2015;10(3):185-192.

Glavaš S, **Valenčić L**, Trbojević N, Tomašić A-M, Tibauth S, Turčić N, Zaputović L, Ružić A. Assessment of erectile function in cardiovascular patients: the graphic questionnaire as a novel diagnostic test. *Cardiologia Croatica.* 2014;9(5-6):251.

Review articles / case reports:

Valenčić L, Koraca Chinchella I, Juričić K. Značajke anestezioloških postupaka kod transplantacije bubrega/Specificities of anesthesia management for kidney transplantation. *Medicina Fluminensis*. 2020;56(4):515-521.

Valković Zujčić P, Grebić D, **Valenčić L**. Chronic Granulomatous Inflammation of the Breast as a First Clinical Manifestation of Primary Sarcoidosis. *Breast Care (Basel)*. 2015;10(1):51-53.

Oral presentations:

Tomulić Brusich K, Protić A, Juričić K, **Valenčić L**. Intenzivističko liječenje bolesnika s komplikacijama nakon operacije aneurizme abdominalne aorte-prikaz slučajeva. Annual Congress of the Croatian Society for Vascular Surgery, CroMA with international participation. Opatija, October 2021

Published in: *Acta Chirurgica Croatica*, 2021;18(Suppl.1).

Valenčić L, Polonijo Ž, Kuharić J, Dangubić B, Sotošek Tokmadžić V, Šustić A. Utjecaj zbrinjavanja dišnog puta supraglotičnim pomagalom i endotrahealnim tubusom na karakteristike opće anestezije tijekom operacija dojke i štitnjače. 3rd Croatian Congress of Airway Management with International Participation "Airway in Emergencies", Zagreb, September 2018.

Poster presentations:

Krušić Alić V, **Valenčić L**, Zrna S, Biberić M, Jagoić T, Tarčuković J, Grabušić K. Identification of microRNA cargo of extracellular vesicles from cerebrospinal fluid of severe traumatic brain injury patients. 3rd Regional Congress of Physiological Societies and 5th Congress of Croatian Physiological Society. September 2022, Plitivička Jezera, Croatia.

Jagoić T, Krušić Alić V, Zrna S, Biberić M, **Valenčić L**, Grabušić K. Antioxidative enzymes from cerebrospinal fluid as protein biomarkers of neurorecovery in patients with severe traumatic brain injury. 8th International Student Congress Graz. June 2022. Graz, Austria.

Krušić Alić V, Malenica M, Zrna S, Biberić M, **Valenčić L**, Kalagac Fabris L, Šuput Aleksandar, Wechtersbach K, Kojc N, Kurtjak M, Kučić N, Grabušić K. Evaluation of four size-exclusion chromatography's to separate extracellular vesicles from human

intracranial cerebrospinal fluid. International Society for Extracellular Vesicles (ISEV) 2022 Annual Meeting. May 2022. Lyon, France.

Jagoić T, Krušić Alić V, Zrna S, Biberić M, **Valenčić L**, Grabušić K. Dynamics of antioxidative enzymes in cerebrospinal fluid of patients with severe traumatic brain injury-a pilot study of potential biomarkers for neuro-recovery. 11th Student Congress of Neuroscience – NeuRi 2022. April 2022. Rijeka-Rab, Croatia.

Glavaš S, **Valenčić L**, Trbojević N, Tibauth S, Turčić N, Zaputović L. Assessment of erectile function in cardiovascular patients: The graphic questionnaire as a novel diagnostic test. June 2014. 22nd Annual Meeting of the Alpe Adria Association of Cardiology. Opatija, Croatia.

Chapters in books and manuals:

Tomulić Brusich K, **Valenčić L**, Polonijo Ž. Physiology and pharmacology of epidurally administered drugs. Epidural administration – new perspectives and uses. December 2022. doi: 10.5772/intechopen.109116.

Sokolić J, **Valenčić L**. Preoperative preparation of patients and operative risk assessment. Handbook of Anesthesiology, Reanimatology, and Intensive Care Medicine. Medicinska naklada. Zagreb, 2021, 5-13.

Knežević D, **Valenčić L**. Regional Anesthesia. Handbook of Anesthesiology, Reanimatology, and Intensive Care Medicine. Medicinska naklada. Zagreb, 2021, 50-59.

Other publications:

Polonijo Ž, **Valenčić L**. Razlika opće i regionalne anestezije. Narodni zdravstveni list. 2022, No. 744-745, pages 7-9.

MEMBERSHIPS

From 2015 until today – Croatian Medical Chamber

AWARDS

Dean's Award for the best student of the 3rd year of the Integrated Undergraduate and Graduate Study of Medicine (2011/2012)